

## Supporting Information for

### Ferrocene-Containing Amphiphilic Polynorbornenes as Biocompatible Drug Carriers

Guirong Qiu,<sup>a</sup> Xiong Liu,<sup>a,b</sup> Binrong Wang,<sup>c</sup> Haibin Gu,<sup>a,b,\*</sup> Weixiang Wang<sup>c,\*</sup>

<sup>a</sup>Key Laboratory of Leather Chemistry and Engineering of Ministry of Education, Sichuan University, Chengdu 610065, China. E-mail: guhaibinkong@126.com (H. Gu)

<sup>b</sup>National Engineering Laboratory for Clean Technology of Leather Manufacture, Sichuan University, Chengdu 610065, China.

<sup>c</sup>College of Food and Bioengineering, Xihua University, Chengdu 610039, China. E-mail: wang\_weixiang@hotmail.com (W. Wang)

#### Table of Contents

Materials and instruments	S6
1. Synthesis of <b>2</b>	S7
Synthesis route of <b>2</b> (Scheme S1)	S7
1.1 Synthesis of <b>1</b>	S7
<sup>1</sup> H NMR spectrum of <b>1</b> (Figure S1)	S7
1.2 Synthesis of <b>2</b>	S7
<sup>1</sup> H NMR spectrum of <b>2</b> (Figure S2)	S8
2. Synthesis of <b>NFc</b>	S8
Synthesis route of <b>NFc</b> (Scheme S2)	S8
2.1 Synthesis of <b>3</b>	S8
<sup>1</sup> H NMR spectrum of <b>3</b> (Figure S3)	S9
IR spectrum of <b>3</b> (Figure S4)	S9
2.1 Synthesis of <b>NFc</b>	S9
<sup>1</sup> H NMR spectrum of <b>NFc</b> (Figure S5)	S10
<sup>13</sup> C NMR (100 MHz) spectrum of <b>NFc</b> (Figure S6)	S10
ESI mass spectrum of <b>NFc</b> (Figure S7)	S11
IR spectrum of <b>NFc</b> (Figure S8)	S11
Uv-vis spectrum of <b>NFc</b> (Figure S9)	S12
CV curve of monomer <b>NFc</b> (Figure S10)	S12
3. ROMP synthesis of homopolymer <b>PNFc</b>	S12
3.1 General Synthesis of homopolymer <b>PNFc</b>	S12
<sup>1</sup> H NMR spectrum of <b>PNFc</b> (Figure S11)	S13
<sup>13</sup> C NMR spectrum of <b>PNFc</b> (Figure S12)	S14
IR spectrum of <b>PNFc</b> (Figure S13)	S14
UV-vis spectrum of <b>PNFc</b> . (Figure S14)	S14
CV curve of polymer <b>PNFc</b> (Figure S15)	S15
MALDI-TOF MS spectrum of polymer <b>PNFc c</b> (Figure S16)	S15
GPC curve of <b>PNFc a</b> (Figure S17)	S15
Molecular weight data of polymers <b>PNFc a</b> by GPC (Table S1)	S16

3.2 Kinetic study for the synthesis of Polymer <b>PNFc-c</b> :	S16
<sup>1</sup> H NMR spectrum of the reaction mixtures in CDCl <sub>3</sub> for the synthesis of <b>PNFc-c</b> <b>(Figure S18)</b>	S16
3.3 Calculation of the polymer degrees of <b>PNFc-a</b> by <sup>1</sup> H NMR end-group analysis and errors	S16
<sup>1</sup> H NMR of <b>PNFc-a</b> in (CD <sub>3</sub> ) <sub>2</sub> SO <b>(Figure S19)</b>	S16
Polymer degree of <b>PNFc-a</b> calculated by using its <sup>1</sup> H NMR spectrum in (CD <sub>3</sub> ) <sub>2</sub> SO <sup>a</sup> <b>(Table S2)</b>	S17
3.4 Calculation of the polymer degrees of <b>PNFc-b</b> by <sup>1</sup> H NMR end-group analysis and errors	S17
<sup>1</sup> H NMR of <b>PNFc-b</b> in (CD <sub>3</sub> ) <sub>2</sub> SO <b>(Figure S20)</b>	S17
Polymer degree of <b>PNFc-b</b> calculated by using its <sup>1</sup> H NMR spectrum in (CD <sub>3</sub> ) <sub>2</sub> SO <sup>a</sup> <b>(Table S3)</b>	S18
3.5 Calculation of the polymer degrees of <b>PNFc-c</b> by <sup>1</sup> H NMR end-group analysis and errors	S18
The <sup>1</sup> H NMR of <b>PNFc-c</b> in (CD <sub>3</sub> ) <sub>2</sub> SO <b>(Figure S21)</b>	S18
Polymer degree of <b>PNFc-c</b> calculated by using its <sup>1</sup> H NMR spectrum in (CD <sub>3</sub> ) <sub>2</sub> SO <b>(Table S4.)</b>	S19
4. Synthesis of monomer <b>NETG</b>	S19
Synthesis route of monomer <b>NETG (Scheme S4)</b>	S19
4.1. Synthesis of <b>5</b>	S20
<sup>1</sup> H NMR (400 MHz) spectrum of <b>5 (Figure S22)</b>	S20
4.2. Synthesis of <b>6</b>	S20
<sup>1</sup> H NMR (400 MHz) spectrum of <b>6 (Figure S23)</b>	S21
<sup>13</sup> C NMR spectrum (100 MHz) of <b>6 (Figure S24)</b>	S21
4.3. Synthesis of <b>7</b>	S21
<sup>1</sup> H NMR (400 MHz) spectrum of <b>7 (Figure S25)</b>	S22
<sup>13</sup> C NMR (100 MHz) spectrum of <b>7 (Figure S26)</b>	S22
ESI Mass spectrum of <b>9 (Figure S27)</b>	S23
4.4. Synthesis of <b>NETG</b>	S23
<sup>1</sup> H NMR (400 MHz) spectrum of <b>NETG (Figure S28)</b>	S24
<sup>13</sup> C NMR (100 MHz) spectrum of <b>NETG (Figure S29)</b>	S24
Mass spectrum of <b>NETG (Figure S30)</b>	S24
IR spectrum of <b>NETG (Figure S31)</b>	S25
5. Synthesis of polymer <b>PNETG</b>	S25
Synthesis route of polymer <b>PNETG (Scheme S5)</b>	S25
5.1. General Synthesis procedure of polymer <b>PNETG</b>	S25
<sup>1</sup> H NMR (400 MHz) spectrum of <b>PNETG (Figure S32)</b>	S26
<sup>1</sup> H NMR (400 MHz) spectrum of <b>PNETG-a (Figure S33)</b>	S26
<sup>1</sup> H NMR (400 MHz) spectrum of <b>PNETG-a</b> in (CD <sub>3</sub> ) <sub>2</sub> SO <b>(Figure S34)</b>	S27
<sup>1</sup> H NMR (400 MHz) spectrum of <b>PNETG-b</b> in D <sub>2</sub> O <b>(Figure S35)</b>	S27
<sup>13</sup> C NMR (100 MHz) spectrum of <b>PNETG</b> in CDCl <sub>3</sub> <b>(Figure S36)</b>	S28
MALDI-TOF mass spectrum of <b>PNETG-a (Figure S37)</b>	S28
IR spectrum of <b>PNETG (Figure S38)</b>	S29

GPC curve of <b>PNETG b (Figure S39)</b>	S29
Molecular weight data of polymer <b>PNETG b</b> by GPC ( <b>Table S5</b> )	S29
5.2 Kinetic study for polymer <b>PNETG-a</b>	S29
<sup>1</sup> H NMR spectra of the reaction mixtures in CDCl <sub>3</sub> for the synthesis of <b>PNETG-a (Figure S40)</b>	S30
5.3 Kinetic study for polymer <b>PNETG-b</b>	S30
<sup>1</sup> H NMR spectra of the reaction mixtures in CDCl <sub>3</sub> for the synthesis of <b>PNETG-b (Figure S41)</b>	S30
6. ROMP synthesis of diblock copolymer <b>PN(Fc-b-TEG)</b>	S31
6.1. Synthesis route of diblock copolymer <b>PN(Fc-b-TEG) (Scheme S6)</b>	S31
<sup>13</sup> C NMR (100 MHz) spectrum of <b>PN(Fc-b-TEG) (Figure S42)</b>	S31
UV-vis spectrum of <b>PN(Fc-b-TEG) (Figure S43)</b>	S31
IR spectrum of <b>PN(Fc-b-TEG) (Figure S44)</b>	S31
DLS curve of <b>PN(Fc-b-TEG)</b> in wate ( <b>Figure S45</b> )	S32
The partial GPC trace of <b>PN(Fc-b-TEG) (Figure S46)</b>	S32
Molecular weight data of black polymer <b>PN(Fc-b-TEG)</b> by GPC ( <b>Table S6</b> )	S32
6.2 <sup>1</sup> H NMR of <b>PN(Fc-b-TEG)</b> in (CD <sub>3</sub> ) <sub>2</sub> SO for ratio analysis ( <b>Figure S47</b> )	S32
Ratio analysis calculated by using the <sup>1</sup> H NMR spectrums in (CD <sub>3</sub> ) <sub>2</sub> SO of <b>PN(Fc-b-TEG) (Table S7)</b>	S33
6.3. Kinetic study for the synthesis of diblock copolymer <b>PN(Fc-b-TEG)</b>	S33
<sup>1</sup> H NMR spectra of the reaction mixtures in CDCl <sub>3</sub> for the synthesis of <b>PN(Fc-b-TEG) (Figure S48)</b>	S34
7. ROMP synthesis of random copolymer <b>PN(Fc-r-TEG)</b>	S34
7.1 General synthetic procedure	S34
<sup>1</sup> H NMR (400 MHz) spectrum of <b>PN(Fc-r-TEG) (Figure S49)</b>	S35
<sup>13</sup> C NMR (100 MHz) spectrum of <b>PN(Fc-r-TEG) (Figure S50)</b>	S35
UV-vis spectrum of <b>PN(Fc-r-TEG) (Figure S51)</b>	S35
IR spectrum of <b>PN(Fc-r-TEG) (Figure S52)</b>	S36
DLS curve of <b>PN(Fc-r-TEG)</b> in water ( <b>Figure S53</b> )	S36
The SEM images of self-assembly random copolymer <b>PN(Fc-r-TEG)</b> in aqueous solutions ( <b>Figure S54</b> )	S36
The partial GPC trace of <b>PN(Fc-r-TEG) (Figure S55)</b>	S37
Molecular weight data of black polymer <b>PN(Fc-r-TEG)</b> by GPC ( <b>Table S8</b> )	S37
7.2. <sup>1</sup> H NMR of <b>PN(Fc-r-TEG)</b> in (CD <sub>3</sub> ) <sub>2</sub> SO for ratio analysis ( <b>Figure S56</b> )	S37
Ratio analysis calculated by using the <sup>1</sup> H NMR spectrums in (CD <sub>3</sub> ) <sub>2</sub> SO of <b>PN(Fc-r-TEG) (Table S9)</b>	S37
7.3. Kinetic study for the synthesis of random copolymer <b>PN(Fc-r-TEG)</b>	S38
<sup>1</sup> H NMR spectra of the reaction mixtures in CDCl <sub>3</sub> for the synthesis of <b>PN(Fc-r-TEG) (Figure S57)</b>	S38
8. Self-assembly of the copolymer in water	S39
The Tyndall effect of <b>PN(Fc-b-TEG)</b> and (a) and <b>PN(Fc-r-TEG)</b> (b) after self-assembly in water( <b>Figure S58</b> )	S39
9. Oxidation and reduction of micelles	S39
9.1 Determination of critical micelle concentration (CMC)	S39

The CMCs of the block <b>PN(Fc-b-TEG)</b> and random copolymers <b>PN(Fc-r-TEG)</b> (Figure S59)	S40
9.2. DLS curves of <b>PN(Fc-r-TEG)</b> micelles	S40
Micelles of <b>PN(Fc-r-TEG)</b> in water (Figure S60)	S40
9.3. Determination of CMC of oxidized micelles	S40
The CMCs of the block <b>PN(Fc-b-TEG)</b> and random copolymers <b>PN(Fc-r-TEG)</b> after oxidation by FeCl <sub>3</sub> (Figure S61)	S41
10. Drug loading and release	S41
10.1 The loading and release of Nile red	S41
The SEM image of micelles of <b>PN(Fc-b-TEG)</b> after loaded Nile red in aqueous (Figure S62)	S41
The DLS curve of micelles of <b>PN(Fc-b-TEG)</b> after loaded Nile red in aqueous (Figure S63)	S42
UV-vis spectrum of the NR-loaded micelles of <b>PN(Fc-b-TEG)</b> in water (Figure S64)	S42
Picture of copolymer <b>PN(Fc-b-TEG)</b> and NR in different solutions (Figure S65)	S42
The UV-vis absorbance variation of <b>PN(Fc-b-TEG)</b> loaded with Nile red (Figure S66)	S43
The UV-vis absorbance variation of NR-loaded micelles of <b>PN(Fc-b-TEG)</b> at 585 nm after oxidized by FeCl <sub>3</sub> in water (Figure S67)	S43
10.2. Loading and release of NR by micelles of <b>PN(Fc-r-TEG)</b>	S43
The SEM image of micelles of <b>PN(Fc-r-TEG)</b> after loaded Nile red in aqueous (Figure S68)	S43
The DLS curve of micelles of <b>PN(Fc-r-TEG)</b> after loaded Nile red in aqueous (Figure S69)	S44
The UV-vis spectrum of the micelles <b>PN(Fc-r-TEG)</b> loaded Nile red in aqueous (Figure S70)	S44
The UV-vis absorption spectra of <b>PN(Fc-r-TEG)</b> loaded with Nile red after oxidized by FeCl <sub>3</sub> at every stage in aqueous (Figure S71)	S44
The UV-vis absorbance variation of <b>PN(Fc-r-TEG)</b> loaded with Nile red (Figure S72)	S45
10.3 The loading and release of DOX	S45
The UV-vis absorption spectra of DOX in water at different concentrations (Figure S73)	S45
The time dependent DLS curves of <b>PN(Fc-b-TEG)</b> -DOX micelles using 1 mg ml <sup>-1</sup> FeCl <sub>3</sub> as oxidants. (Figure S74)	S45
The UV-vis absorption spectra of DOX release in 2 mg ml <sup>-1</sup> FeCl <sub>3</sub> aqueous solution from <b>PN(Fc-b-TEG)</b> -DOX micelles at different time intervals (Figure S75)	S46
The UV-vis absorption spectra of DOX release in 1 mg ml <sup>-1</sup> FeCl <sub>3</sub> aqueous solution from <b>PN(Fc-b-TEG)</b> -DOX micelles at different time intervals (Figure S76)	S46
The UV-vis absorption spectra of DOX release in 0.5 mg ml <sup>-1</sup> FeCl <sub>3</sub> aqueous solution from <b>PN(Fc-b-TEG)</b> -DOX micelles at different time intervals (Figure S77)	S46
10.4. Loading and release of DOX by micelles of <b>PN(Fc-r-TEG)</b>	S47
The UV-vis absorption spectra of the micelles of random copolymer <b>PN(Fc-r-TEG)</b> after loaded DOX <b>PN(Fc-r-TEG)</b> -DOX (Figure S78)	S47
The DLS curve of the micelles of random copolymer <b>PN(Fc-r-TEG)</b> loaded DOX (Figure S79)	S47

The SEM image (A) and size distribution (B) of the micelles of random copolymer <b>PN(Fc-r-TEG)</b> after loaded DOX ( <b>Figure S80</b> )	S47
The time dependent DLS curves of <b>PN(Fc-r-TEG)-DOX</b> micelles using FeCl <sub>3</sub> - as oxidants. ( <b>Figure S81</b> )	S48
The UV-vis absorption spectra of DOX release in 1 mg ml <sup>-1</sup> FeCl <sub>3</sub> aqueous solution from <b>PN(Fc-r-TEG)-DOX</b> micelles at different time intervals ( <b>Figure S82</b> )	S48
The cumulative release of DOX at different time intervals using 1mg ml <sup>-1</sup> FeCl <sub>3</sub> as oxidants for <b>PN(Fc-r-TEG)-DOX</b> micelles ( <b>Figure S83</b> )	S49
11. Biototoxicity evaluation	S49
11.1 Evaluation of the biototoxicity by murine fibroblast cells (L-929 cell)	S49
The relationship between cell relative proliferation rate and cytotoxicity grade ( <b>Table S10</b> )	S49
11.2 Evaluation of the biototoxicity by zebrafish embryo	S49
The photos of the zebrafish at 24 hpf, ( <b>Figure S84</b> )	S49
The photos of the zebrafish at 48 hpf ( <b>Figure S85</b> )	S50
The photos of the zebrafish at 72 hpf ( <b>Figure S86</b> )	S50
The photos of the zebrafish at 96 hpf ( <b>Figure S87</b> )	S51
The photos of the zebrafish dyed by acridine orange at 96 hpf ( <b>Figure S88</b> )	S51
12. References	S51

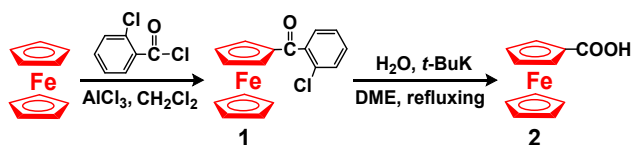
## Materials

ethyl vinyl ether (99%, EVE), propargylamine, Grubb's 3rd generation catalyst, Nile red (NE), DOX, fetal bovine serum (FBS), penicillin, streptomycin, murine fibroblast cells (L-929 cell), Cell Counting Kit, acridine orange (AO), zebrafish. All the chemicals and solvents used in this paper were purchased from the reagent company Energy Chemical.

## Instruments

$^1\text{H}$  NMR (400 MHz) and  $^{13}\text{C}$  NMR (100 MHz) spectra were recorded at 25 °C using a Bruker AC (400 MHz) spectrometer. All the chemical shifts are reported in parts per million ( $\delta$ , ppm) with reference to tetramethylsilane (TMS). Mass spectra were recorded using an Applied Biosystems Voyager-DE STR-MALDI-TOF spectrometer. The infrared spectra were recorded on an ATI Mattson Genesis series FT-IR spectrophotometer the range 400–4000  $\text{cm}^{-1}$ . UV–visible absorption spectra were measured with a Perkin-Elmer Lambda 19 UV–visible spectrometer. Gel permeation Chromatography (GPC) measurements were conducted in N, N-dimethyl formamide (DMF) using Shimadzu high performance liquid chromatography (HPLC) system equipped with PLgel 5  $\mu\text{m}$  MIXED-D columns, refractometric and UV detectors, column oven and integrated degasser. Polymer molecular weights were calculated based on the multiangle light scattering data using the Wyatt Astra software, with  $\text{dn}/\text{dc}$  values of the polymers determined from the RI detector using Astra. Column calibration was performed using polystyrene (PS) standards from Polymer Laboratories. Dynamic light scattering (DLS) measurements were made using Malvern Zetasizer Nano-ZS series equipment (Malvern Instruments, UK) at 25 °C at an angle of 90°. Scanning electron microscopy (SEM) observations were conducted with a SM-7500F field emission SEM instrument (JEOL). Samples for SEM were prepared by casting a drop of the solution on a silicon grid, followed by drying at room temperature (r.t., 25 °C).

## 1. Synthesis of carboxylferrocene 2



**Scheme S1.** Synthesis route of carboxylferrocene **2**

**1.1. Synthesis of *o*-chlorobenzoylferrocene **1****<sup>[S1]</sup>: Anhydrous AlCl<sub>3</sub> (21.5 g, 0.16 mol, 1.2 equiv) was suspended in CH<sub>2</sub>Cl<sub>2</sub> (30 ml), and the *o*-chlorobenzoyl chloride (23.5 g, 0.13 mol, 1 equiv) was added dropwise into the suspension. After 30 min of stirring at 0 °C under N<sub>2</sub> atmosphere, the suspension was added into the ferrocene (30.0 g, 0.16 mol, 1.2 equiv) solution in CH<sub>2</sub>Cl<sub>2</sub> (50 ml), and the obtained mixture was further stirred at r. t. for 1.5 h. The organic layer was washed by diluted hydrochloric acid (HCl) solution (1 mol l<sup>-1</sup>, 100 ml × 4), then by saturated NaHCO<sub>3</sub>, and dried over anhydrous Na<sub>2</sub>SO<sub>4</sub> and evaporated under vacuum. Purification was conducted by column chromatography with petroleum ether/ethyl acetate as eluent to get *o*-chlorobenzoylferrocene **1** as brown-red solid. Yield: 35.7 g, 82%. <sup>1</sup>H NMR (400 MHz, CDCl<sub>3</sub>, 25 °C, TMS), δ<sub>ppm</sub>: 7.51-7.31 (m, 4H, ph), 4.73 (t, *J* = 3.8 Hz, 2H, sub. Cp, Cp = η<sup>5</sup>-C<sub>5</sub>H<sub>5</sub>), 4.59 (t, *J* = 3.8 Hz, 2H, sub. Cp), 4.27 (s, 5H, free Cp).

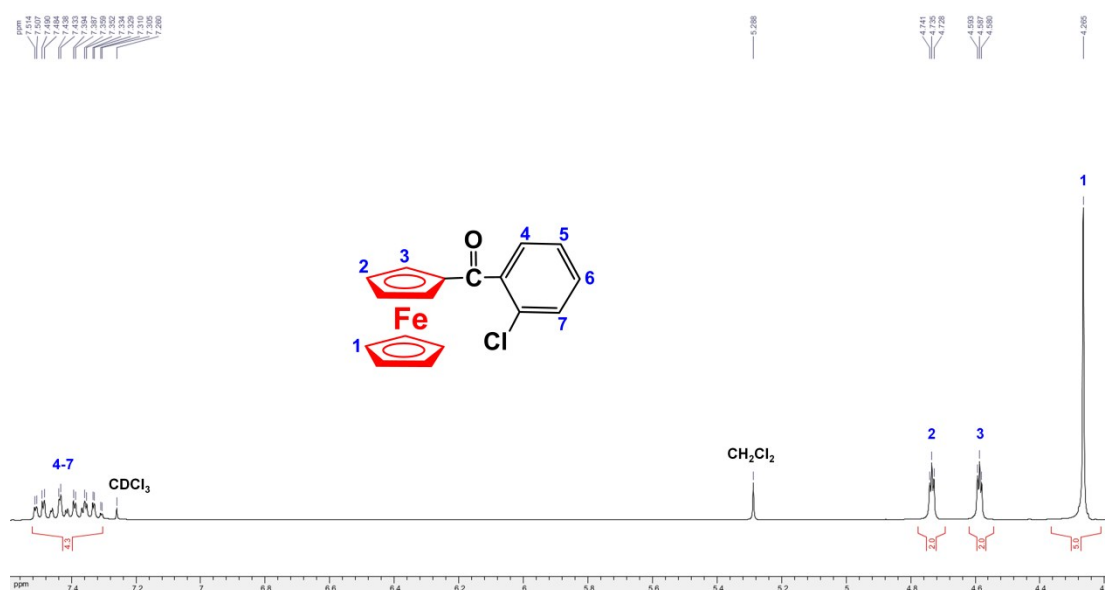


**Figure S1.** <sup>1</sup>H NMR (400 MHz) spectrum of **1** in CDCl<sub>3</sub>

**1.2. Synthesis of carboxylferrocene **2****<sup>[S1]</sup>: *o*-Chlorobenzoylferrocene **1** (35.7 g, 0.11 mol, 1 equiv) and potassium *tert*-butoxide (*t*-BuK, 30.8 g, 0.27 mol, 2.5 equiv) were dissolved in the mixture of ethylene glycol dimethyl ether (DME, 100 ml) and H<sub>2</sub>O (3.0 g, 0.17 mol, 1.5 equiv), and the reaction mixture was refluxed at 120 °C for 2 h under N<sub>2</sub> atmosphere. 10% NaOH (44 g, 1.1 mol, 10 equiv) solution (400 ml) was then added to get ferrocene carboxylate. The water solution was washed by diethyl ether (Et<sub>2</sub>O, 100 ml × 4), adjusted to pH 2.0 by adding HCl solution. The obtained precipitate was collected by suction filtration, and purified by column chromatography with CH<sub>2</sub>Cl<sub>2</sub>/methanol as eluent to get carboxylferrocene **2** as yellow solid. Yield: 23.18 g, 86%. <sup>1</sup>H NMR (400 MHz, (CD<sub>3</sub>)<sub>2</sub>SO, 25 °C, TMS), δ<sub>ppm</sub>: 4.75 (t, *J* = 3.9 Hz, 2H, sub. Cp), 4.44 (t, *J* = 3.9 Hz,

2H, sub. Cp), 4.22 (s, 5H, free Cp).

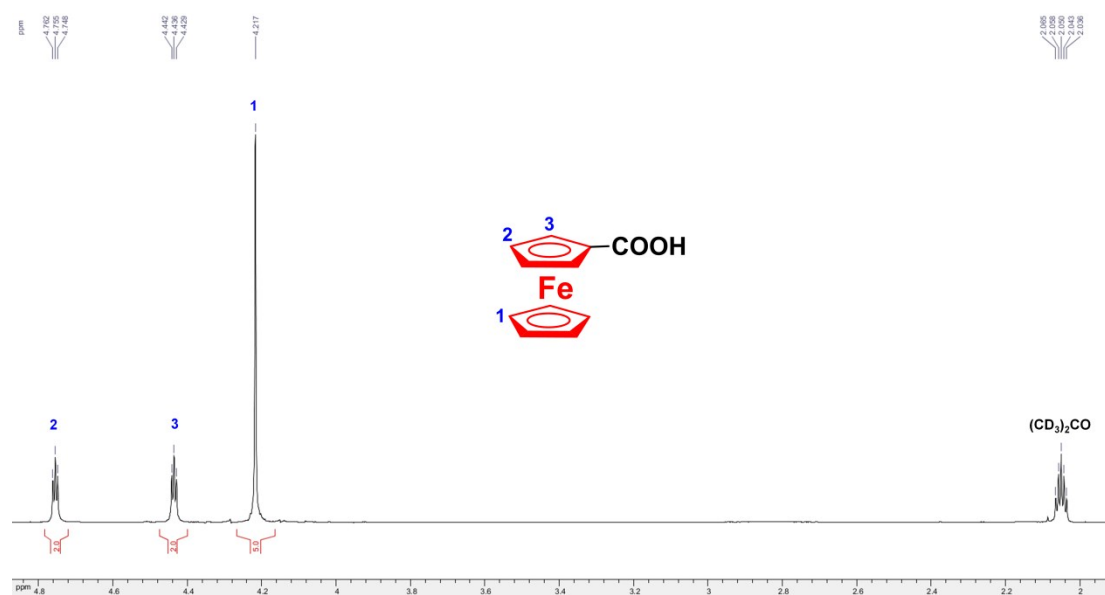
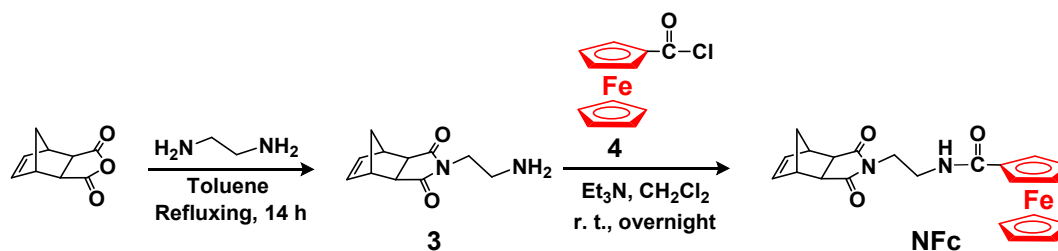


Figure S2.  $^1\text{H}$  NMR (400 MHz) spectrum of **2** in  $(\text{CD}_3)_2\text{SO}$ .

## 2. Synthesis of monomer NFc



Scheme S2. Synthesis route of monomer NFc

**2.1. Synthesis of **3****<sup>[S2]</sup>: To a solution of freshly distilled ethanediamine (3.59 g, 4.0 ml, 0.06 mol, 9.8 equiv) in toluene (10 ml) was added a solution of *cis*-5-norbornene-*exo*-2,3-dicarboxylic anhydride (1.0 g, 6.09 mmol, 1 equiv) in toluene (40 ml) dropwise at room temperature (r. t.) over 15 min with vigorous stirring. The obtained mixture was refluxed at 145 °C under  $\text{N}_2$  atmosphere for 14 h with a Dean-Stark apparatus before the solvent were removed *via* distillation *in vacuo*. Purification was achieved by column chromatography with  $\text{CH}_2\text{Cl}_2$ /methanol (1%→20%) as eluent, and the product **3** was obtained as pale white solid. Yield: 0.69 g, 55%.  $^1\text{H}$  NMR (400 MHz,  $\text{CDCl}_3$ , 25 °C, TMS),  $\delta_{\text{ppm}}$ : 6.30 (s, 2H, CH=CH), 3.56 (t,  $J = 12.5$  Hz, 2H, CONCH<sub>2</sub>), 3.28 (s, 2H, =C-CH), 2.91 (t,  $J = 12.4$  Hz, 2H, CH<sub>2</sub>NH<sub>2</sub>), 2.70 (s, 2H, CO-CH), 1.52 (d,  $J = 10.0$  Hz, 1H, CH<sub>2</sub>-bridge), 1.43 (br, 2H, NH<sub>2</sub>), 1.35 (d,  $J = 10.0$  Hz, 1H, CH<sub>2</sub>-bridge). Selected IR (KBr,  $\text{cm}^{-1}$ ): 3375 ( $\nu_{\text{NH}_2}$ ), 1767, 1696 ( $\nu_{\text{C=O}}$ ), 1396, 1149.

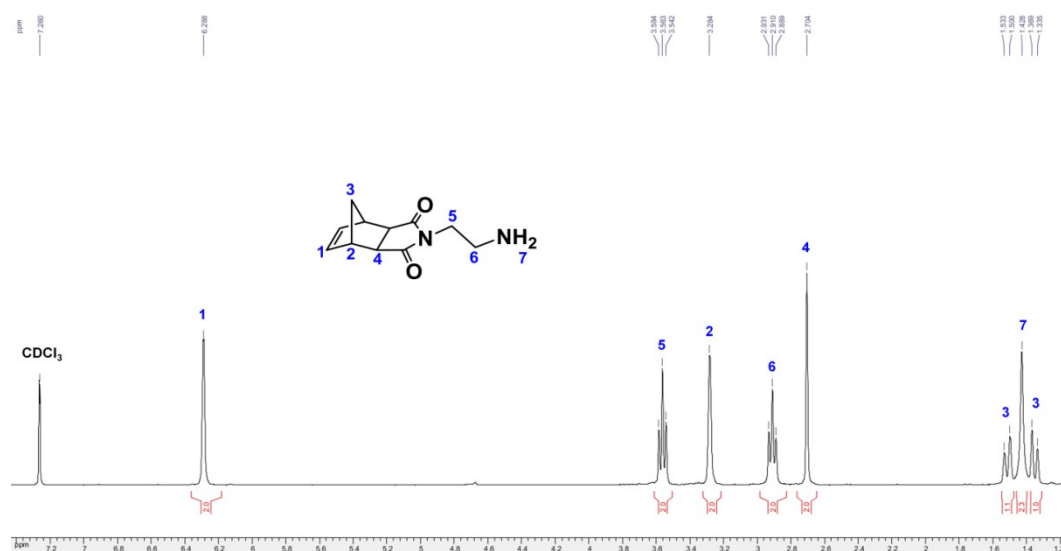


Figure S3.  $^1\text{H}$  NMR (400 MHz) spectrum of **3** in  $\text{CDCl}_3$ .

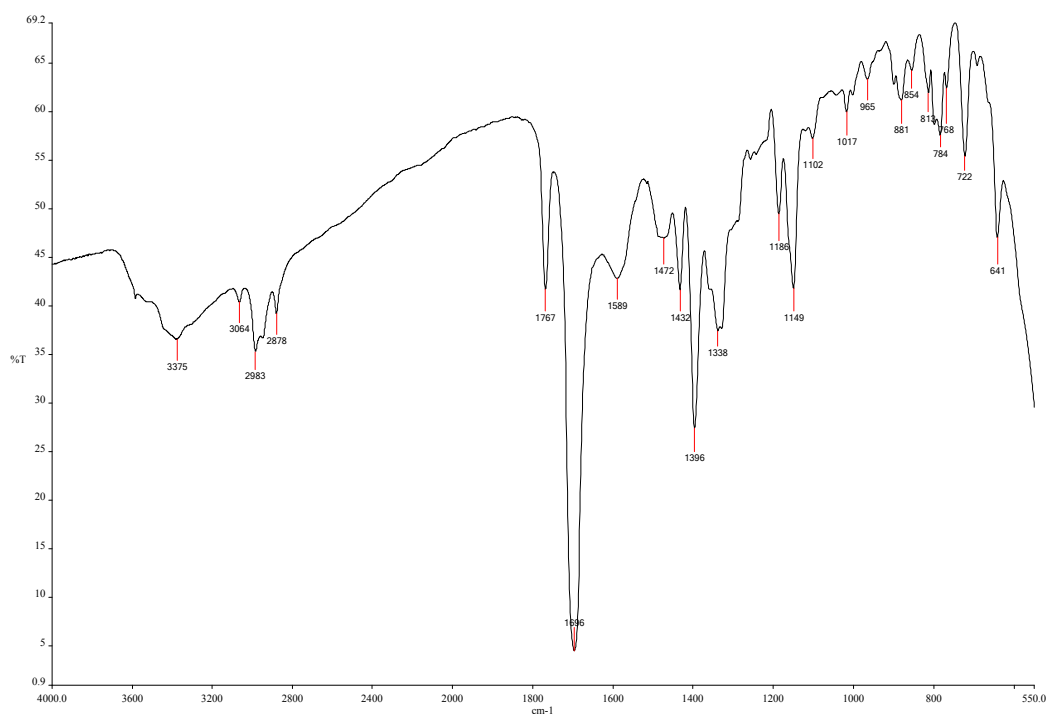


Figure S4. IR spectrum of **3**.

**2.2 Synthesis of NFc:** Triethylamine ( $\text{Et}_3\text{N}$ , 0.1 ml, 0.72 mmol) was injected dropwise into the  $\text{CH}_2\text{Cl}_2$  (40 ml) suspension of carboxylferrocene **2** (0.5 g, 2.17 mmol) at  $0^\circ\text{C}$  under  $\text{N}_2$  atmosphere. Oxalyl chloride (0.7 ml, 8.2 mmol) was then added dropwise into the solution. The reaction mixture was stirred at r. t. overnight. Next day, the solvent was removed *in vacuo*, and the residue red solid, crude chlorocarbonyl ferrocene **4**, was then dissolved in dry  $\text{CH}_2\text{Cl}_2$  (20 ml), added dropwise into the  $\text{CH}_2\text{Cl}_2$  solution (10 ml) of **3** (0.38 g, 1.85 mmol) and  $\text{Et}_3\text{N}$  (1.5 ml, 10.7 mmol). The obtained mixture was further stirred overnight at r. t. under  $\text{N}_2$  atmosphere, and then washed successively with saturated  $\text{NaHCO}_3$  solution ( $1 \times 100$  ml) and distilled water ( $3 \times 100$  ml). The organic layer was dried with anhydrous  $\text{Na}_2\text{SO}_4$ , and vacuumed to afford crude product **NFc** that was then purified by column chromatography with  $\text{CH}_2\text{Cl}_2$ /methanol (0% $\rightarrow$ 10%)

as the eluent and obtained as yellow-brown solid. Yield: 0.66 g, 85%.  $^1\text{H}$  NMR (400 MHz,  $\text{CDCl}_3$ , 25 °C, TMS),  $\delta_{\text{ppm}}$ : 6.39 (s, 1H, NHCO), 6.29 (t,  $J = 3.3$  Hz, 2H, CH=CH), 4.66 (t,  $J = 3.4$  Hz, 2H, sub. Cp), Cp, Cp =  $\eta^5\text{-C}_5\text{H}_5$ , 4.33 (t,  $J = 3.1$  Hz, 2H, sub. Cp), 4.19 (s, 5H, free Cp), 3.80-3.76 (m, 2H,  $\text{CH}_2\text{NH}$ ), 3.60-3.54 (m, 2H,  $\text{CONCH}_2$ ), 3.29 (t,  $J = 3.0$  Hz, 2H, =CH-CH), 2.75 (d,  $J = 1.0$  Hz, 2H, CO-CH), 1.52 (d,  $J = 9.8$  Hz, 1H,  $\text{CH}_2$ -bridge), 1.22 (d,  $J = 10.0$  Hz, 1H,  $\text{CH}_2$ -bridge).  $^{13}\text{C}$  NMR (100 MHz,  $\text{CDCl}_3$ , 25 °C, TMS),  $\delta_{\text{ppm}}$ : 178.9 (CON), 170.9 (CONH), 70.6, 70.4, 69.9, 68.3 (Cp), 48.1 (CO-CH), 45.4 (=CH-CH), 42.9 ( $\text{CH}_2$ -bridge), 39.8 ( $\text{CH}_2$ ), 38.2 ( $\text{CH}_2$ ). MS (ESI,  $m/z$ ), calcd. for  $\text{C}_{22}\text{H}_{22}\text{FeN}_2\text{O}_3$ : 418.27; found: 419.1(M+H<sup>+</sup>), 441.1 (M + Na<sup>+</sup>), 859.2 (2M + Na<sup>+</sup>). Selected IR (KBr,  $\text{cm}^{-1}$ ): 3348 ( $\nu_{\text{NH}}$ ), 2985, 2879 ( $\nu_{\text{CH}_2}$ ), 1769 ( $\nu_{\text{C=O}}$  of NHCO), 1694 ( $\nu_{\text{C=O}}$  of NCO), 1640, 1533, 1433 ( $\nu_{\text{C=C}}$  of Cp), 1395, 1296 ( $\nu_{\text{C-N}}$ ), 1183, 1106, 1002, 821 ( $\nu_{\text{FeII}}$ ).

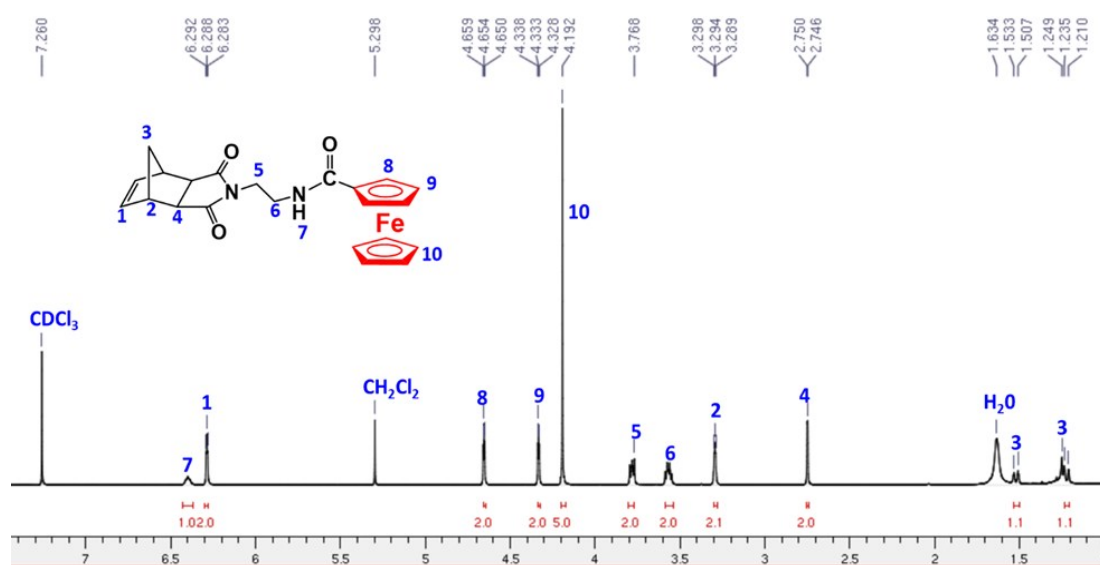


Figure S5.  $^1\text{H}$  NMR (400 MHz) spectrum of **NfC** in  $\text{CDCl}_3$ .

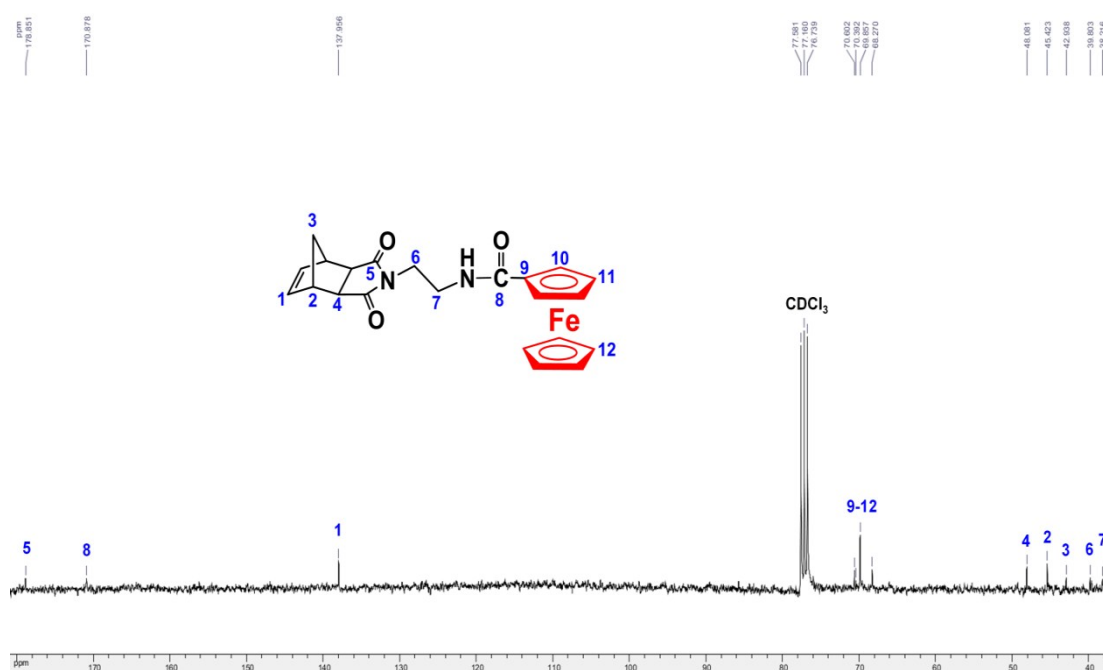
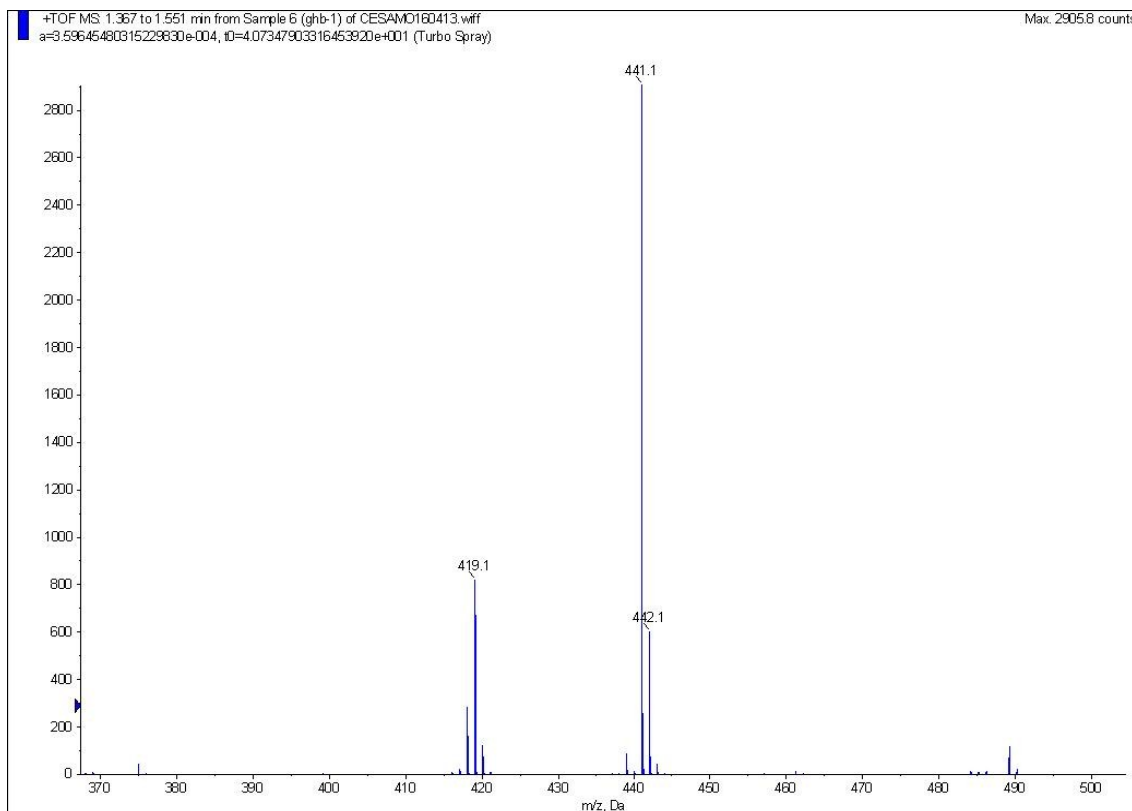
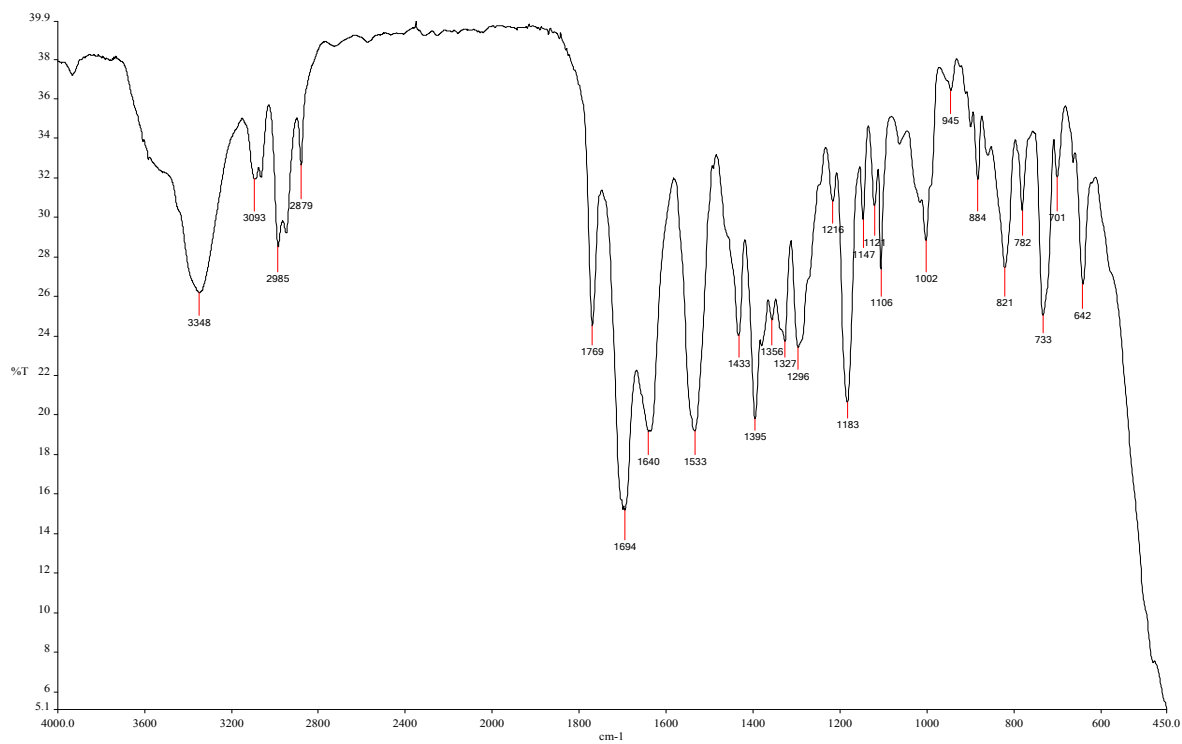


Figure S6.  $^{13}\text{C}$  NMR (100 MHz) spectrum of **NfC** in  $\text{CDCl}_3$ .



**Figure S7.** ESI mass spectrum of NfC.



**Figure S8.** IR spectrum of NfC.

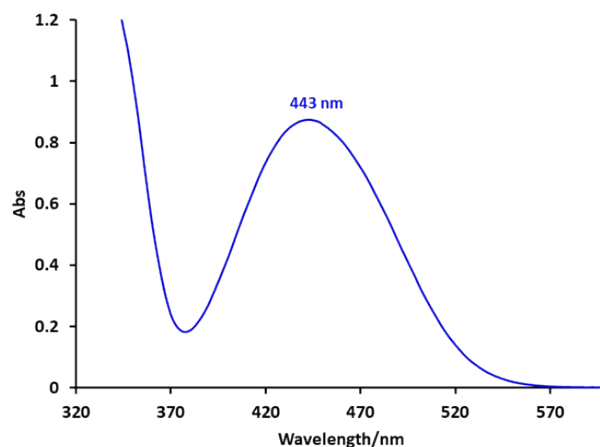


**Figure S9.** Uv-vis spectrum of **NFc** in  $\text{CH}_2\text{Cl}_2$ .

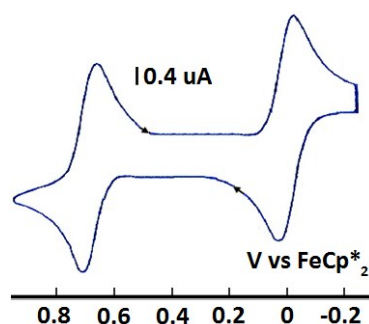
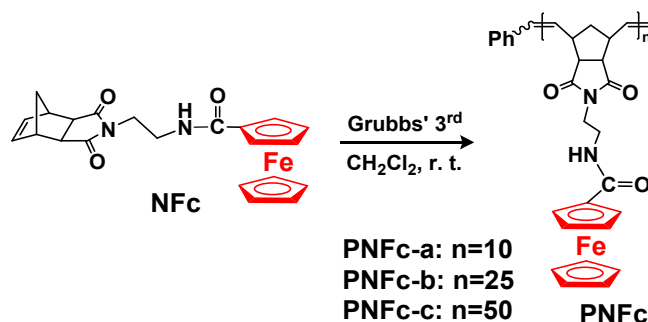


**Figure S10.** CV curve of monomer **NFc** in  $\text{CH}_2\text{Cl}_2$ . Internal reference,  $\text{FeCp}^*_2$ ; reference electrode, Ag; working and counter electrodes, Pt; scan rate,  $0.4 \text{ mV s}^{-1}$ ; supporting electrolyte,  $[\text{n-Bu}_4\text{N}][\text{PF}_6]$ . The wave at 0.0 V is that of the reference [ $\text{FeCp}^*_2$ ].  $\text{Fe}^{\text{III/II}}$  oxidation potential is 0.672 V.

### 3. ROMP synthesis of homopolymer PNFc



**Scheme S3.** Synthesis of homopolymer **PNFc**

**3.1. General synthetic procedure:** The desired amount of Grubbs' 3<sup>rd</sup> was dissolved by a minimum amount of dry  $\text{CH}_2\text{Cl}_2$  in a small Schlenk flask under  $\text{N}_2$  atmosphere. A known amount of monomer **NFc** in dry  $\text{CH}_2\text{Cl}_2$  (1 ml per 100 mg of monomer **NFc**) was added to the catalyst

solution under N<sub>2</sub> atmosphere with vigorous stirring. The obtained reaction mixture was stirred vigorously until the signal of olefinic protons of monomer **NFc** at 6.29 ppm disappeared by checking *in situ* <sup>1</sup>H NMR of reaction mixture, which indicated the monomer conversion reached 100%. Then, 0.3 ml of ethyl vinyl ether (EVE) was added to quench the catalyst. All the samples were collected, purified by precipitating from CH<sub>2</sub>Cl<sub>2</sub> with Et<sub>2</sub>O three times, and dried *in vacuo* until constant weight to get the polymer **PNFc** as a yellow-brown powder. Yield: 95% (**PNFc-a**), 96% (**PNFc-b**) and 96% (**PNFc-c**). <sup>1</sup>H NMR (400 MHz, (CD<sub>3</sub>)<sub>2</sub>SO, 25 °C, TMS) δ<sub>ppm</sub>: 7.83 (s, 1H, NHCO), 5.59 (m, 2H, =CH), 4.69 (s, 2H, sub. Cp), 4.30 (s, 2H, sub. Cp), 4.15 (d, *J* = 4.2 Hz, 6H, free Cp), 3.47 (s, 2H, CONH<sub>2</sub>), 3.39 (m, 2H, =C-CH), 2.94 (m, 4H, CH<sub>2</sub>NH<sub>2</sub> and CHCO), 1.92 (s, 1H, CH<sub>2</sub>-bridge), 1.41 (s, 1H, CH<sub>2</sub>-bridge). <sup>13</sup>C NMR (100 MHz, (CD<sub>3</sub>)<sub>2</sub>SO, 25 °C, TMS) δ<sub>ppm</sub>: 178.1 (CON), 169.3 (NHCO), 131.6 (CH-CH), 76.6 (Cp), 69.8 (Cp), 68.1 (Cp), 68.9 (Cp), 51.7 (CHCO), 50.6 (CH<sub>2</sub>-bridge), 44.2 (=C-CH), 38.4 (CONCH<sub>2</sub>), 36.3 (CH<sub>2</sub>NH). Selected IR (KBr, cm<sup>-1</sup>): 3446 (ν<sub>NH</sub>), 2923 (ν<sub>CH2</sub>), 1769 (ν<sub>C=O</sub> of NHCO), 1694 (ν<sub>C=O</sub> of NCO), 1633, 1536, 1433 (ν<sub>C=C</sub> of Cp), 1397, 1330 (ν<sub>C-N</sub>), 1178, 1105, 1002, 820 (ν<sub>FeII</sub>).

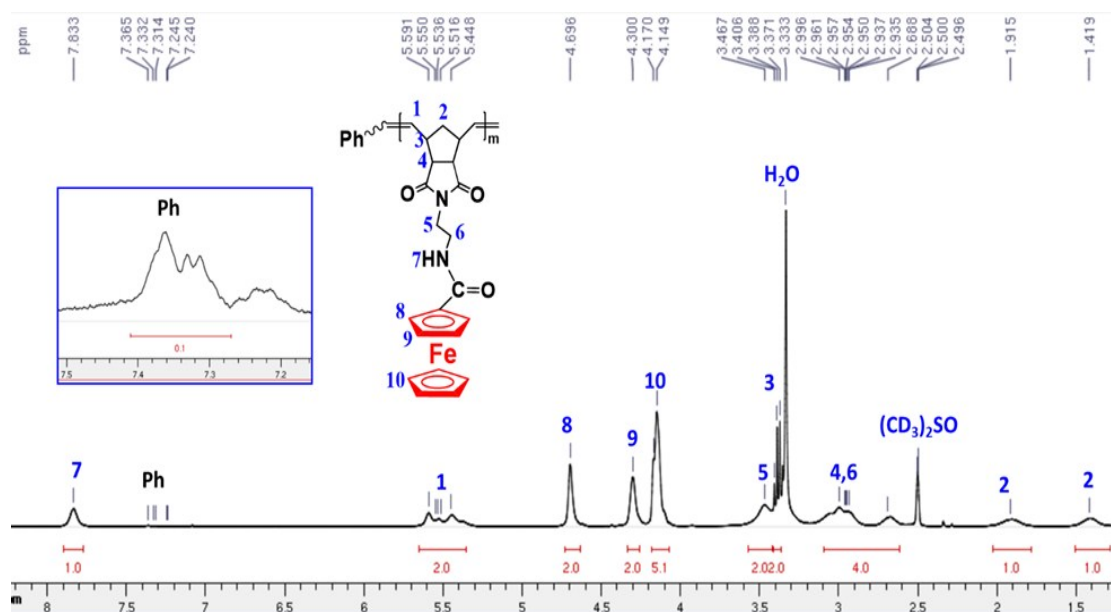
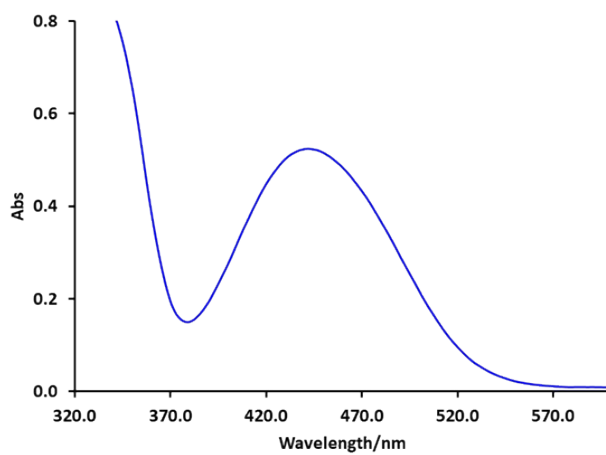
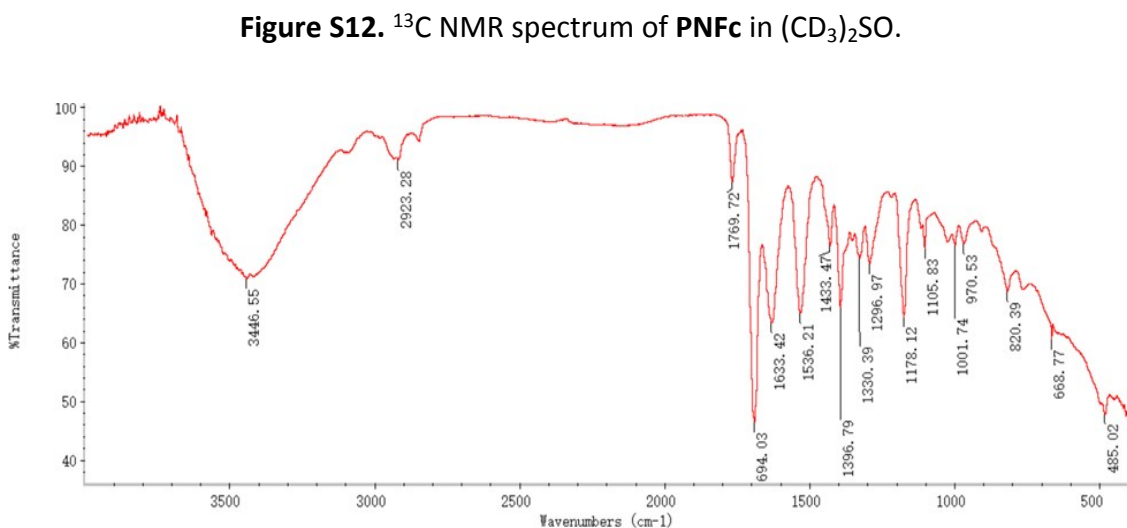
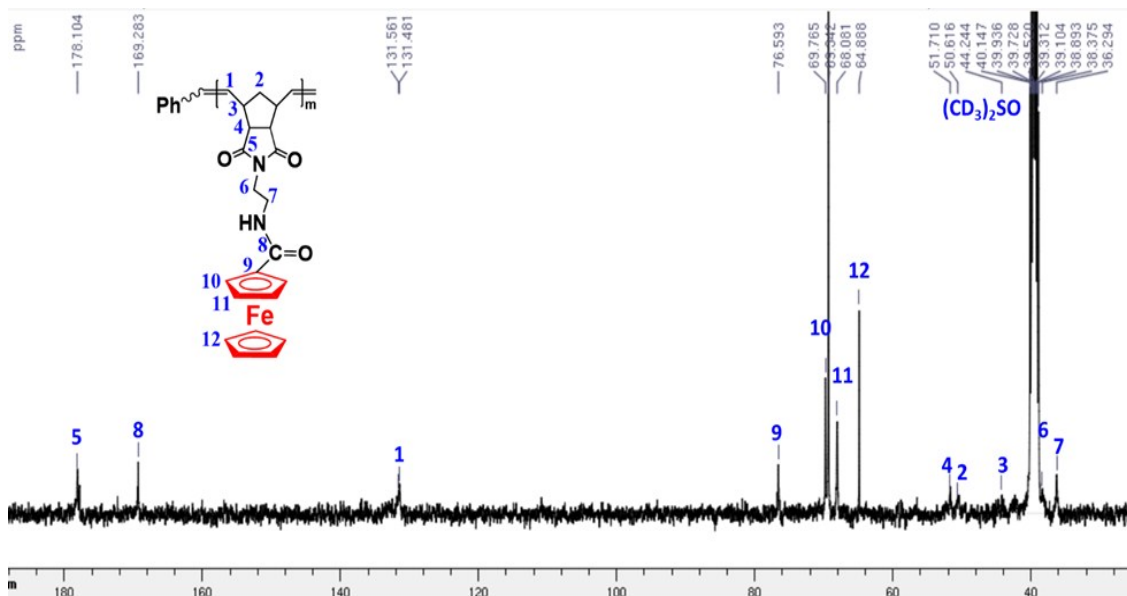
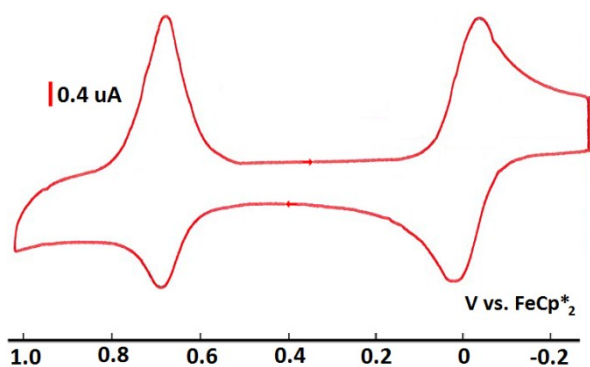
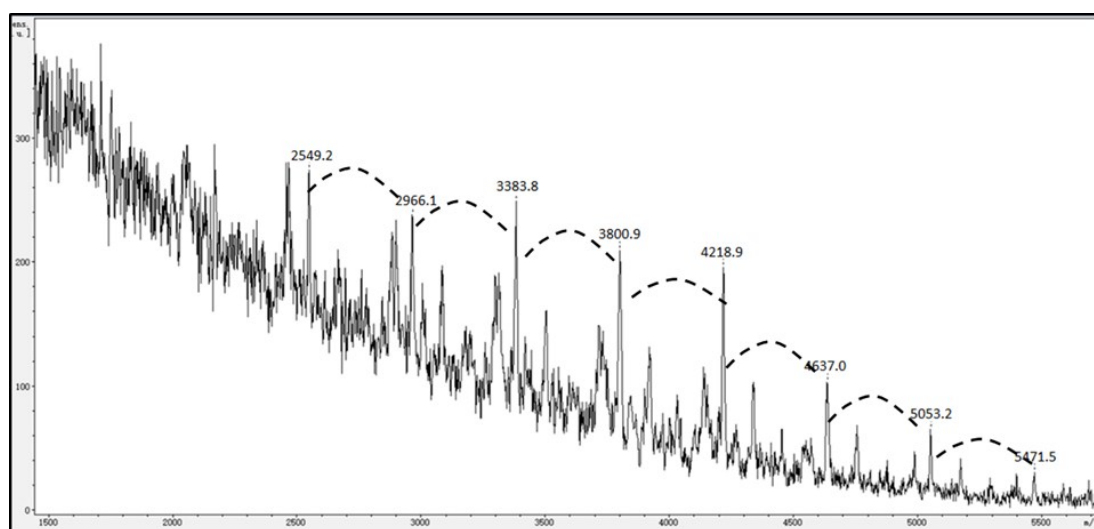


Figure S11. <sup>1</sup>H NMR spectrum of **PNFc** in (CD<sub>3</sub>)<sub>2</sub>SO.





**Figure S15.** CV curve of polymer **PNFc** in  $\text{CH}_2\text{Cl}_2$ . Internal reference,  $\text{FeCp}^*_2$ ; reference electrode, Ag; working and counter electrodes, Pt; scan rate,  $0.4 \text{ mV s}^{-1}$ ; supporting electrolyte,  $[\text{n-Bu}_4\text{N}][\text{PF}_6]$ . The wave at 0.0 V is that of the reference  $[\text{FeCp}^*_2]$ .  $\text{Fe}^{\text{III/II}}$  oxidation potential is 0.675 V.



**Figure S16.** MALDI-TOF MS spectrum of polymer **PNFc-c** at the region of 1500-6000 Da. The polymerization degree is 50. The black dotted lines correspond to the difference between molecular peaks of a value of  $418.26 \pm 1 \text{ Da}$  (MW of monomer **NFc**).

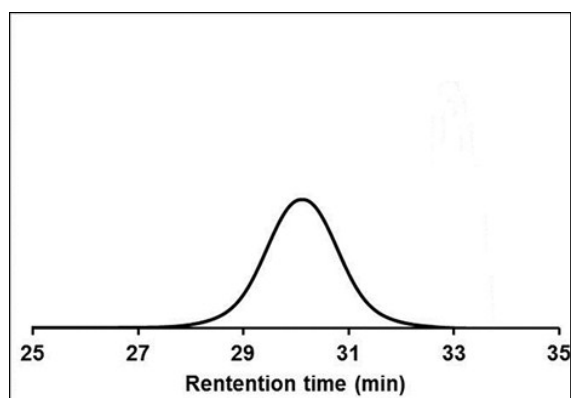


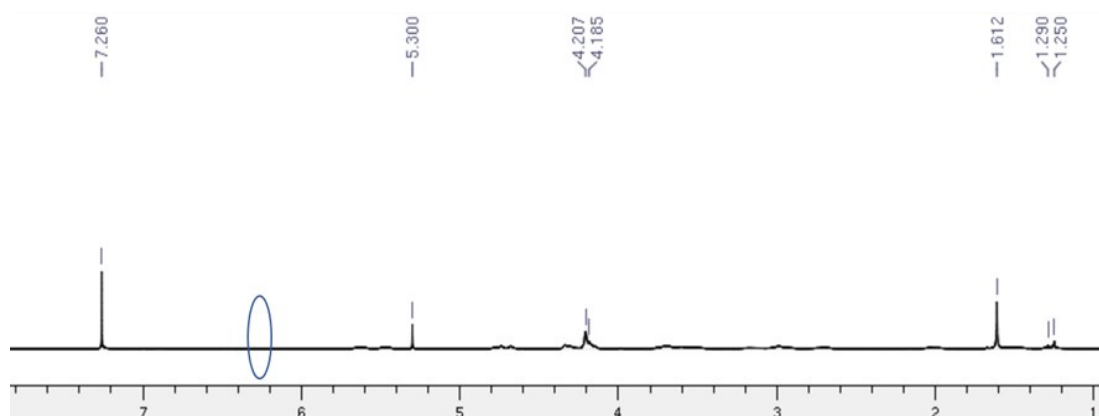
**Figure S17.** GPC curve of **PNFc-a** in DMF.

**Table S1.** Molecular weight data of polymers **PNFc-a** by GPC in DMF (PS standard)

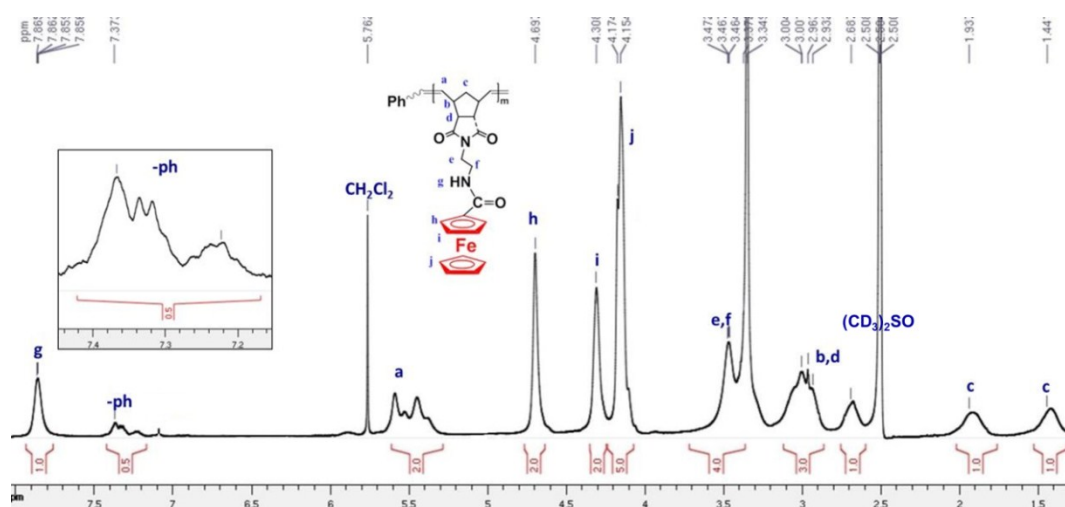
Polymers	$M_p$	$M_n$	$M_w$	$M_z$	$M_{z+1}$	$M_w/M_n$
<b>PNFc-a</b>	8534	8196	8814	9469	10152	1.07

### 3.2 Kinetic study for the synthesis of Polymer **PNFc-c**:

In order to determine when the ROMP of monomer **NFc** was completed at a feed mole ratio of 50:1, a kinetic study was conducted as follows: monomer **NFc** (26.52 mg, 0.0634 mmol, 50 equiv) in 0.3 ml dry  $\text{CH}_2\text{Cl}_2$  was added into the solution of Grubbs 3<sup>rd</sup> (1.12 mg, 0.00127 mmol, 1 equiv) in 0.2 ml dry  $\text{CH}_2\text{Cl}_2$ . The reaction mixture was vigorously stirred at r. t. under  $\text{N}_2$  atmosphere. After 5 min, 0.02 ml of samples were removed and quenched with 0.01 ml of EVE. The *in situ*  $^1\text{H}$  NMR analysis in  $\text{CDCl}_3$  of the dried reaction mixture was conducted. The monomer conversion was deemed to be 100% when the signal of the olefin protons for monomer **NFc** at 6.29 ppm disappeared.

**Figure S18.**  $^1\text{H}$  NMR spectrum of the reaction mixture in  $\text{CDCl}_3$  for the synthesis of **PNFc-c** after the addition of **NFc** with further 5 min of stirring.

### 3.3. Calculation of polymer degree of **PNFc-a** by $^1\text{H}$ NMR end-group analysis

**Figure S19.**  $^1\text{H}$  NMR spectrum of **PNFc-a** in  $(\text{CD}_3)_2\text{SO}$ .

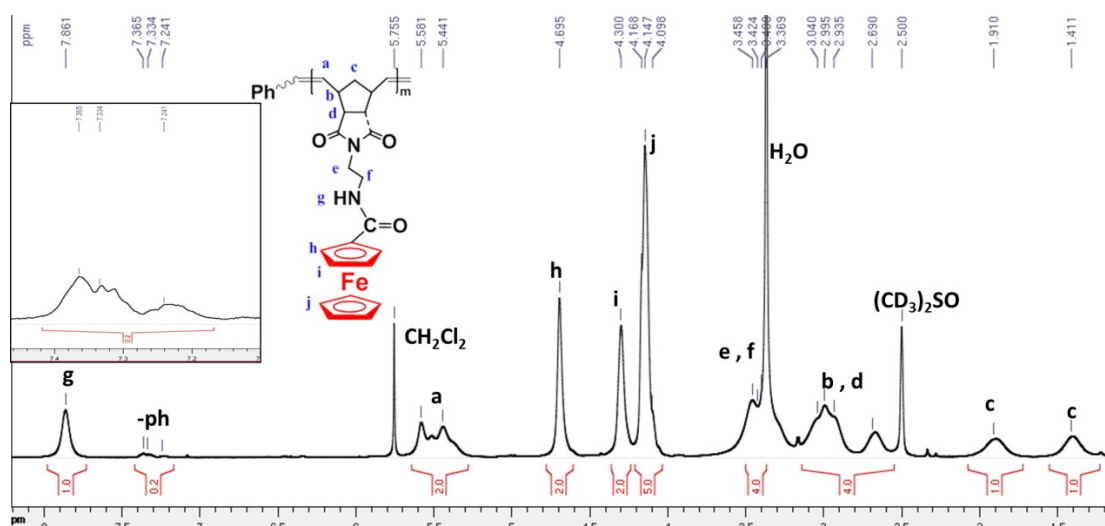
**Table S2.** Polymer degree of **PNFc-a** calculated by using its  $^1\text{H}$  NMR spectrum in  $(\text{CD}_3)_2\text{SO}^a$ 

Proton peak	End-ph	NHCO	Olefinic	Sub. Cp	Sub. Cp	Free Cp
$\delta_{\text{ppm}}$	7.22-7.37	7.86	5.59 and 5.45	4.69	4.30	4.15
Integra	0.5	1	2	2	2	5
$n_{p1a}^b$	1	9.67-10.0	10.0-10.28	9.98-10.09	10.03-10.12	9.88-10.42
$n_{p1b}^c$	$10 \pm 0.4$					

<sup>a</sup> **Figure S19** is used for the calculation of polymer degree of **PNFc-a**. <sup>b</sup> Calculated polymer degrees based on integral of each peak. <sup>c</sup> Average polymer degree according to  $n_{p1a}$  values.

As shown in **Table S2**, the  $^1\text{H}$  NMR end-group analysis provides the value of  $10 \pm 0.4$  for the polymer degree of **PNFc-a**. These calculations were conducted by comparing the intensities of the signals of the five protons of the end-phenyl group with those of characteristic protons in the homopolymer **PNFc-a**. Namely, the proton integration for end-phenyl group (7.22-7.37 ppm) was compared with those of the proton of acylamino (7.86 ppm), olefin protons (5.59 and 5.45 ppm), and Fc group (4.69, 4.30 and 4.15 ppm), respectively. The obtained values are 9.67-10.00, 10.0-10.28, 9.98-10.09, 10.03-10.12 and 9.88-10.42, respectively. Thus, the average value of the polymer degree is  $10 \pm 0.4$ . The error is due to the integration error on each signal.

### 3.4. Calculation of polymer degree of **PNFc-b** by $^1\text{H}$ NMR end-group analysis

**Figure S20.**  $^1\text{H}$  NMR spectrum of **PNFc-b** in  $(\text{CD}_3)_2\text{SO}$ .

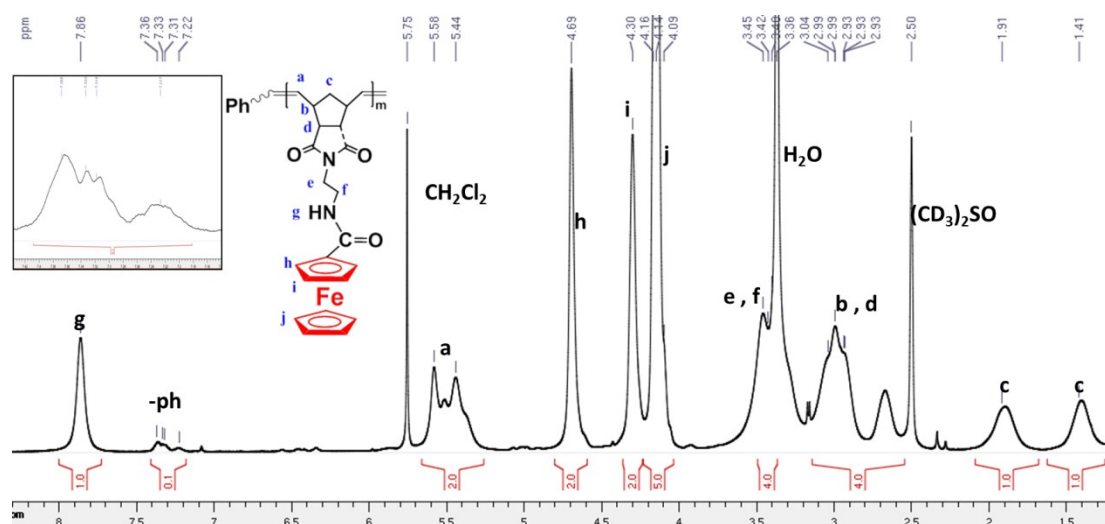
**Table S3.** Polymer degree of **PNFc-b** calculated by using its  $^1\text{H}$  NMR spectrum in  $(\text{CD}_3)_2\text{SO}^a$ 

Proton peak	End-ph	NHCO	Olefinic	Sub. Cp	Sub. Cp	Free Cp
$\delta_{\text{ppm}}$	7.22-7.37	7.86	5.59 and 5.45	4.69	4.30	4.15
Integra.	0.2	1	2	2	2	5
$n_{\text{p1a}}^b$	1	24-26	23-25	24-25	24-25	25-27
$n_{\text{p1b}}^c$	$25 \pm 2$					

<sup>a</sup> **Figure S20** is used for the calculation of polymer degree of **PNFc-b**. <sup>b</sup> Calculated polymer degrees based on integral of each peak. <sup>c</sup> Average polymer degree according to  $n_{\text{p1a}}$  values.

As shown in **Table S3**, the  $^1\text{H}$  NMR end-group analysis provides the value of  $25 \pm 2$  for the polymer degree of **PNFc-b**. These calculations were conducted by comparing the intensities of the signals of the five protons of the end-phenyl group with those of characteristic protons in the homopolymer **PNFc-b**. Namely, the proton integration for end-phenyl group (7.22-7.37 ppm) was compared with those of the proton of acylamino (7.86 ppm), olefin protons (5.59 and 5.45 ppm), and Fc group (4.69, 4.30 and 4.15 ppm), respectively. The obtained values are 24-26, 23-25, 24-25 and 24-25, respectively. Thus, the average value of the polymer degree is  $25 \pm 2$ . The error is due to the integration error on each signal.

### 3.5. Calculation of polymer degree of **PNFc-c** by $^1\text{H}$ NMR end-group analysis

**Figure S21.**  $^1\text{H}$  NMR spectrum of **PNFc-c** in  $(\text{CD}_3)_2\text{SO}$ .

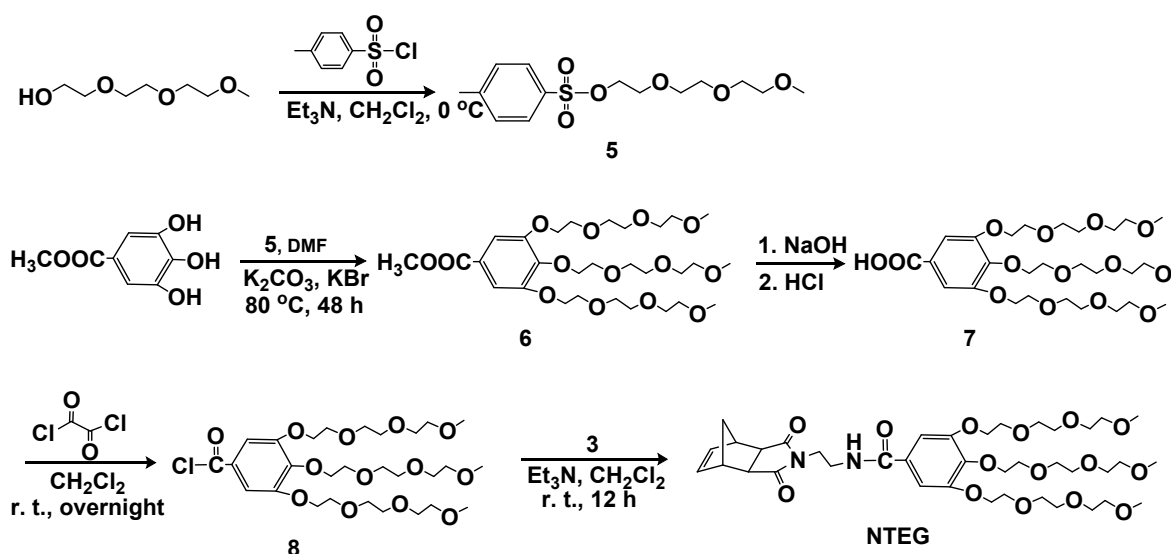
**Table S4.** Polymer degree of **PNFc-c** calculated by using its  $^1\text{H}$  NMR spectrum in  $(\text{CD}_3)_2\text{SO}^a$ 

Proton peak	End-ph	NHCO	Olefinic	Sub. Cp	Sub. Cp	Free Cp
$\delta_{\text{ppm}}$	7.22-7.37	7.86	5.59 and 5.45	4.69	4.30	4.15
Integra.	0.1	0.98-1.02	1.88-2.01	1.93-2.06	1.91-2.1	4.88-5.15
$n_{\text{p1a}}^b$	1	49-51	47-51	47-52	48-53	47-52
$n_{\text{p1b}}^c$	$50 \pm 3$					

<sup>a</sup> **Figure S21** is used for the calculation of polymer degree of **PNFc-c**. <sup>b</sup> Calculated polymer degrees based on integral of each peak. <sup>c</sup> Average polymer degree according to the obtained  $n_{\text{p1a}}$  values.

As shown in **Table S4**, the  $^1\text{H}$  NMR end-group analysis provides the value of  $50 \pm 3$  for the polymer degree of **PNFc-c**. These calculations were conducted by comparing the intensities of the signals of the five protons of the end-phenyl group with those of characteristic protons in the homopolymer **PNFc-c**. Namely, the proton integration for end-phenyl group (7.22-7.37 ppm) was compared with those of the proton of acylamino (7.86 ppm), olefin protons (5.59 and 5.45 ppm), and Fc group (4.69, 4.30 and 4.15 ppm), respectively. The obtained values are 49-51, 47-51, 47-52, 48-53 and 47-52, respectively. Thus, the average value of the polymer degree is  $50 \pm 3$ . The error is due to the integration error on each signal.

#### 4. Synthesis of monomer NTEG



**4.1. Synthesis of 5<sup>[S3]</sup>:** Tosyl chloride (40.2 g, 210 mmol, 1 equiv) in dry CH<sub>2</sub>Cl<sub>2</sub> (100 ml) was added dropwise into the CH<sub>2</sub>Cl<sub>2</sub> solution (100 ml) of triethylene glycol mono methyl ether (33 ml, 210 mmol, 1 equiv) and Et<sub>3</sub>N (43.5 ml, 315 mmol, 1.5 equiv) at 0 °C. The obtained reaction mixture was stirred for 2 h at 0 °C under N<sub>2</sub> atmosphere, and further at r. t. for 30 min. Then Et<sub>2</sub>O (100 ml) was added into the mixture, and the resulting precipitate was removed by suction filtration. The filtrate was collected, vacuumed to dryness. The residue was purified by column chromatography with Et<sub>2</sub>O as eluent to afford **5** as colorless oil. Yield: 48.9 g, 73%. <sup>1</sup>H NMR (400 MHz, CDCl<sub>3</sub>, 25 °C, TMS), δ<sub>ppm</sub>: 2.40 (s, 3H, CH<sub>3</sub>), 3.32 (s, 3H, OCH<sub>3</sub>), 3.46-3.65 (m, 10H, 5 × CH<sub>2</sub>), 4.10 (t, 2H, CH<sub>2</sub>OSO<sub>2</sub>), 7.30 (d, 2H, ph), 7.74 (d, 2H, ph).

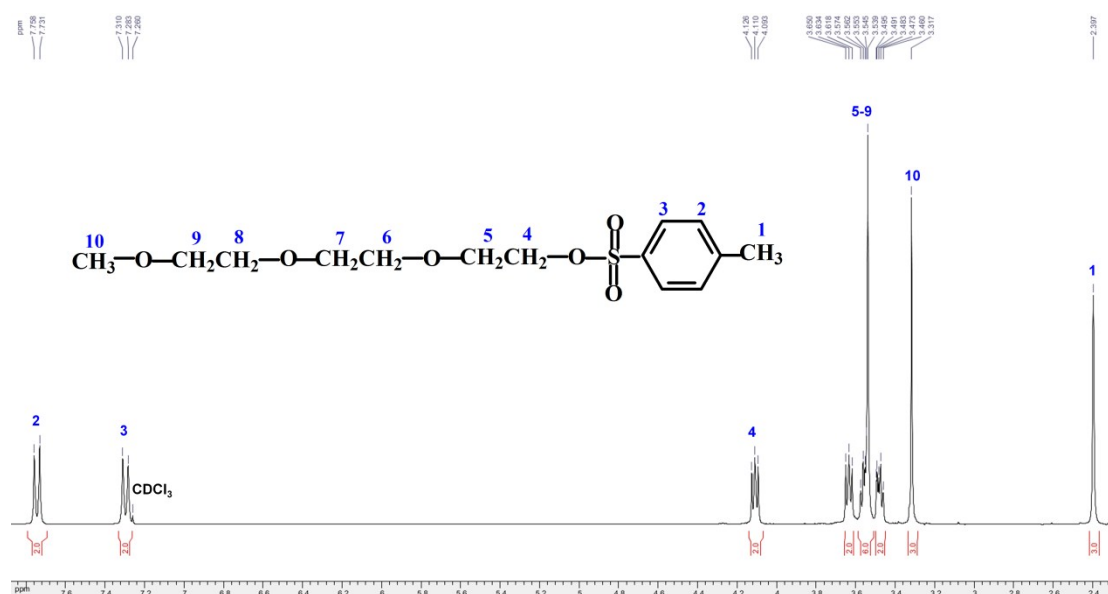


**Figure S22.** <sup>1</sup>H NMR (400 MHz) spectrum of **5** in CDCl<sub>3</sub>.

**4.2. Synthesis of 6<sup>[S4]</sup>:** Compound **5** (14.88 g, 0.048 mol), methyl gallate (2.55 g, 13.761 mmol), K<sub>2</sub>CO<sub>3</sub> (19.02 g, 0.138 mol), a little KBr as catalyst and DMF (80 ml) were added together into a small Schlenk flask, and the obtained mixture was refluxed for 48 h at 80 °C under N<sub>2</sub> atmosphere. The final reaction mixture was diluted with a large amount of water (150 ml) and extracted with CH<sub>2</sub>Cl<sub>2</sub> (100 ml × 3). The organic layer was washed with water (100 ml × 5) and evaporated under vacuum. Purification was achieved by column chromatography with CH<sub>2</sub>Cl<sub>2</sub>/methanol (0%→30%) as eluent, and methyl 3,4,5-tris(2-(2-(2-methoxyethoxy)ethoxy)ethoxy)benzoate **6** was obtained as light-brown oil. Yield: 6.57 g, 76.8%. <sup>1</sup>H NMR (400 MHz, CDCl<sub>3</sub>, 25 °C, TMS), δ<sub>ppm</sub>: 7.29 (s, 2H, ph), 4.23-4.17 (m, 6H, ph-OCH<sub>2</sub>), 3.88 (s, 3H, CH<sub>3</sub>OOC), 3.88-3.52 (m, 30H, 3 × CH<sub>2</sub>OCH<sub>2</sub>CH<sub>2</sub>OCH<sub>2</sub>CH<sub>2</sub>), 3.37 (s, 9H, 3 × OCH<sub>3</sub>). <sup>13</sup>C NMR (100 MHz, CDCl<sub>3</sub>, 25 °C, TMS), δ<sub>ppm</sub>: 166.7 (COO), 152.4, 142.7, 125.1, 109.1 (ph), 72.5, 72.0, 70.9, 70.8, 70.7, 69.7, 68.9 (CH<sub>2</sub>O), 59.1(OCH<sub>3</sub>), 52.2 (OOCH<sub>3</sub>).



Figure S23.  $^1\text{H}$  NMR (400 MHz) spectrum of **6** in  $\text{CDCl}_3$ .

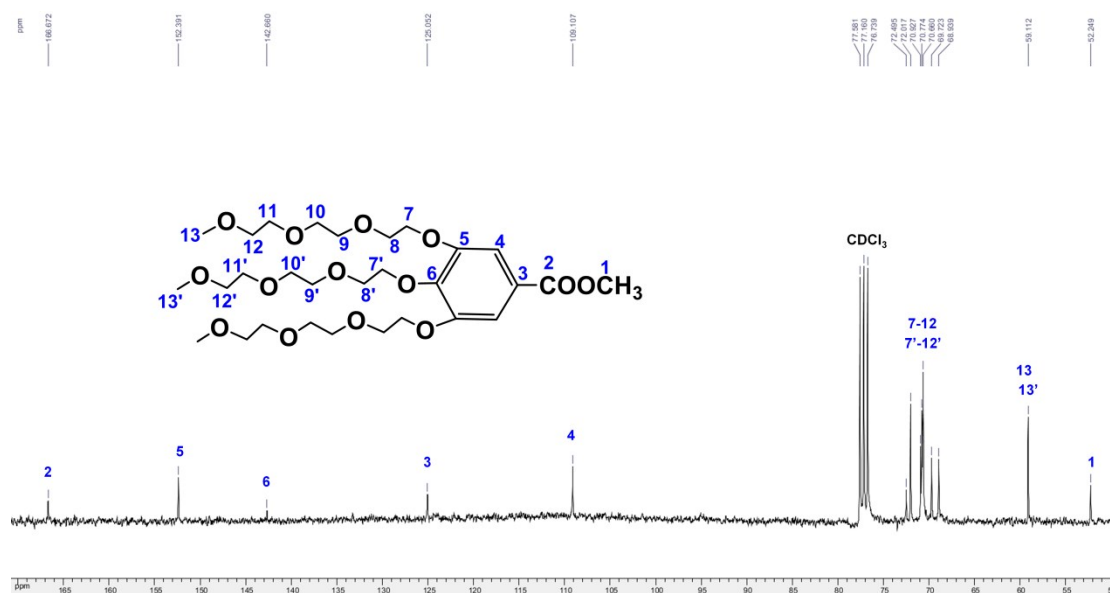


Figure S24.  $^{13}\text{C}$  NMR spectrum (100 MHz) of **6** in  $\text{CDCl}_3$ .

**4.3. Synthesis of 7<sup>[S4]</sup>:** **6** (6.53 g, 10.49 mmol, 1.0 equiv) and NaOH (3.15 g, 78.75 mmol, 7.5 equiv) were dissolved in 50 ml of distilled water, and refluxed at 110 °C for 4 h under  $\text{N}_2$  atmosphere. The reaction mixture was cooled to r. t., adjusted to pH 2.0-3.0 by adding concentrated HCl, and then extracted by  $\text{CH}_2\text{Cl}_2$  (100 ml  $\times$  3). The organic layers were combined, dried with anhydrous  $\text{Na}_2\text{SO}_4$ , vacuumed to dryness to get **7** as light-brown oil without further purification. Yield: 5.85 g, 91.5%.  $^1\text{H}$  NMR (400 MHz,  $\text{CDCl}_3$ , 25 °C, TMS),  $\delta_{\text{ppm}}$ : 7.35 (s, 2H, ph), 4.26-4.18 (m, 6H, ph- $\text{OCH}_2$ ), 3.88-3.52 (m, 30H,  $(\text{CH}_2\text{OCH}_2\text{CH}_2\text{OCH}_2\text{CH}_2)_3$ ), 3.37 and 3.37 (ds, 9H, 3  $\times$   $\text{OCH}_3$ ).  $^{13}\text{C}$  NMR (100 MHz,  $\text{CDCl}_3$ , 25 °C, TMS),  $\delta_{\text{ppm}}$ : 170.1 (COOH), 152.2, 142.8, 124.8, 109.4 (ph), 72.4, 71.9, 70.8, 70.7, 70.5, 69.6, 68.8 ( $\text{CH}_2\text{O}$ ), 59.0 ( $\text{OCH}_3$ ). MS (ESI,  $m/z$ ), calcd. for  $\text{C}_{28}\text{H}_{48}\text{O}_{14}$ : 608.7; found: 653.3 ( $\text{M} + 2\text{Na}^+$ ).

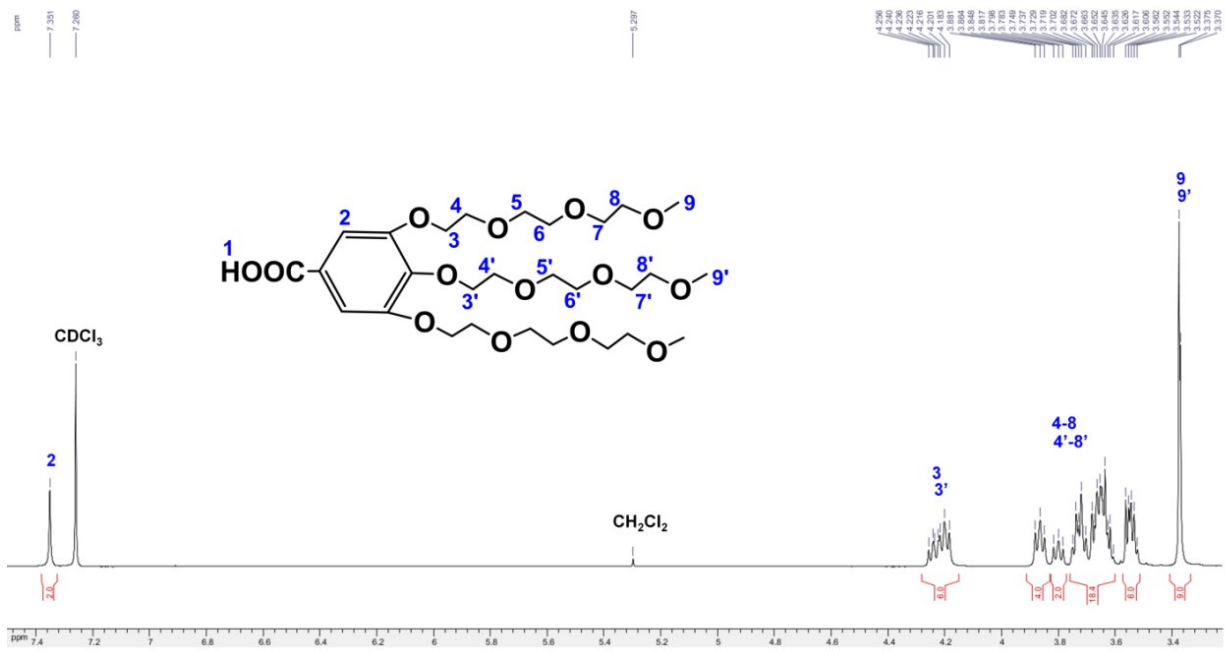


Figure S25. <sup>1</sup>H NMR (400 MHz) spectrum of **7** in CDCl<sub>3</sub>.

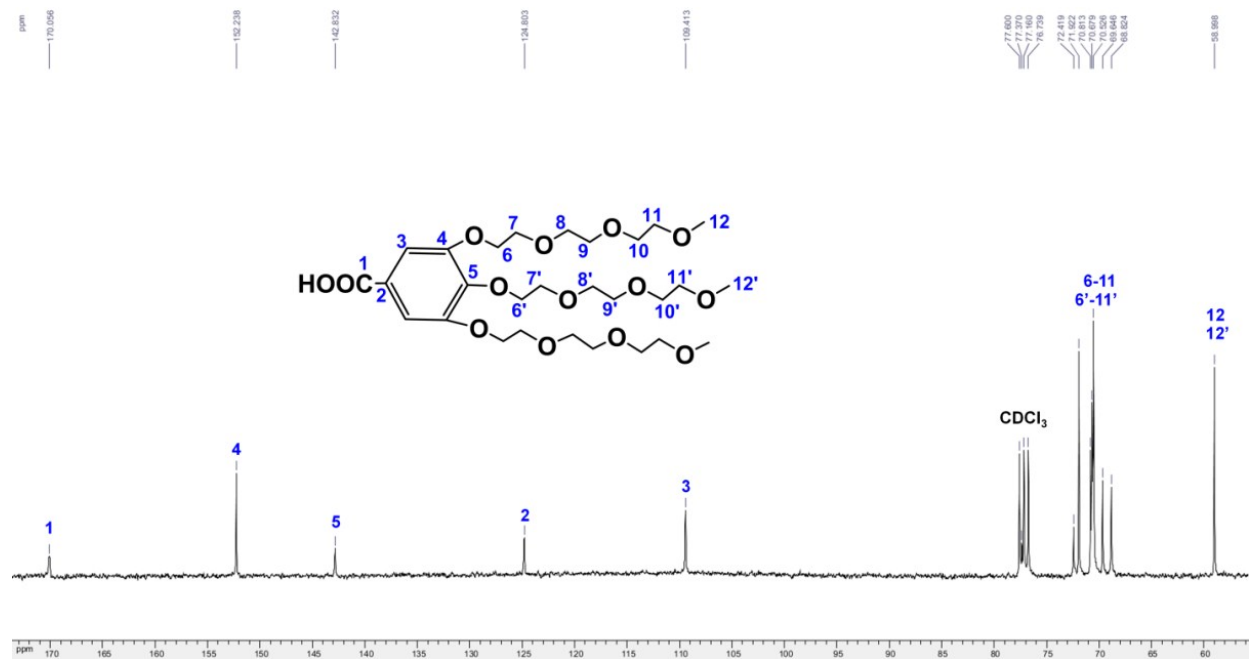
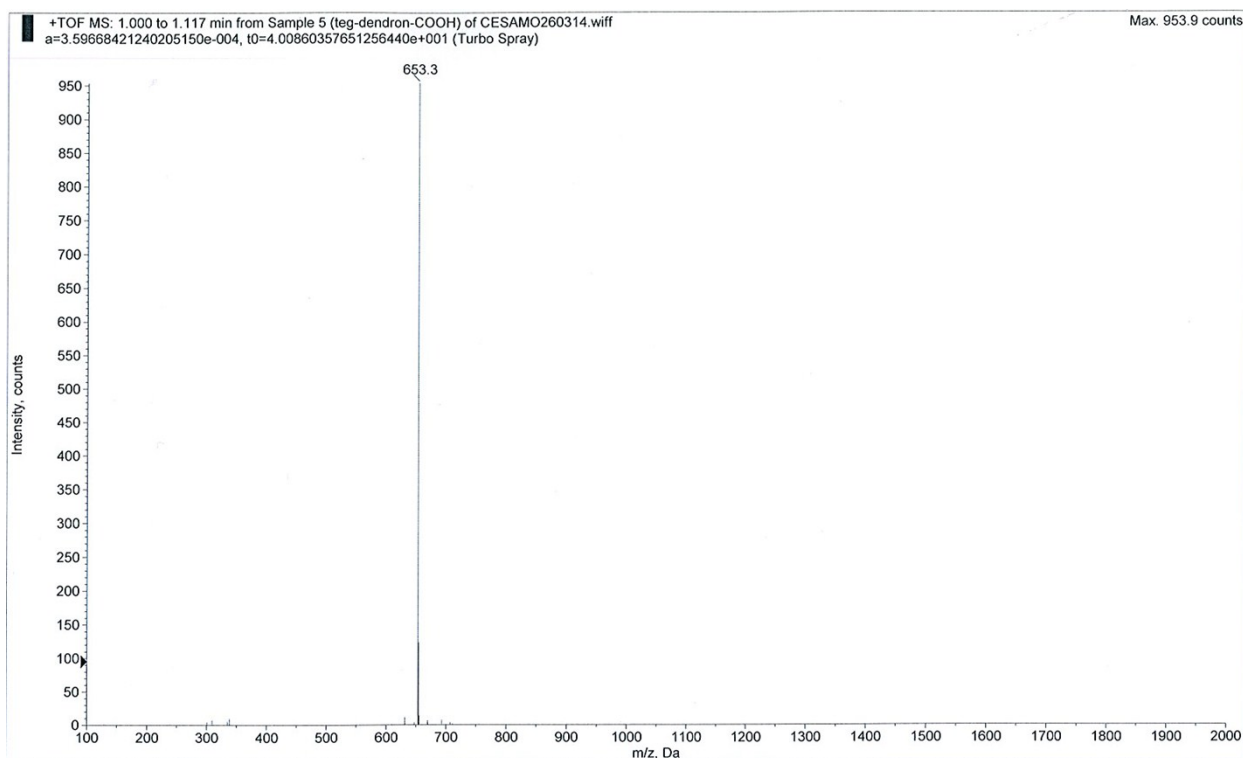


Figure S26. <sup>13</sup>C NMR (100 MHz) spectrum of **7** in CDCl<sub>3</sub>.



**Figure S27.** ESI Mass spectrum of **7**.

**4.4 Synthesis of NTEG**<sup>[S4]</sup>: To a solution of **7** (1.9 g, 3.12 mmol, 1 equiv) in dry CH<sub>2</sub>Cl<sub>2</sub> (25 ml) was added oxalyl dichloride (3.96 g, 31.2 mmol, 10 equiv) dropwise at 0 °C under N<sub>2</sub> atmosphere. The mixture was stirred overnight at r. t. under N<sub>2</sub> atmosphere. Then the mixture was concentrated to give crude **8** that was used in the next step without further purification. To a mixture of **3** (0.644 g, 3.12 mmol, 1 equiv) and Et<sub>3</sub>N (1.58 g, 2.2 ml, 15.6 mmol, 5 equiv) in dry CH<sub>2</sub>Cl<sub>2</sub> (15 ml) was added the crude **8** in dry CH<sub>2</sub>Cl<sub>2</sub> (20 ml) dropwise at 0 °C. The mixture was stirred at r. t. overnight, vacuumed to remove all the solvent and excess Et<sub>3</sub>N. The obtained dried residue was purified by column chromatography using CH<sub>2</sub>Cl<sub>2</sub>/methanol (50:1) as eluent to give monomer **NTEG** as colorless sticky oil. Yield: 1.9 g, 76.3%. <sup>1</sup>H NMR (400 MHz, CDCl<sub>3</sub>, 25 °C, TMS) δ<sub>ppm</sub>: 7.03 (s, 2H, phenyl), 6.93 (s, 1H, phenyl), 6.27 (t, *J* = 2.0 Hz, 2H, CH=CH), 4.23-4.18 (m, 6H, 3 × phenyl-OCH<sub>2</sub>), 3.88-3.52 (m, 34H, NCH<sub>2</sub>CH<sub>2</sub>N and 3 × CH<sub>2</sub>OCH<sub>2</sub>CH<sub>2</sub>OCH<sub>2</sub>CH<sub>2</sub>O), 3.37 and 3.36 (ds, 9H, 3 × OCH<sub>3</sub>), 3.23 (t, *J* = 1.5 Hz, 2H, =CH-CH), 2.71 (d, *J* = 0.8 Hz, 2H, CHCON), 1.46 (d, *J* = 9.6 Hz, 1H, CH<sub>2</sub>-bridge), 1.18 (d, *J* = 9.6 Hz, 1H, CH<sub>2</sub>-bridge). <sup>13</sup>C NMR (100 MHz, CDCl<sub>3</sub>, 25 °C, TMS) δ<sub>ppm</sub>: 177.6 (CON), 166.0 (CONH), 151.5 (ph), 140.2 (ph), 136.8 (CH=CH), 128.1 (ph), 105.6 (ph), 71.4, 70.9, 69.8, 69.7, 69.5, 68.7, 67.9 (OCH<sub>2</sub>), 58.0 (OCH<sub>3</sub>), 46.9 (CHCON), 44.2 (=CHCH), 41.8 (CH<sub>2</sub>-bridge), 38.6, 36.9 (NCH<sub>2</sub>CH<sub>2</sub>NH). MS (ESI *m/z*), calcd. for C<sub>39</sub>H<sub>60</sub>N<sub>2</sub>O<sub>15</sub>: 796.91; found: 797.41 [M + H<sup>+</sup>] and 819.39 [M + Na<sup>+</sup>]. Selected IR (KBr, cm<sup>-1</sup>): 3452 cm<sup>-1</sup> (ν<sub>NH</sub>), 2877 cm<sup>-1</sup> (ν<sub>CH2</sub>), 1769 cm<sup>-1</sup> (δ<sub>C=C</sub>), 1697 cm<sup>-1</sup> (δ<sub>NC=O</sub>), 1650 cm<sup>-1</sup> (δ<sub>NHC=O</sub>).

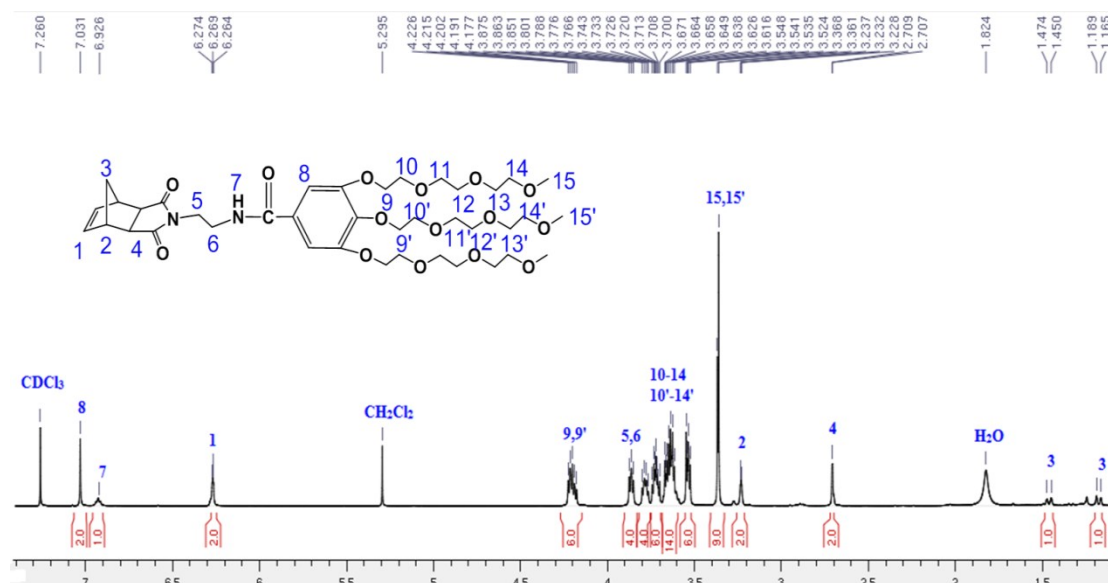
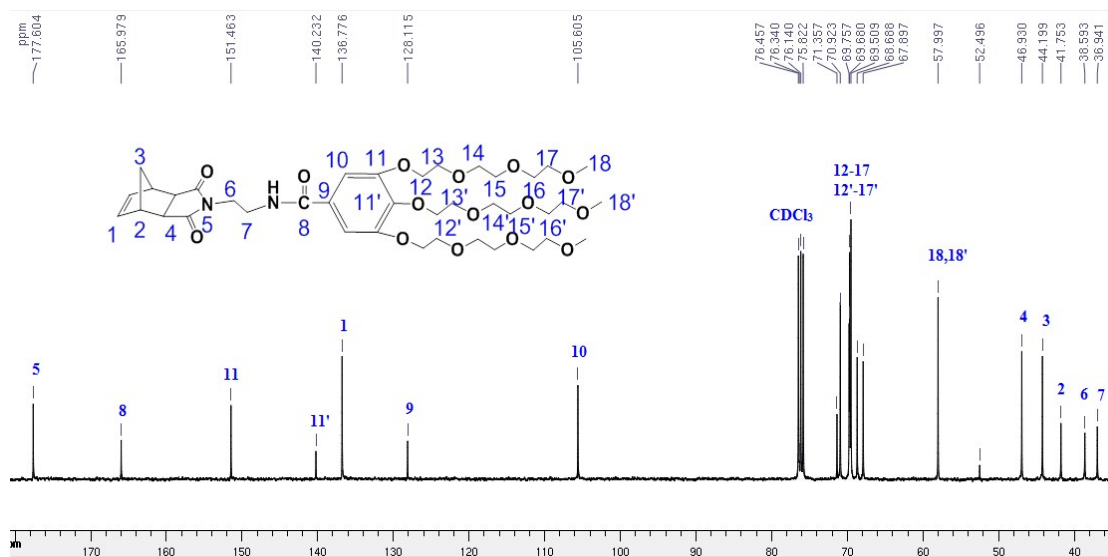


Figure S28. <sup>1</sup>H NMR (400 MHz) spectrum of NTEG in CDCl<sub>3</sub>.



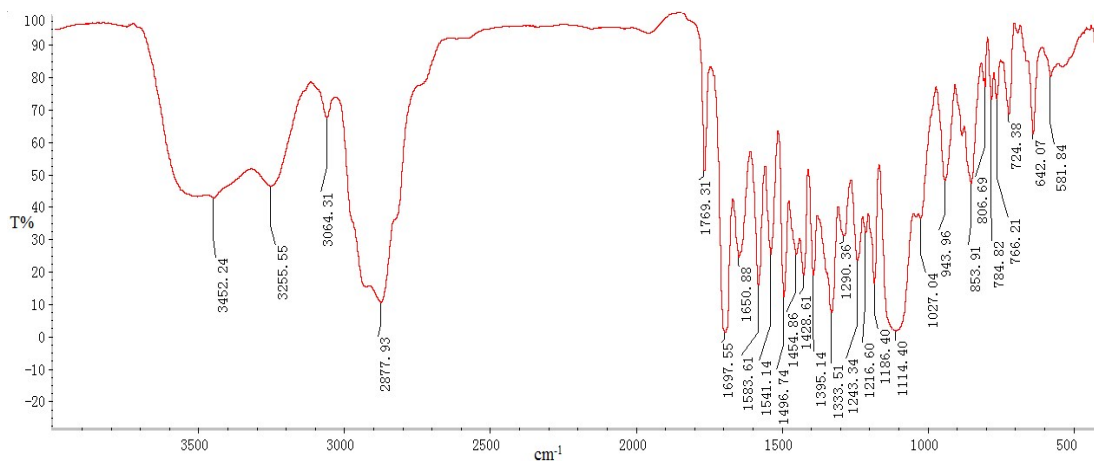
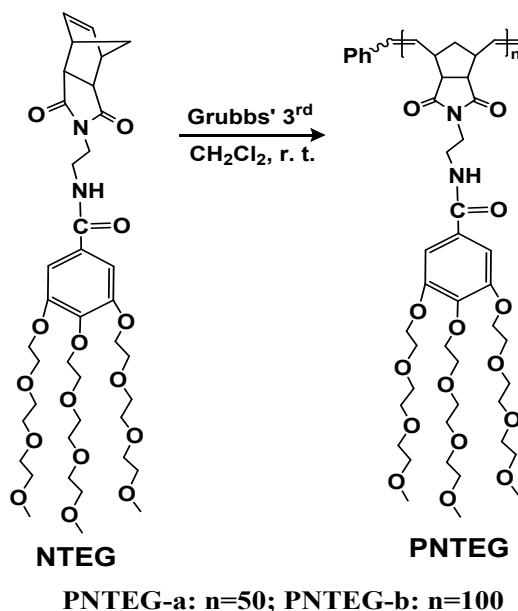


Figure S31. IR spectrum of NTEG.

## 5. Synthesis of homopolymer PNTEG



Scheme S5. Synthesis route of polymer PNTEG

**5.1. General Synthesis procedure of homopolymer PNTEG:** The desired amount of Grubbs' 3<sup>rd</sup> was dissolved by a minimum amount of dry CH<sub>2</sub>Cl<sub>2</sub> in a small Schlenk flask under N<sub>2</sub> atmosphere. A known amount of monomer **NTEG** in dry CH<sub>2</sub>Cl<sub>2</sub> (1.0 ml per 100 mg of monomer **NTEG**) was added to the catalyst solution under N<sub>2</sub> atmosphere with vigorous stirring. The obtained reaction mixture was stirred vigorously until the signal of olefinic protons of monomer **NTEG** at 6.27 ppm disappeared by checking *in situ* <sup>1</sup>H NMR of reaction mixture in CDCl<sub>3</sub>, which indicates the monomer conversion reached 100%. Then, 0.3 ml of ethyl vinyl ether (EVE) was added to quench the catalyst. All the samples were evaporated under reduced pressure, washed with Et<sub>2</sub>O three times, and dried *in vacuo* until constant weight to get the polymer **PNTEG** as colorless sticky oil. Yield: 98% (**PNTEG-a**) and 97% (**PNTEG-b**). <sup>1</sup>H NMR (400 MHz, CDCl<sub>3</sub>, 25 °C, TMS), δ<sub>ppm</sub>: 7.76 and 7.63 (br, 1H, NHCO), 7.07 (br, 2H, ph), 5.60 (br, 1H, CH=), 5.49 (br, 1H, CH=),

4.18-4.11 (m, 6H, 3 × ph-OCH<sub>2</sub>), 3.82-3.52 (m, 34H, NCH<sub>2</sub>CH<sub>2</sub>N and OCH<sub>2</sub>), 3.35-3.33 (m, 9H, 3 × OCH<sub>3</sub>), 3.22, 3.00 and 2.66 (br, 4H, =CH-CH and CH-CO), 2.05 and 1.51 (br, 2H, CH=CHCHCH<sub>2</sub>). <sup>13</sup>C NMR (100 MHz, CDCl<sub>3</sub>, 25 °C, TMS), δ<sub>ppm</sub>: 178.6 (CON), 167.2 (NHCO), 152.3 (ph), 140.8 (ph), 133.3, 132.2 (CH=CH), 129.4 and 129.3 (ph), 106.8 and 106.6 (ph), 72.3, 71.9, 70.7, 70.6, 70.4, 69.6, 68.8, 68.7 (OCH<sub>2</sub>), 58.9 (OCH<sub>3</sub>), 53.5 (ph-OCH<sub>2</sub>), 50.9 (CHCON), 45.8 (=CHCH), 43.2 (CH<sub>2</sub>-bridge), 41.2, 38.3 (NCH<sub>2</sub>CH<sub>2</sub>N). Selected IR (KBr, cm<sup>-1</sup>): 3455 cm<sup>-1</sup> (ν<sub>NH</sub>), 2923 cm<sup>-1</sup> (ν<sub>CH<sub>2</sub></sub>), 1770 cm<sup>-1</sup> (δ<sub>C=C</sub>), 1700 cm<sup>-1</sup> (δ<sub>NC=O</sub>), 1649 cm<sup>-1</sup> (δ<sub>NHC=O</sub>).

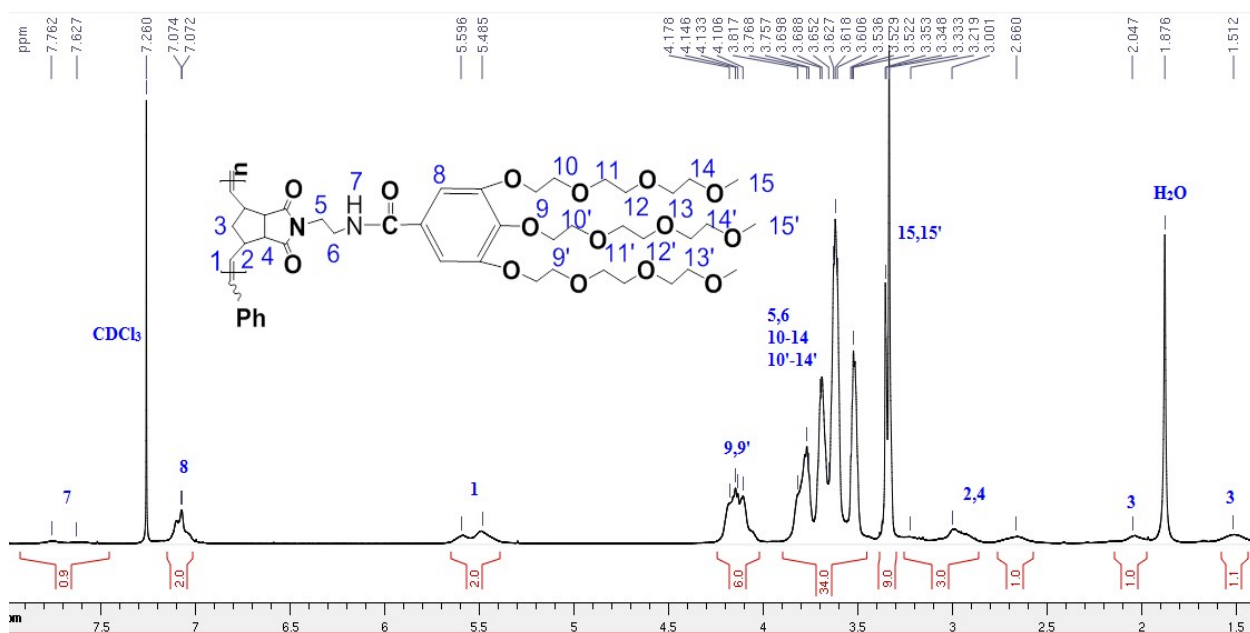


Figure S32. <sup>1</sup>H NMR (400 MHz) spectrum of PNTEG in CDCl<sub>3</sub>.

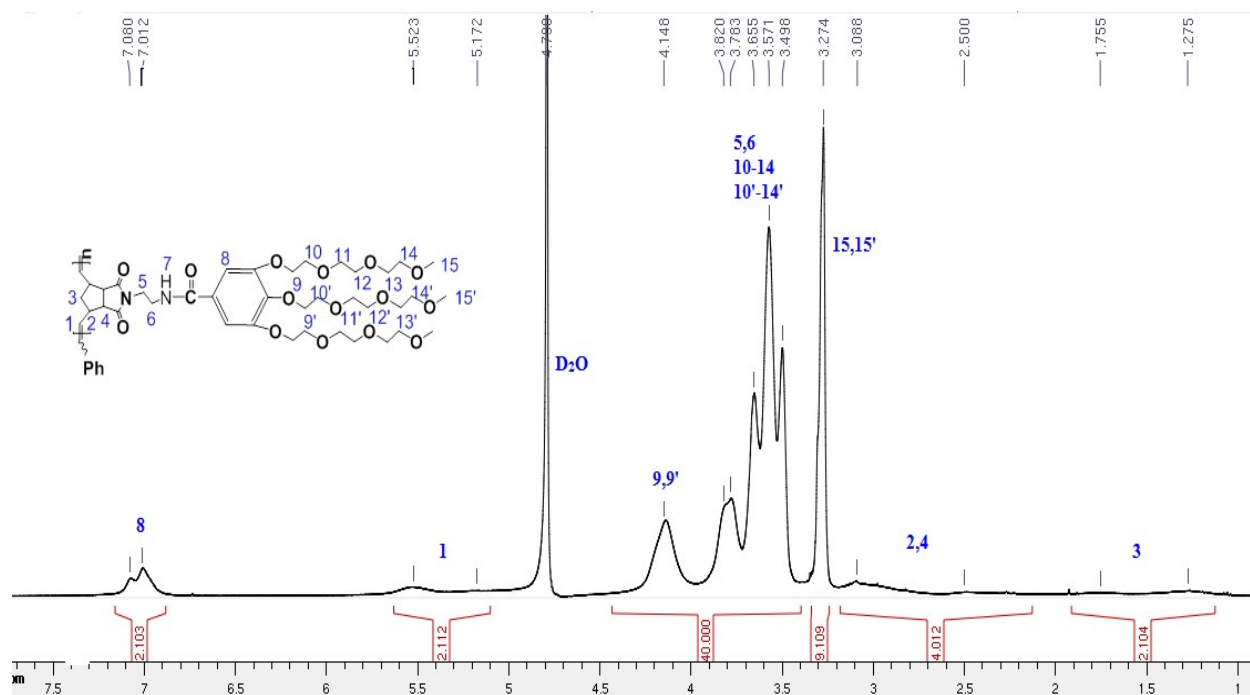


Figure S33. <sup>1</sup>H NMR (400 MHz) spectrum of PNTEG-a in D<sub>2</sub>O.

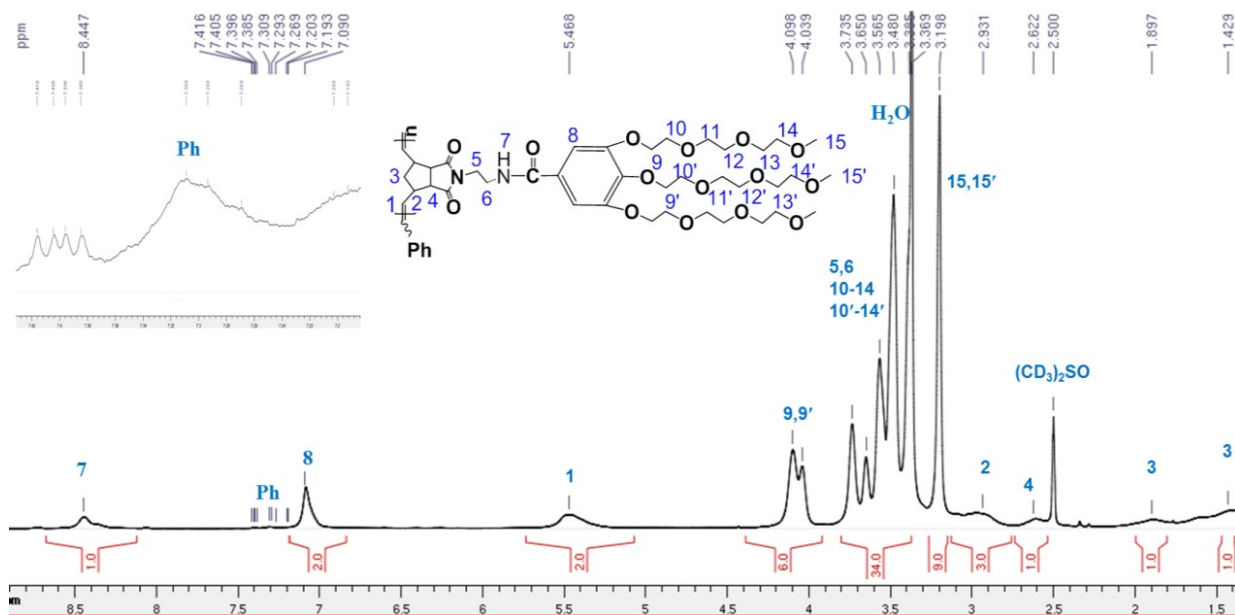


Figure S34.  $^1\text{H}$  NMR (400 MHz) spectrum of PNTEG-a in  $(\text{CD}_3)_2\text{SO}$ .

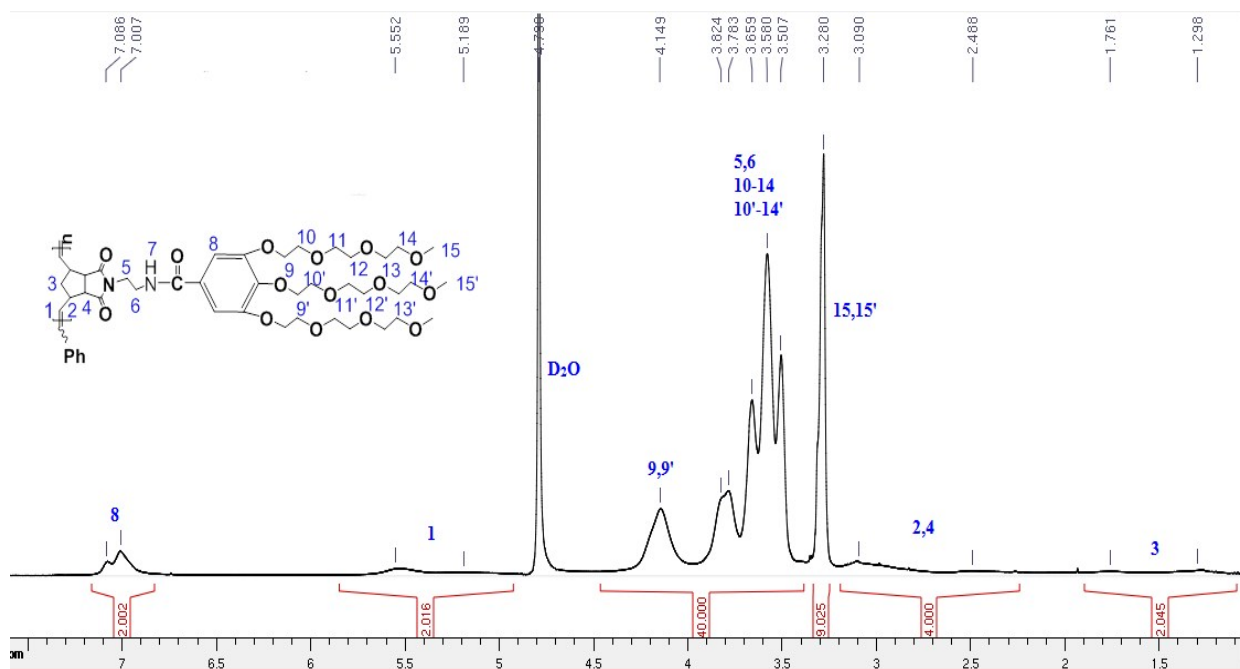
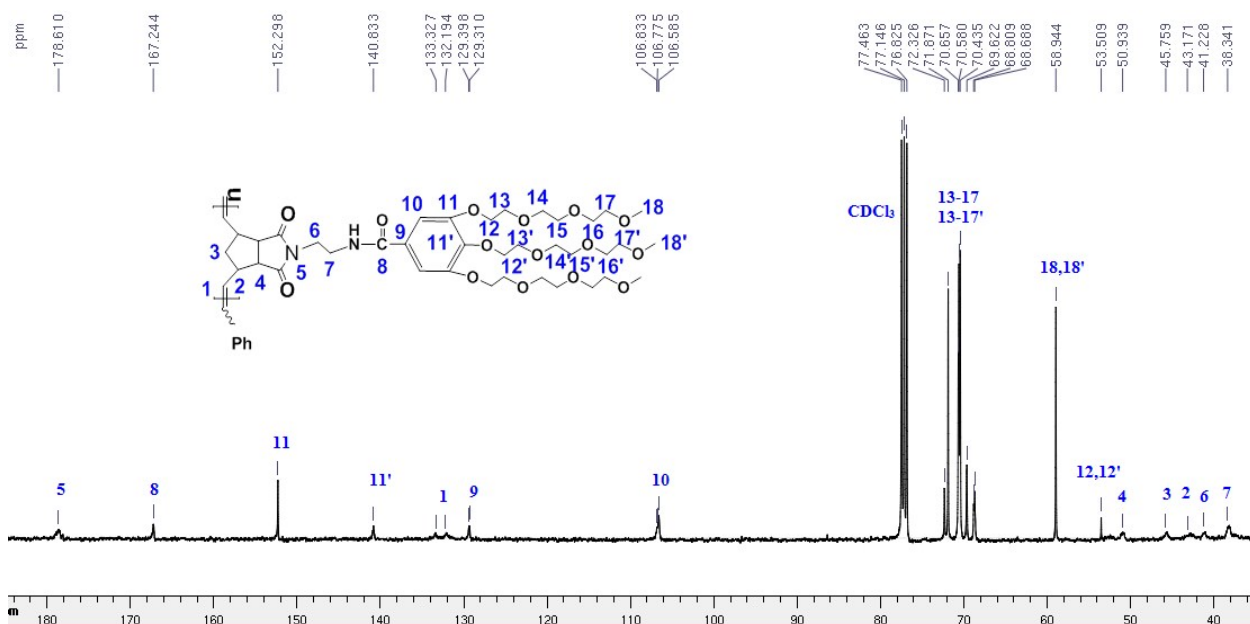
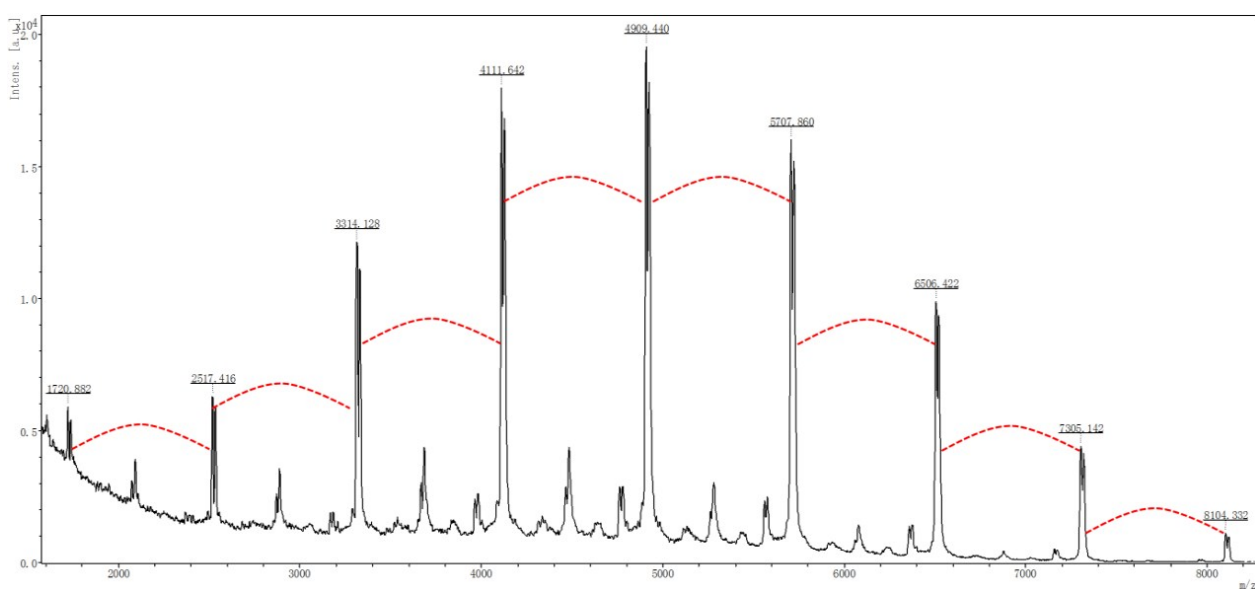


Figure S35.  $^1\text{H}$  NMR (400 MHz) spectrum of PNTEG-b in  $\text{D}_2\text{O}$ .



**Figure S36.**  $^{13}\text{C}$  NMR (100 MHz) spectrum of **PNTEG** in  $\text{CDCl}_3$ .



**Figure S37.** MALDI-TOF mass spectrum of **PNTEG**. The feed molar ratio of monomer **NTEG** to Grubbs' 3<sup>rd</sup> generation catalyst is 5:1. The red dotted lines are corresponding to the difference between molecular peaks of a value of  $797 \pm 1$  Da which is consistent with the molecular weight of the monomer **NTEG** (MW = 796.91 Da).

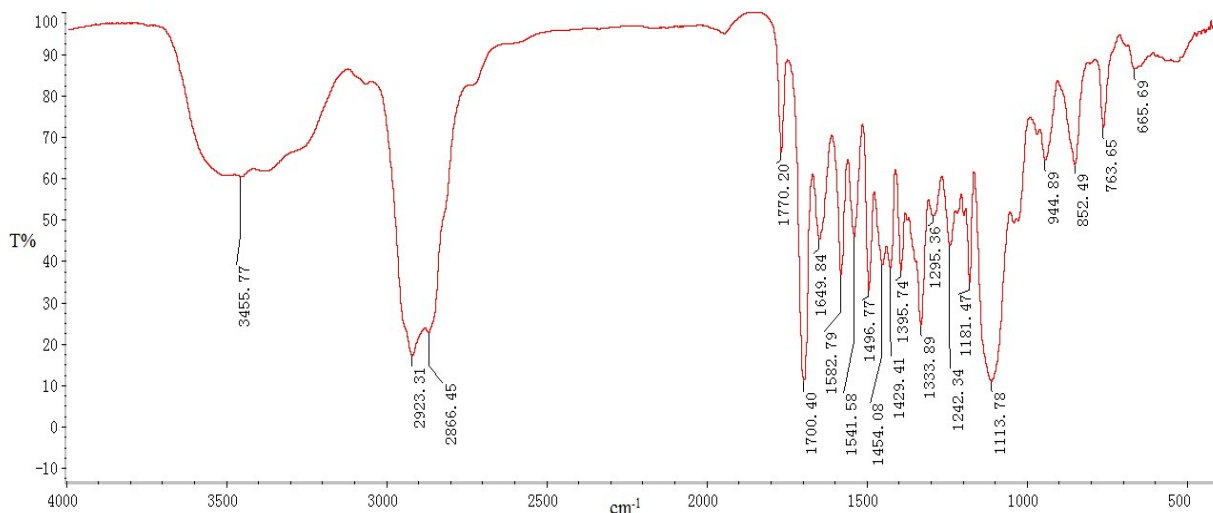


**Figure S38.** IR spectrum of PNTEG.

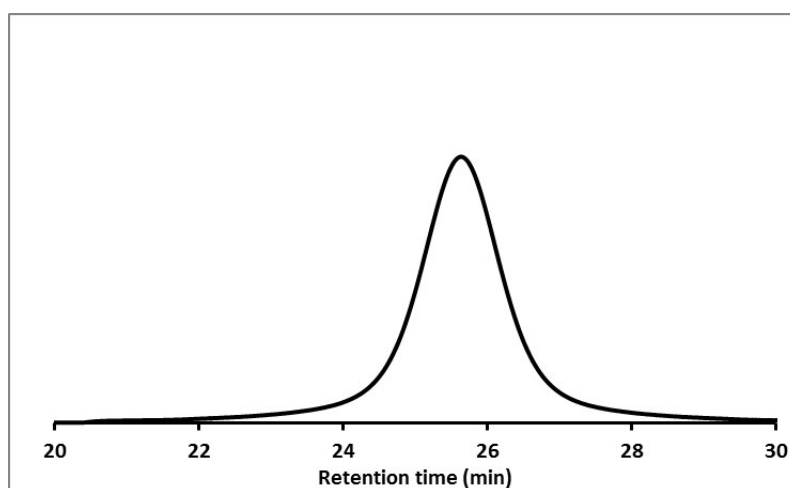


**Figure S39.** GPC curve of PNTEG-b in DMF

**Table S5.** Molecular weight data of polymer PNTEG-b by GPC in DMF (Ps standard)

Polymer	$M_p$	$M_n$	$M_w$	$M_z$	$M_{z+1}$	PDI
<b>PNTEG-b</b>	63680	64490	68130	72500	77750	1.06

**5.2. Kinetic study for polymer PNTEG-a:** In order to determine when the ROMP of monomer NTEG was completed at a feed mole ratio of 50:1, a kinetic study was conducted as follows: monomer NTEG (300 mg, 0.3765 mmol, 50 equiv) in 1.5 ml dry  $\text{CH}_2\text{Cl}_2$  was added into the solution of Grubbs 3<sup>rd</sup> (6.66 mg, 0.00753 mmol, 1 equiv) in 0.5 ml dry  $\text{CH}_2\text{Cl}_2$ . The reaction mixture was vigorously stirred at r. t. under  $\text{N}_2$  atmosphere. After 10, 20, 30 and 60 min, respectively, 0.02 ml of sample were removed and quenched with 0.01 ml of EVE. The *in situ*  $^1\text{H}$  NMR analysis of the dried reaction mixture in  $\text{CDCl}_3$  was conducted. The monomer conversion was deemed to be 100% when the signal of the olefin protons for monomer NTEG at 6.27 ppm disappeared.

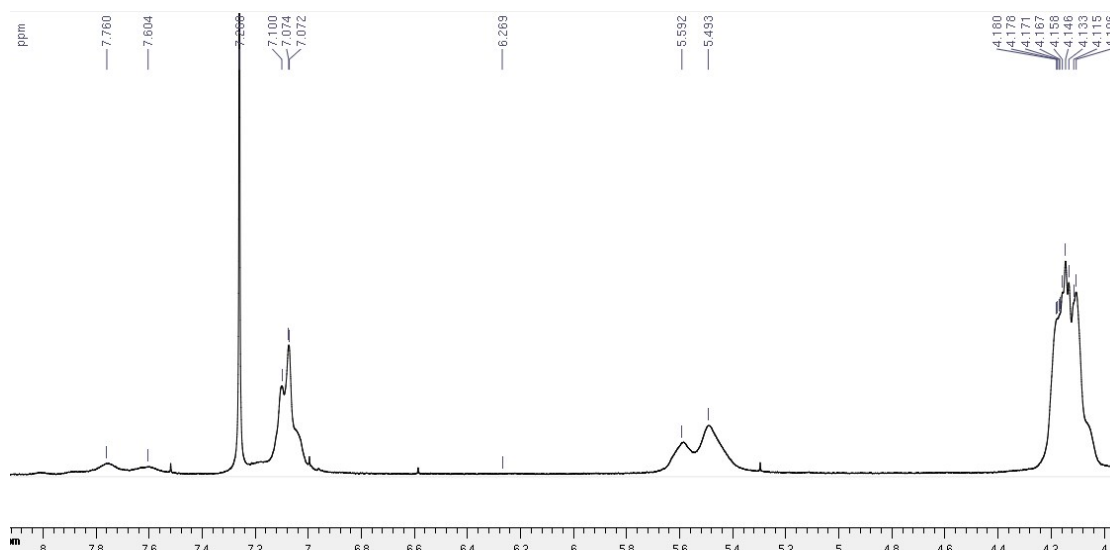


**Figure S40.**  $^1\text{H}$  NMR spectrum of the reaction mixture in  $\text{CDCl}_3$  for the synthesis of **PNTEG-a** after 10 min of stirring.

**5.3. Kinetic study for polymer PNTEG-b:** In order to determine when the ROMP of monomer **NTEG** was completed at a feed mole ratio of 100:1, a kinetic study was conducted as follows: monomer **NTEG** (394 mg, 0.4944 mmol, 100 equiv) in 1.5 ml dry  $\text{CH}_2\text{Cl}_2$  was added into the solution of Grubbs 3<sup>rd</sup> (4.38 mg, 0.004944 mmol, 1 equiv) in 0.5 ml dry  $\text{CH}_2\text{Cl}_2$ . The reaction mixture was vigorously stirred at r. t. under  $\text{N}_2$  atmosphere. After 10, 20, 30 and 60 min, respectively, 0.02 ml of sample were removed and quenched with 0.01 ml of EVE. The *in situ*  $^1\text{H}$  NMR analysis of the dried reaction mixture in  $\text{CDCl}_3$  was conducted. The monomer conversion was deemed to be 100% when the signal of the olefin protons for monomer **NTEG** at 6.27 ppm disappeared.

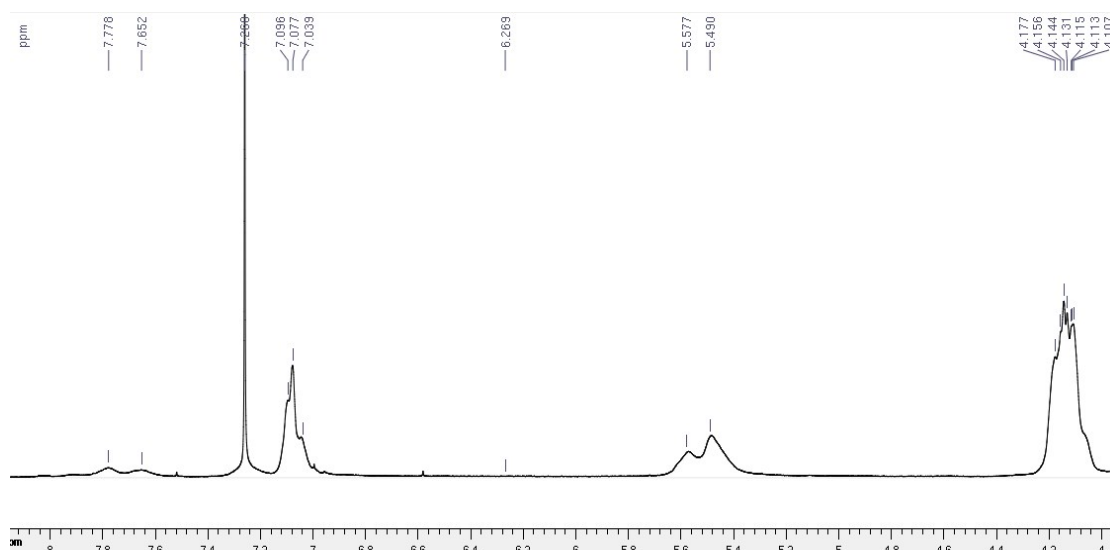


**Figure S41.**  $^1\text{H}$  NMR spectrum of the reaction mixture in  $\text{CDCl}_3$  for the synthesis of **PNTEG-b** after 10 min of stirring.

## 6. Synthesis of diblock copolymer PN(Fc-*b*-TEG)

### 6.1. Synthesis

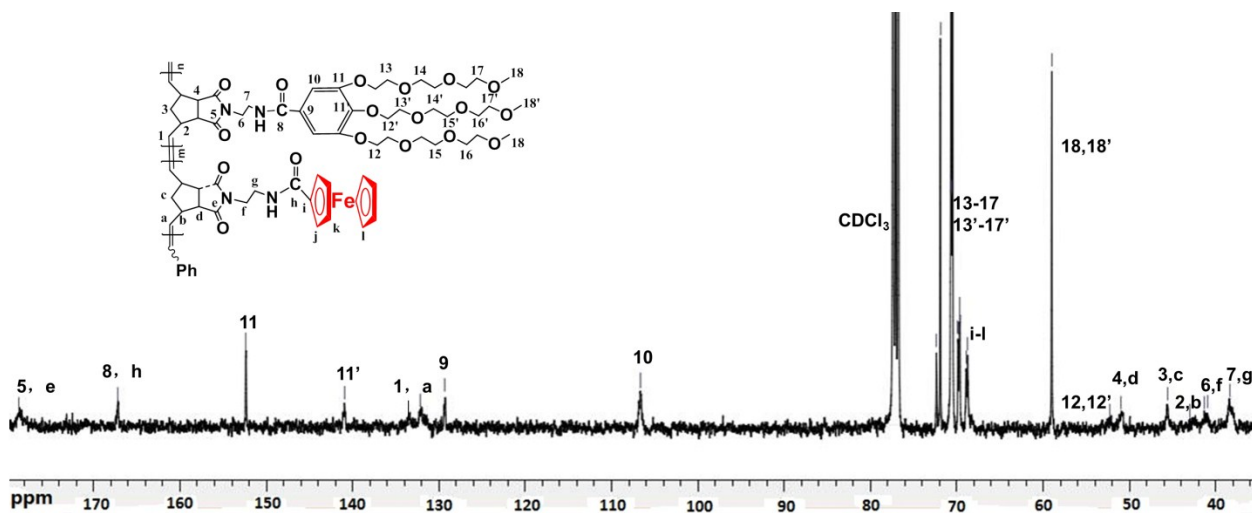


Figure S42. The  $^{13}\text{C}$  NMR spectrum of PN(Fc-*b*-TEG) in  $\text{CDCl}_3$ .

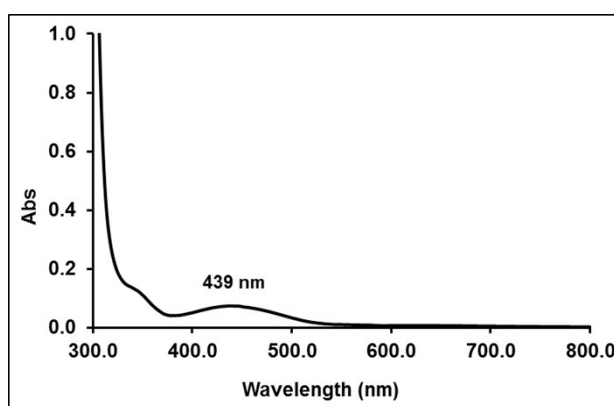


Figure S43. UV-vis spectrum of PN(Fc-*b*-TEG) in  $\text{CH}_2\text{Cl}_2$ .

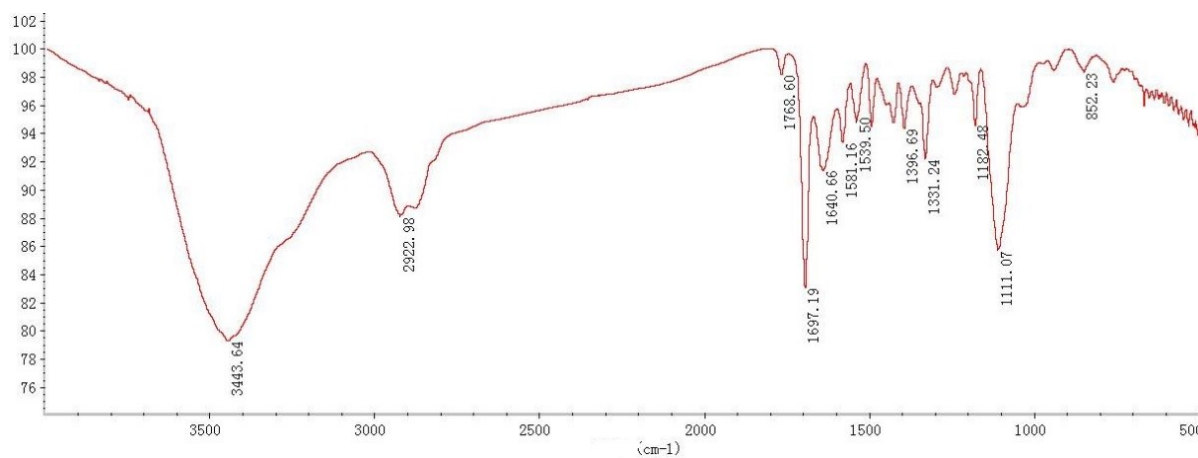


Figure S44. IR spectrum of PN(Fc-*b*-TEG).

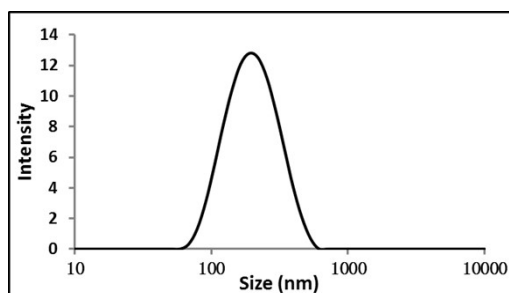


Figure S45. DLS curve of **PN(Fc-*b*-TEG)** in water (PDI=0.246, Z-average: 156 nm).

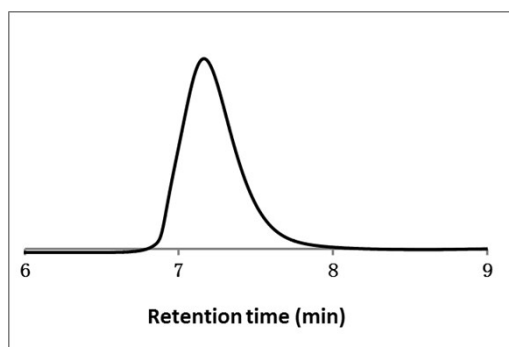


Figure S46. The GPC curve of **PN(Fc-*b*-TEG)**.

Table S6. Molecular weight data of block copolymer **PN(Fc-*b*-TEG)** by GPC in THF (Ps standard)

Polymer	$M_p$	$M_n$	$M_w$	$M_z$	$M_{z+1}$	$M_v$	$M_w/M_n$
<b>PN(Fc-<i>b</i>-TEG)</b>	27925	24922	28553	31727	34678	28553	1.146

## 6.2. Calculation of polymer degree of **PN(Fc-*b*-TEG)** by $^1\text{H}$ NMR end-group analysis

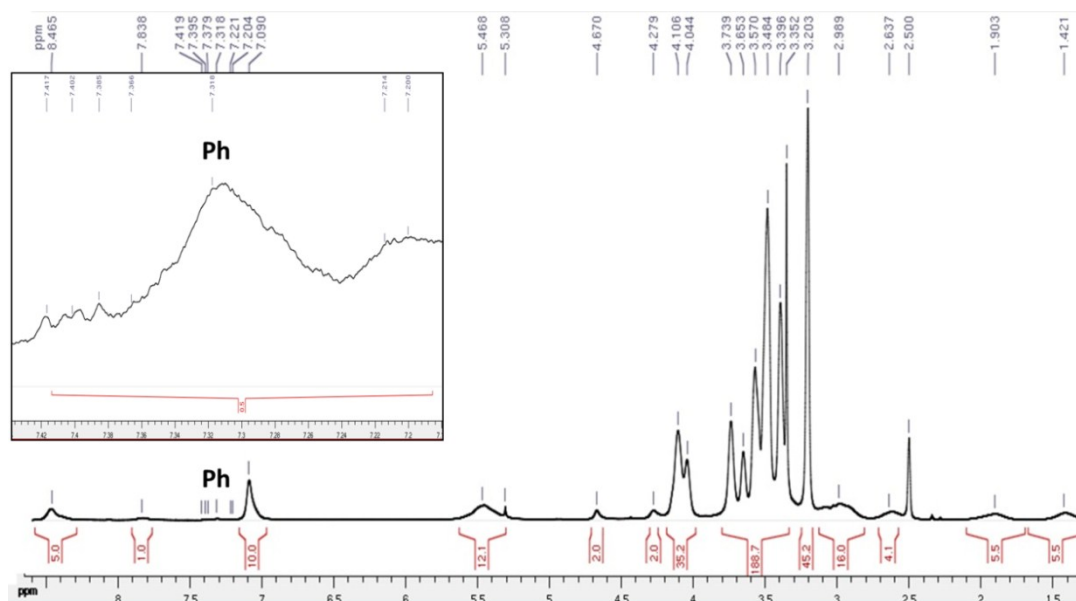


Figure S47.  $^1\text{H}$  NMR spectrum of **PN(Fc-*b*-TEG)** in  $(\text{CD}_3)_2\text{SO}$ .

**Table S7.** Polymer degrees calculated by using the  $^1\text{H}$  NMR spectrum in  $(\text{CD}_3)_2\text{SO}$  of **PN(Fc-*b*-TEG)**

Proton peak	Sub. Cp of Fc block	NHCO of TEG block	Side-chain phenyl of TEG block	OCH <sub>3</sub> of TEG block
$\delta_{\text{ppm}}$	4.67	8.46	7.09	3.20
Integra.	1.98-2.00	4.89-5.00	9.89-10.00	45.11-45.20
$n_{\text{p2a}}^{\text{b}}$	9.9-10	48.9-50	49.45-50	54.1-54.2
$n_{\text{p2b}}^{\text{c}}$	10: (50 $\pm$ 5)			

**Figure S47** is used for the calculation of ratio of  $n/m$ . <sup>b</sup> Calculated value of  $n/m$  based on integral of each peak. <sup>c</sup> Average polymer ratio according to  $n_{\text{p2a}}$  values.

As shown in **Table S7**, the  $^1\text{H}$  NMR ratio analysis in  $(\text{CD}_3)_2\text{SO}$  of diblock copolymer **PN(Fc-*b*-TEG)** provided the value of 10: (50  $\pm$  5) for the ratio of the Fc-containing and TEG-containing blocks. The used polymerization degree ( $n$ ) for the Fc-containing segment is 10 calculated by the end-group analysis in Table S2. These calculations were conducted by comparing the signals of the proton of the substituted Fc group (Cp) with those of characteristic protons in the TEG-containing blocks. Namely, the proton integration for Cp (4.67 ppm) was compared with those of the acylamino in the TEG block (8.46 ppm), side-chain phenyl in the second TEG block (7.09 ppm), and OCH<sub>3</sub> (3.20 ppm) of TEG, respectively. The obtained ratios are 9.9-10, 48.9-50, 49.45-50 and 54.1-54.2, respectively. Thus, the average value of polymerization degree for the diblock copolymer ( $n$ :  $m$ ) is 10: (50  $\pm$  5). The error was due to the integration error on each signal.

**6.3. Kinetic study for the synthesis of diblock copolymer PN(Fc-*b*-TEG):** In order to know when the polymerization of the second TEG block can finish, the kinetic study was conducted as following: Monomer **NFc** (50 mg, 0.200 mmol, 10 equiv) in 1.5 ml of dry  $\text{CH}_2\text{Cl}_2$  was added into the solution of Grubbs catalyst 3<sup>rd</sup> (10.6 mg, 0.020 mmol, 1 equiv) in 0.2 ml of dry  $\text{CH}_2\text{Cl}_2$ . The reaction mixture was stirred vigorously for 10 min at r. t. under  $\text{N}_2$  atmosphere. Then, monomer **NTEG** (476.6 mg, 0.432 mmol, 50 equiv) in 2 ml of dry  $\text{CH}_2\text{Cl}_2$  was added, and after 5, 10, 20 and 30 min, respectively, 0.1 ml of sample was taken out and quenched with 0.1 ml of EVE. The *in situ*  $^1\text{H}$  NMR analysis in  $\text{CDCl}_3$  was conducted, and the conversion of monomer **NTEG** was deemed to be 100% when the peak at 6.27 ppm, the signal of olefinic protons for monomer **NTEG** disappeared. Actually, the polymerization of the second TEG block can finish in 10 min with 100% monomer conversion from the *In situ*  $^1\text{H}$  NMR analysis.

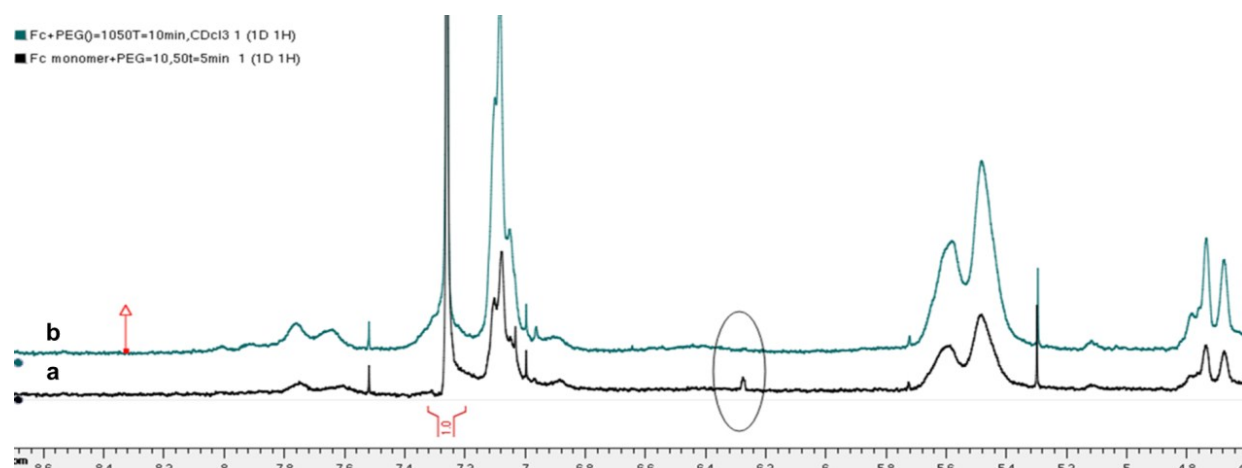


**Figure S48.**  $^1\text{H}$  NMR spectra of the reaction mixture in  $\text{CDCl}_3$  for the synthesis of **PN(Fc-*b*-TEG)** (a: 5 min, b: 10 min).

## 7. ROMP synthesis of random copolymer **PN(Fc-*r*-TEG)**

**7.1. General synthetic procedure:** Monomers **NFc** (34 mg, 0.081 mmol, 10 equiv) and **NTEG** (324.1 mg, 0.407 mmol, 50 equiv) were added into a small glass tube, and dissolved in 2 ml of dry  $\text{CH}_2\text{Cl}_2$ . The desired amount of Grubbs' 3<sup>rd</sup> (7.19 mg, 0.00813 mmol, 1 equiv) was added into another small Schlenk flask, flushed with  $\text{N}_2$ , and dissolved in 0.03 ml of dry  $\text{CH}_2\text{Cl}_2$ . The mixture solution of monomers **NFc** and **NTEG** was transferred to the flask containing the catalyst *via* a small syringe. The reaction mixture was stirred vigorously for 10 min at r. t. under  $\text{N}_2$  atmosphere, and then, 0.5 ml of EVE was added to quench the catalyst. All the samples were collected, purified by precipitating from  $\text{CH}_2\text{Cl}_2$  with  $\text{Et}_2\text{O}$  three times, and dried *in vacuo* until constant weight to get the random copolymer **14** as yellow solid. Yield: 94%.  $^1\text{H}$  NMR (400 MHz,  $\text{CDCl}_3$ , 25 °C, TMS)  $\delta_{\text{ppm}}$ : 7.74 and 7.60 (br, NHCO of Fc and TEG segments), 7.09-7.06 (br, ph), 5.61 and 5.49 (br, CH=), 4.65 (br, sub. Cp), 4.17-4.10 (s, sub. Cp and ph- $\text{OCH}_2\text{CH}_2\text{O}$ ), 3.81-3.51 (m,  $\text{NCH}_2\text{CH}_2\text{N}$  of TEG segment, ph- $\text{OCH}_2\text{CH}_2\text{O}$  and  $\text{OCH}_2\text{CH}_2\text{O}$ ), 3.35 (s, 3  $\times$   $\text{OCH}_3$ ), 3.22 (br,  $\text{NCH}_2\text{CH}_2\text{N}$  of Fc segment), 2.99, 2.98 (s, =CH-CH of norbornene), 2.66 and 2.18 (br, CH-CO of norbornene), 2.03 (br, =CHCH $\text{CH}_2$ ), 1.51 (br, CH=CHCH $\text{CH}_2$ ).  $^{13}\text{C}$  NMR (100 MHz,  $\text{CDCl}_3$ , 25 °C, TMS),  $\delta_{\text{ppm}}$ : 178.4 (CON), 167.1 (NHCO), 152.3 (ph), 140.9 (ph), 132.5, 131.7 (=CHCH), 129.3 (ph), 106.7 (ph), 72.3-68.7 (Cp and  $\text{OCH}_2$ ), 59.0 ( $\text{OCH}_3$ ), 52.5 (ph-O- $\text{CH}_2$ ), 51.0 (=CHCHCH), 45.5 ( $\text{CH}_2$ -bridge), 42.7 (=CH-CH), 41.4 ( $\text{NCH}_2\text{CH}_2\text{N}$ ), 38.2 ( $\text{NCH}_2\text{CH}_2\text{N}$ ). Selected IR (KBr,  $\text{cm}^{-1}$ ): 3443  $\text{cm}^{-1}$  ( $\nu_{\text{NH}}$ ), 2922  $\text{cm}^{-1}$  ( $\nu_{\text{CH}_2}$ ), 1768  $\text{cm}^{-1}$  ( $\delta_{\text{C}=\text{C}}$ ), 1697  $\text{cm}^{-1}$  ( $\delta_{\text{NC}=\text{O}}$ ), 1640  $\text{cm}^{-1}$  ( $\delta_{\text{NHC}=\text{O}}$ ), 1111  $\text{cm}^{-1}$  ( $\nu_{\text{C-O-C}}$ ), 852  $\text{cm}^{-1}$  ( $\nu_{\text{FeII}}$ ).

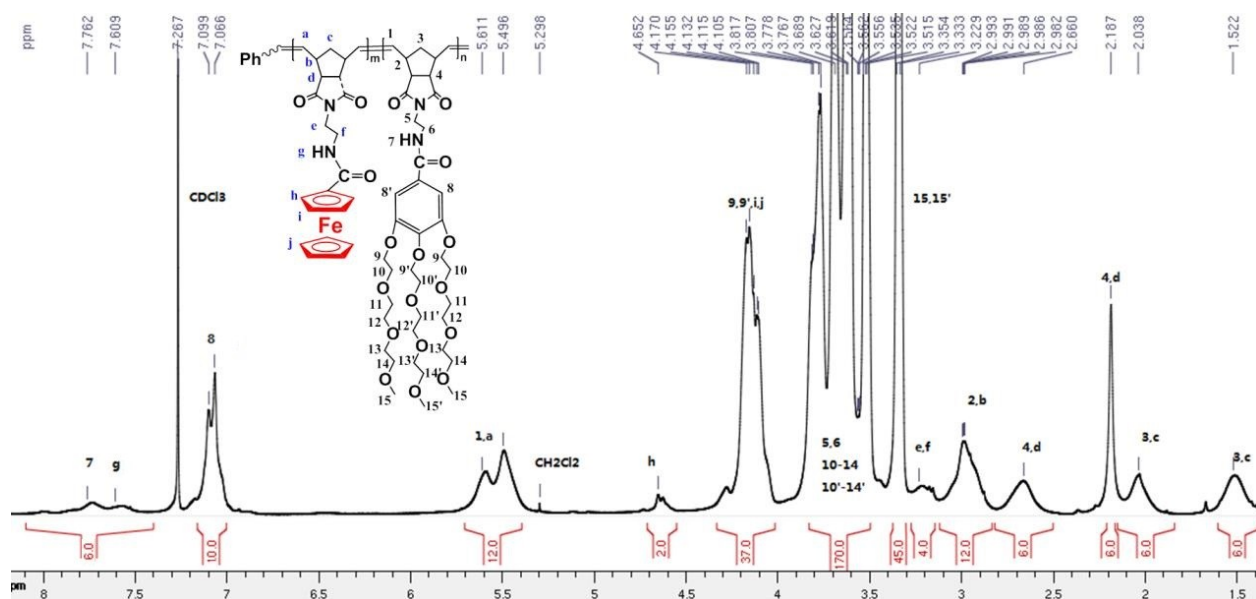


Figure S49.  $^1\text{H}$  NMR (400 MHz) spectrum of  $\text{PN}(\text{Fc-r-TEG})$  in  $\text{CDCl}_3$ .

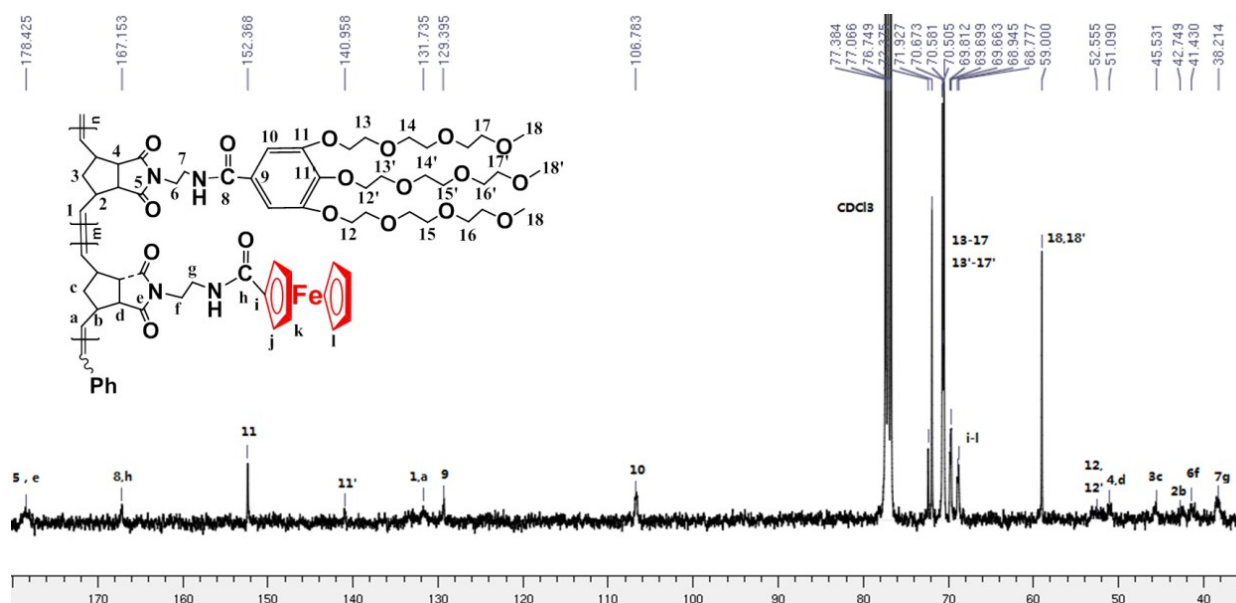


Figure S50.  $^{13}\text{C}$  NMR (100 MHz) spectrum of  $\text{PN}(\text{Fc-r-TEG})$  in  $\text{CDCl}_3$ .

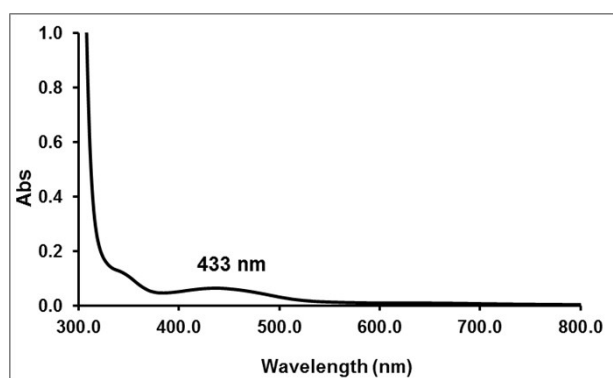
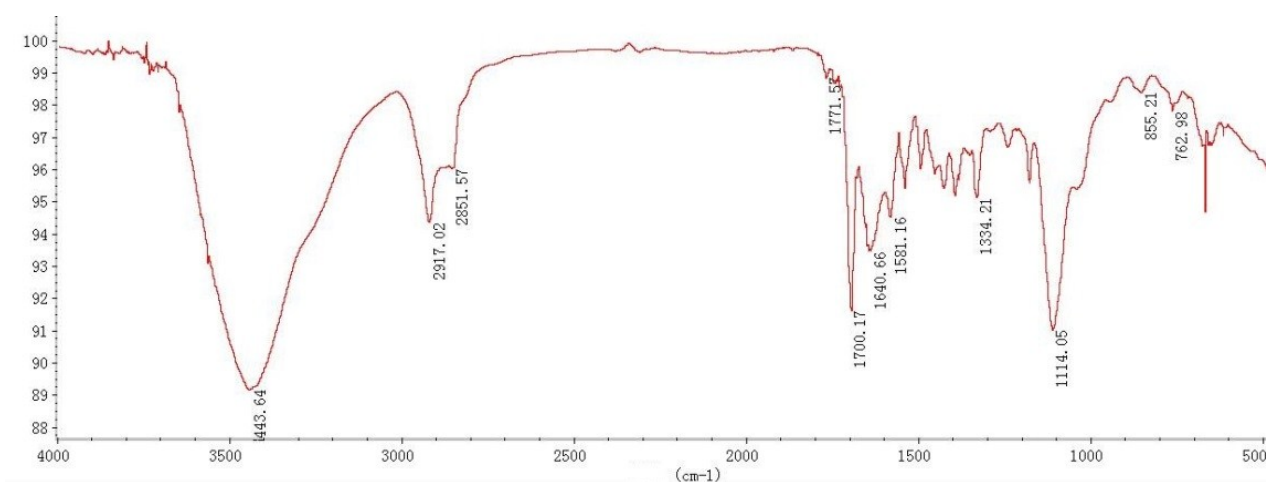
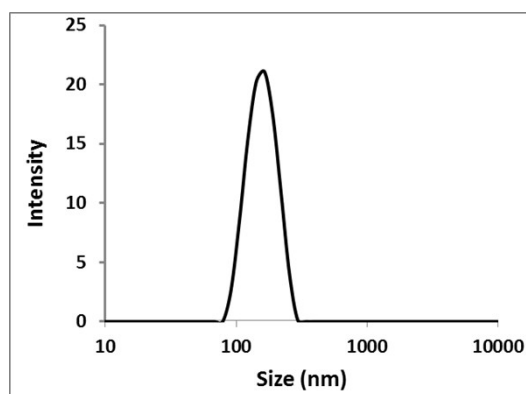


Figure S51. UV-vis spectrum of  $\text{PN}(\text{Fc-r-TEG})$  in  $\text{CH}_2\text{Cl}_2$ .



**Figure S52.** IR spectrum of **PN(Fc-r-TEG)**.



**Figure S53.** DLS curve of **PN(Fc-r-TEG)** in water (PDI=0.288, Z-average = 159 nm).

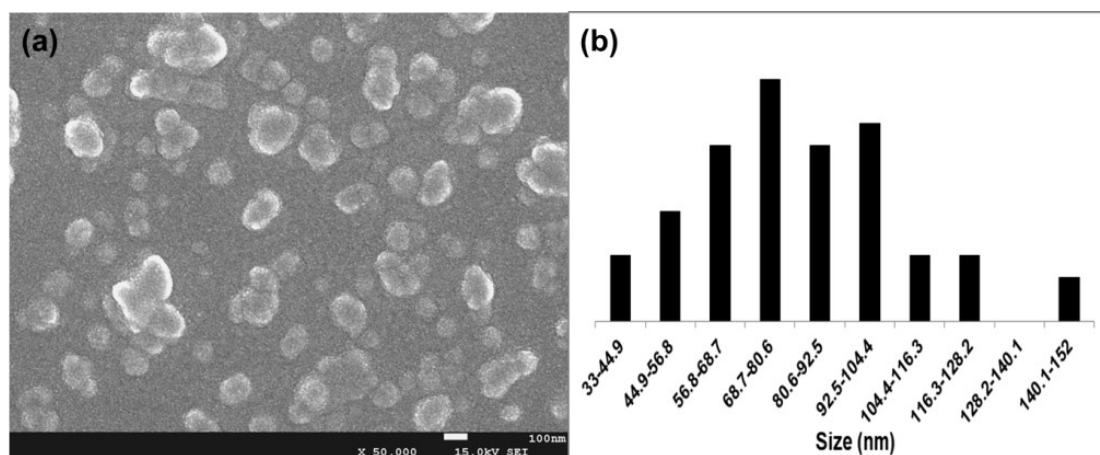


**Figure S54.** The SEM images of self-assembly random copolymer **PN(Fc-r-TEG)** in aqueous solutions (mean diameter  $81 \pm 25$  nm)

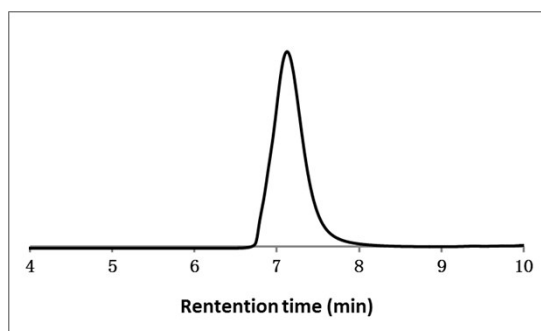


**Figure S55.** GPC trace of **PN(Fc-r-TEG)**.

**Table S8.** Molecular weight data of random polymer **PN(Fc-r-TEG)** by GPC in THF (Ps standard)

Polymer	$M_p$	$M_n$	$M_w$	$M_z$	$M_{z+1}$	$M_v$	$M_w/M_n$
<b>PN(Fc-r-TEG)</b>	31879	26877	32106	36514	40650	32106	1.195

## 7.2. Calculation of polymer degree of **PN(Fc-r-TEG)** by $^1\text{H}$ NMR end-group analysis

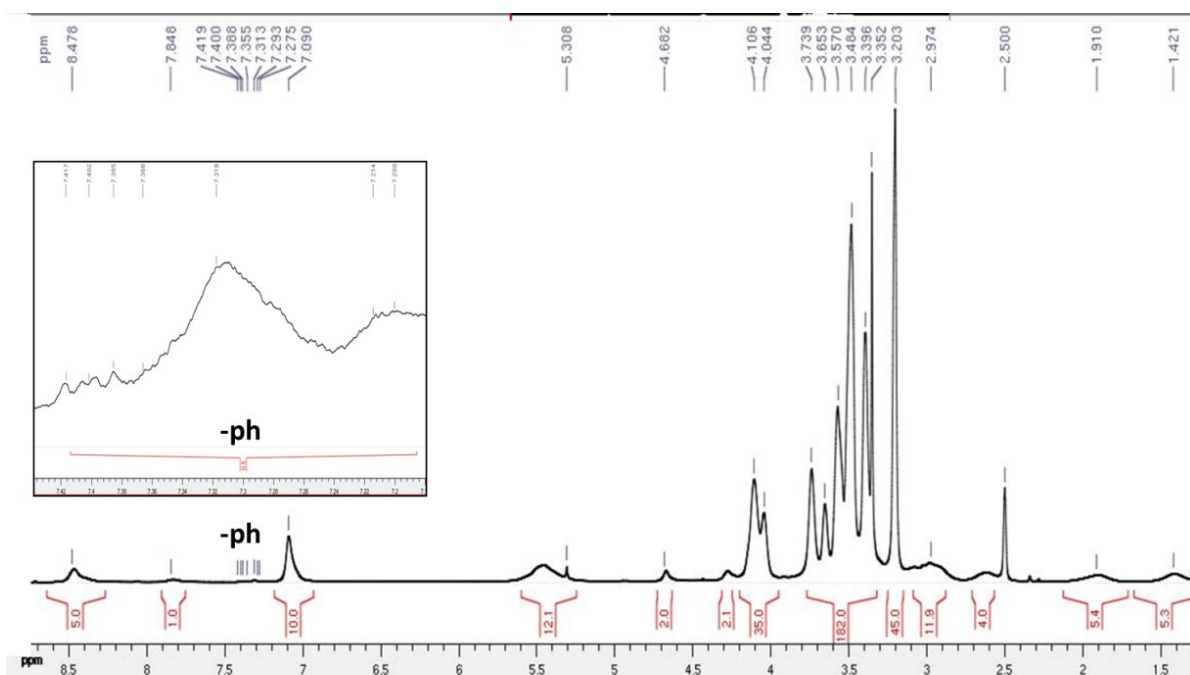


**Figure S56.**  $^1\text{H}$  NMR of **PN(Fc-r-TEG)** in  $(\text{CD}_3)_2\text{SO}$ .

**Table S9.** Polymer degrees calculated by using the  $^1\text{H}$  NMR spectrum in  $(\text{CD}_3)_2\text{SO}$  of **PN(Fc-r-TEG)**

Proton peak	NHCO of Fc part	NHCO of TEG part	Side-chain phenyl of TEG part	$\text{OCH}_3$ of TEG part
$\delta_{\text{ppm}}$	7.84	8.47	7.09	3.20
Integra.	0.92-0.98	4.79-4.98	10.02-10.30	44.23-46.40
$\eta_{\text{p2a}}^b$	9.2-9.8	47.9-49.8	50.1-51.5	53.1-55.7

$n_{p2b}^c$	10: (50 ± 6)
-------------	--------------

**Figure S56** is used for the calculation of ratio of n/m. <sup>b</sup> Calculated value of n/m based on integral of each peak. <sup>c</sup> Average polymer ratio according to  $n_{p2a}$  values.

As shown in **Table S9**, the <sup>1</sup>H NMR ratio analysis in (CD<sub>3</sub>)<sub>2</sub>SO of random copolymer **PN(Fc-r-TEG)** provided the value of 10: (50 ± 6) for the ratio of the Fc-containing and TEG-containing segments. The used polymerization degree (n) for the Fc-containing segment is 10 calculated by the end-group analysis in Table S2. These calculations were conducted by comparing the signals of the proton of the acylamino in the Fc (7.84 ppm) segment with those of characteristic protons in the TEG-containing parts. Namely, the proton integration for the acylamino in the Fc (7.84 ppm) was compared with those of the acylamino in the TEG segment (8.47 ppm), side-chain phenyl in the TEG segment (7.09 ppm), and OCH<sub>3</sub> (3.20 ppm) of TEG, respectively. The obtained ratios are 9.2-9.8, 47.9-49.8, 50.1-51.5 and 53.1-55.7, respectively. Thus, the average value of polymerization degree for the random copolymer (m: n) is 10: (50 ± 6). The error was due to the integration error on each signal.

**7.3. Kinetic study for the synthesis of random copolymer PN(Fc-r-TEG):** In order to know when the polymerization can finish, the kinetic study was conducted as following: Monomers **NFc** (34 mg, 0.081 mmol, 10 equiv) and **NTEG** (324.1 mg, 0.407 mmol, 50 equiv) were added into a small glass tube, and dissolved in 2 ml of dry CH<sub>2</sub>Cl<sub>2</sub>. The desired amount of Grubbs' 3<sup>rd</sup> (7.19 mg, 0.00813 mmol, 1 equiv) was added into another small Schlenk flask, flushed with N<sub>2</sub>, and dissolved in 0.03 ml of dry CH<sub>2</sub>Cl<sub>2</sub>. The mixture solution of monomers **NFc** and **NTEG** was transferred to the flask containing the catalyst *via* a small syringe. 0.1 ml of sample was taken out in a certain interval time and quenched with 0.1 ml of EVE. The *in situ* <sup>1</sup>H NMR analysis in CDCl<sub>3</sub> was conducted, and the conversion of monomers **NFc** and **NTEG** were deemed to be 100% when the peak at 6.27 ppm, the signal of olefinic protons for monomers disappeared. Actually, the polymerization of the monomers can finish in 10 min with 100% monomer conversion from the *in situ* <sup>1</sup>H NMR analysis.

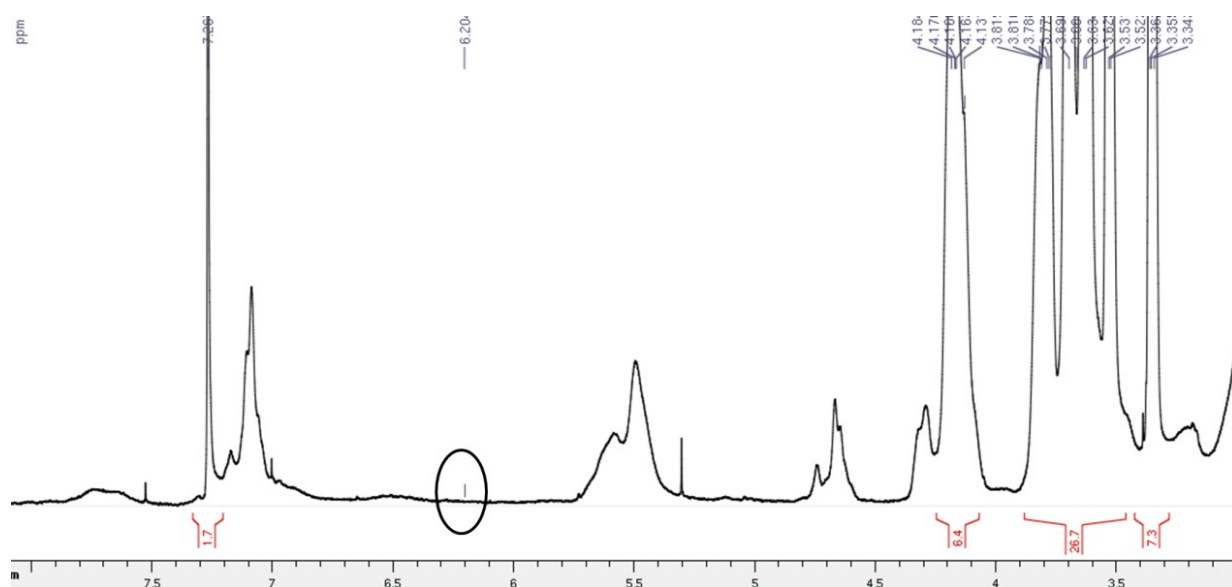


**Figure S57.** <sup>1</sup>H NMR spectrum of the reaction mixture in CDCl<sub>3</sub> for the synthesis of **PN(Fc-r-TEG)**

after 10 min of stirring.

## 8. Self-assembly of the copolymer in water.

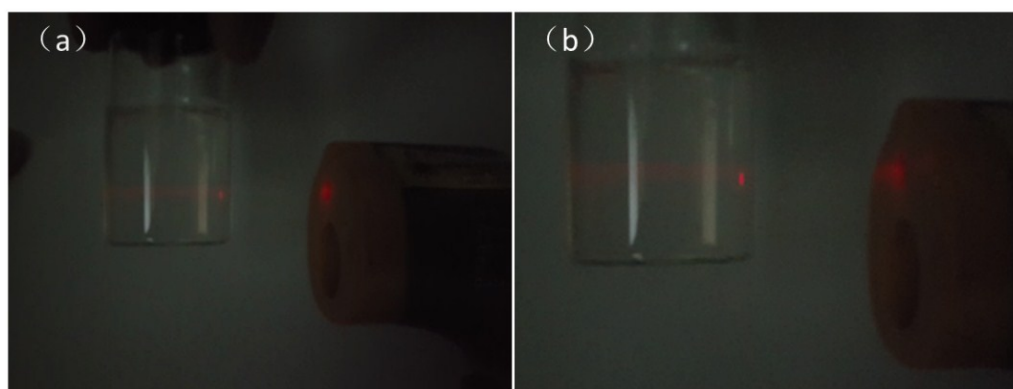


**Figure S58.** Tyndall effects of **PN(Fc-*b*-TEG)** (a) and **PN(Fc-*r*-TEG)** (b) after self-assembly in water.

## 9. Oxidation and reduction of micelles

### 9.1. Determination of CMC<sup>[55]</sup> of original micelles

The pyrene fluorescence probe technique was adopted to determine the CMCs of **PN(Fc-*b*-TEG)** and **PN(Fc-*r*-TEG)**. Concretely, a known amount of pyrene in acetone was added to a battery of 10 ml volumetric flask to give a pyrene concentration of  $2.0 \times 10^{-6}$  M, followed the volatilization of acetone in vacuum condition. A measured amount of the micelle aggregate solutions with concentration ranging from 2.0 to  $2.5 \times 10^{-4}$  mg ml<sup>-1</sup> was then added to the above each flask, and stirred at r. t. overnight to equilibrate the micelle aggregates and pyrene. The fluorescence spectra were detected by using a fluorescence spectrophotometer (RF-5310PC, SHIMADZU, Japan). The excitation wavelength was 339 nm. The plot of  $I_3/I_1$  intensity ratios versus concentration of aggregate solutions was drawn to estimate the CMC by the tangent method.

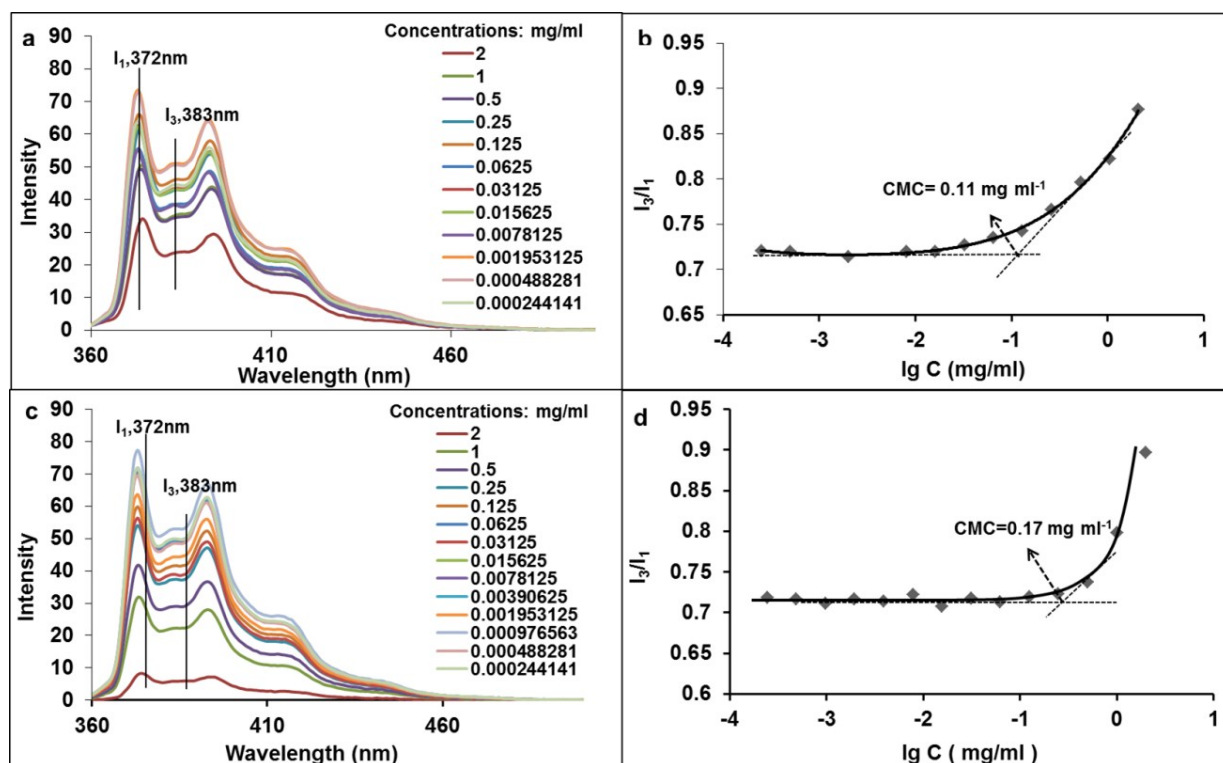


**Figure S59.** The CMCs of the block (**PN(Fc-*b*-TEG)**) and random copolymers (**PN(Fc-*r*-TEG)**). (a) Fluorescence emission spectra of micelles of diblock copolymer **PN(Fc-*b*-TEG)** in water using pyrene as probe. (b) Plots of  $I_3/I_1$  intensity ratio vs logarithmic concentrations of the block copolymer in water from 2 to  $2.5 \times 10^{-4}$  mg ml<sup>-1</sup>. (c) Fluorescence emission spectra of micelles of random copolymer **PN(Fc-*r*-TEG)** in water using pyrene as probe. (d) Plots of  $I_3/I_1$  intensity ratio vs logarithmic concentrations of the random copolymer in water from 2 to  $2 \times 10^{-4}$  mg ml<sup>-1</sup>.

## 9.2. DLS curves of PN(Fc-*r*-TEG) micelles

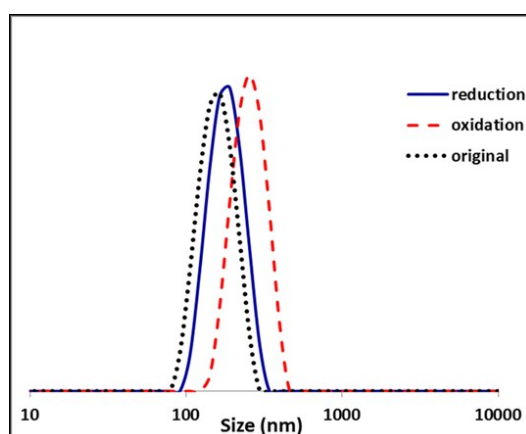


**Figure S60.** DLS curves of **PN(Fc-*r*-TEG)** micelles in water during an oxidation-reduction cycle. (Original: PDI = 0.246, Z-average = 159 nm; Oxidized: PDI = 0.408, Z-average = 250.0 nm; Reduced: PDI = 0.304, Z-average = 164.3 nm).

## 9.3. Determination of CMC of oxidized micelles

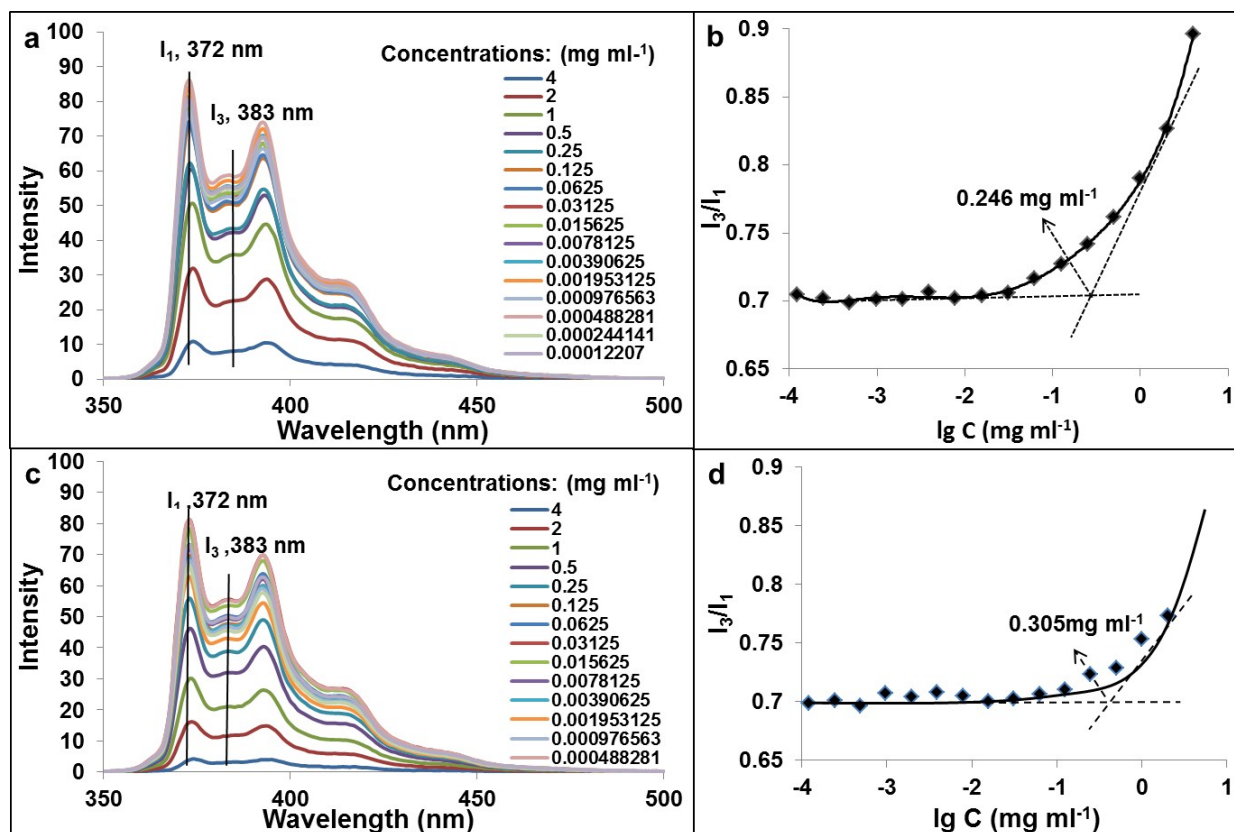


**Figure S61.** CMCs of PN(Fc-*b*-TEG) and PN(Fc-*r*-TEG) after oxidation by FeCl<sub>3</sub>. (a) Fluorescence emission spectra of micelles of diblock copolymer PN(Fc-*b*-TEG) in water using pyrene as probe. (b) Plots of  $I_3/I_1$  intensity ratio vs logarithmic concentrations of the block copolymer in water from 4 to  $2.5 \times 10^{-4}$  mg ml<sup>-1</sup>. (c) Fluorescence emission spectra of micelles of random copolymer PN(Fc-*r*-TEG) in water using pyrene as probe. (d) Plots of  $I_3/I_1$  intensity ratio vs logarithmic concentrations of the random copolymer in water from 4 to  $2 \times 10^{-4}$  mg ml<sup>-1</sup>.

## 10. Drug loading and release

### 10.1. Loading and release of NR by micelles of PN(Fc-*b*-TEG)

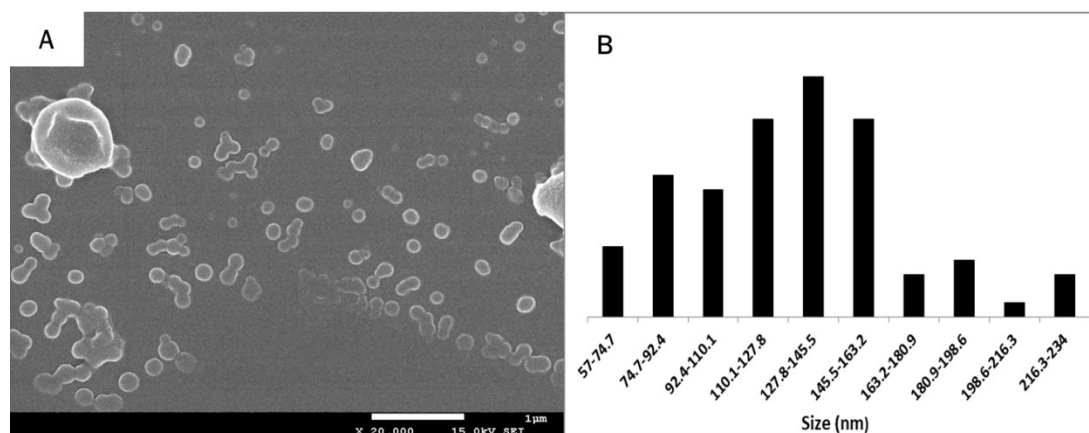


**Figure S62.** SEM image of micelles of PN(Fc-*b*-TEG) after loading NR in water (A) and the statistical diameter distribution of these micelles (B). (Average diameter of  $130 \pm 15$  nm).

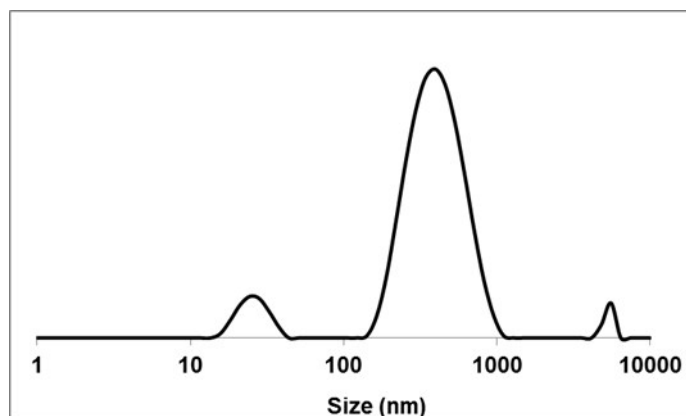


**Figure S63.** DLS curve of micelles of **PN(Fc-*b*-TEG)** after loading NR in water. (PDI = 0.654 nm, average size = 226 nm).

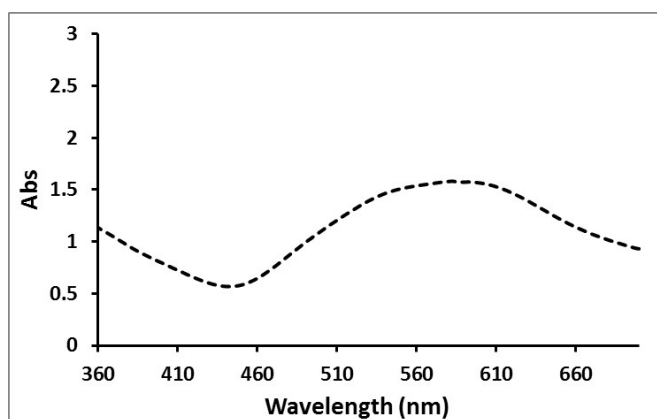


**Figure S64.** UV-vis spectrum of the NR-loaded micelles of **PN(Fc-*b*-TEG)** in water.

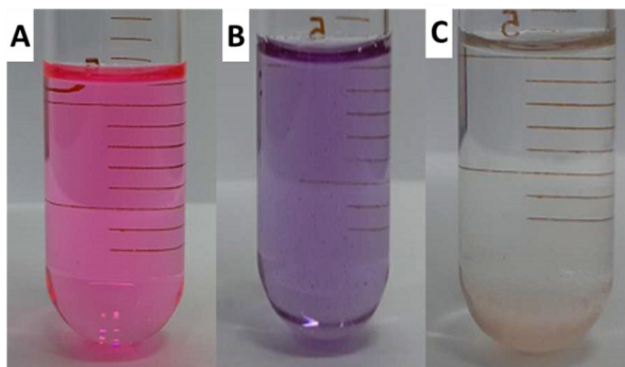


**Figure S65.** Picture of the THF solution of copolymer **PN(Fc-*b*-TEG)** and NR (**A**). Pictures of NR-loaded micelles of **PN(Fc-*b*-TEG)** in water (**B**), and the corresponding polymer solution and NR precipitate resulted from the addition of  $\text{FeCl}_3$ .

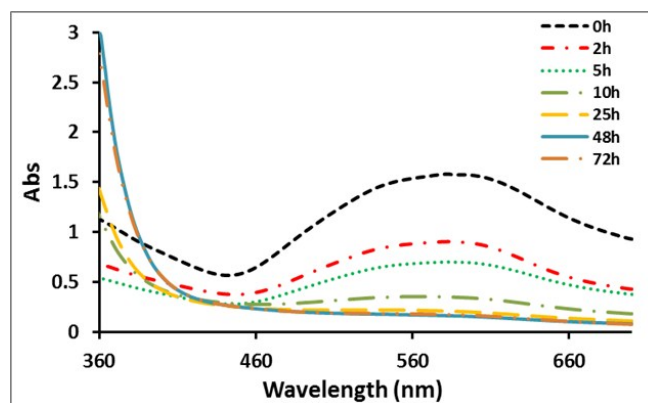


**Figure S66.** UV-vis absorption spectra of NR-loaded micelles of **PN(Fc-*b*-TEG)** after oxidized by  $\text{FeCl}_3$  at different intervals.

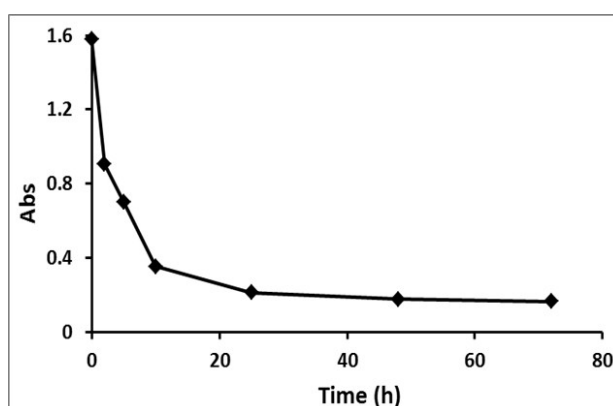


**Figure S67.** The UV-vis absorbance variation of NR-loaded micelles of **PN(Fc-*b*-TEG)** at 585 nm after oxidized by  $\text{FeCl}_3$  in water.

## 10.2. Loading and release of NR by micelles of PN(Fc-*r*-TEG)

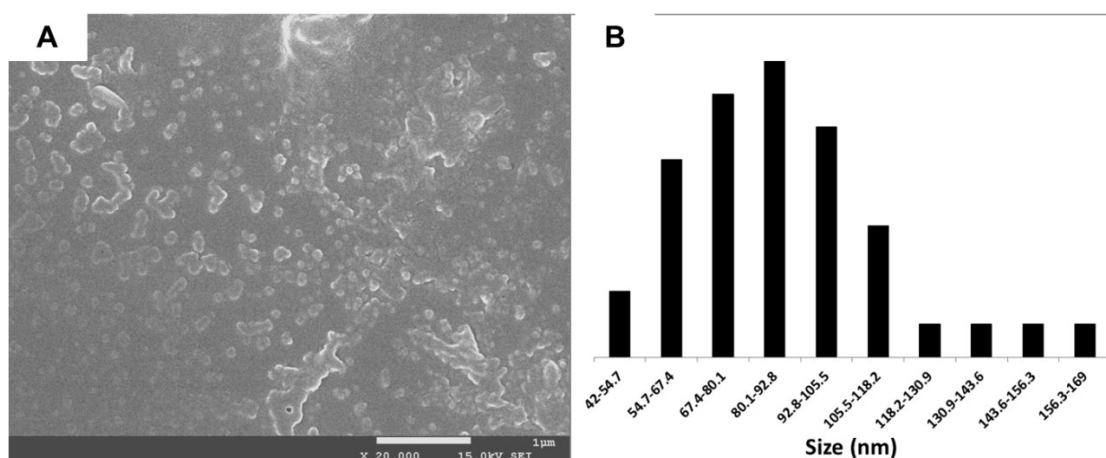


**Figure S68.** SEM image of NR-loaded micelles of **PN(Fc-*r*-TEG)** in water (A) and the statistical diameter distribution of these micelles (B) (Average diameter of  $93 \pm 30$  nm).

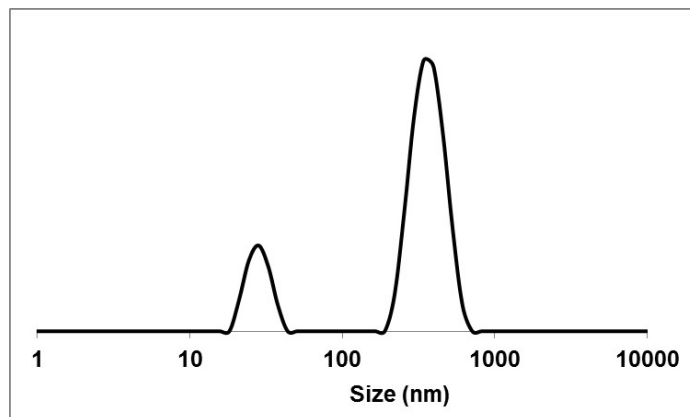


**Figure S69.** DLS curve of NR-loaded micelles of **PN(Fc-r-TEG)** in water (PDI = 0.472 nm, average size = 308 nm).

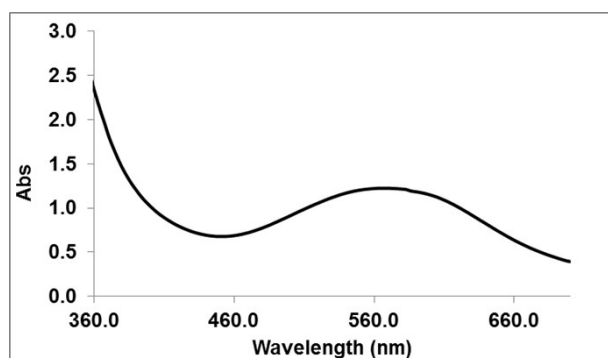


**Figure S70.** UV-vis spectrum of NR-loaded micelles of **PN(Fc-r-TEG)** in water.

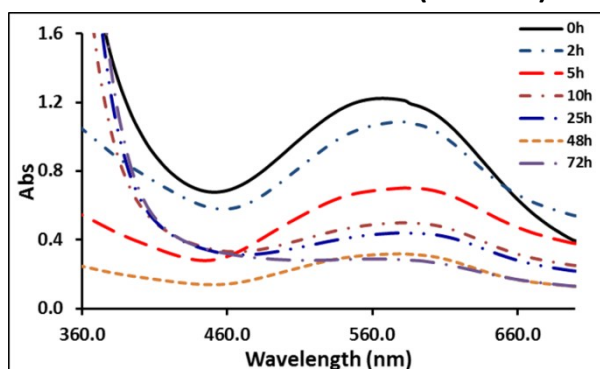


**Figure S71.** UV-vis absorption spectra of NR-loaded micelles of **PN(Fc-r-TEG)** after oxidized by  $\text{FeCl}_3$  at different intervals.

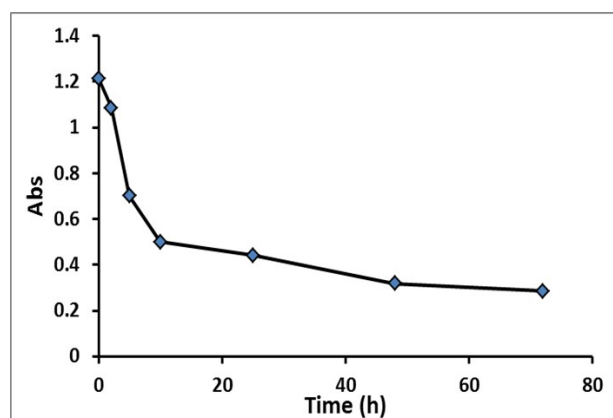


**Figure S72.** The UV-vis absorbance variation of NR-loaded micelles of **PN(Fc-r-TEG)** at 585 nm after oxidized by  $\text{FeCl}_3$  in water.

### 10.3. Loading and release of DOX by micelles of **PN(Fc-b-TEG)**

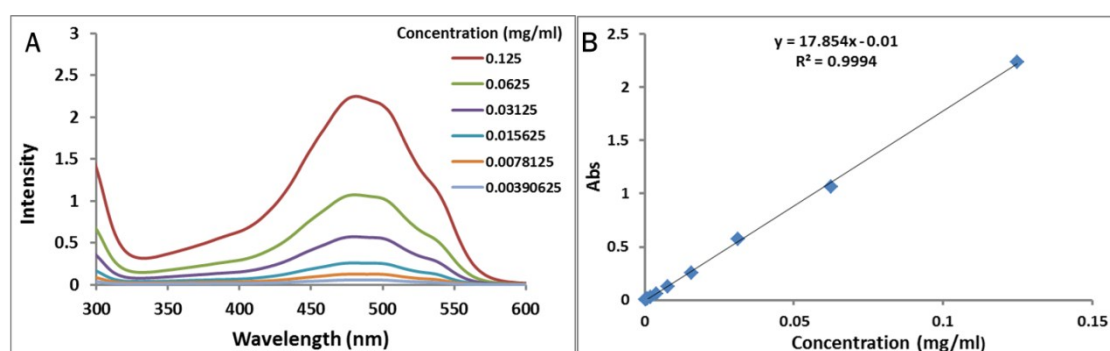


**Figure S73.** (A) The UV-vis absorption spectra of DOX in water at different concentrations. (B) The standard profile of DOX at 480 nm according to the UV-vis absorption spectra.

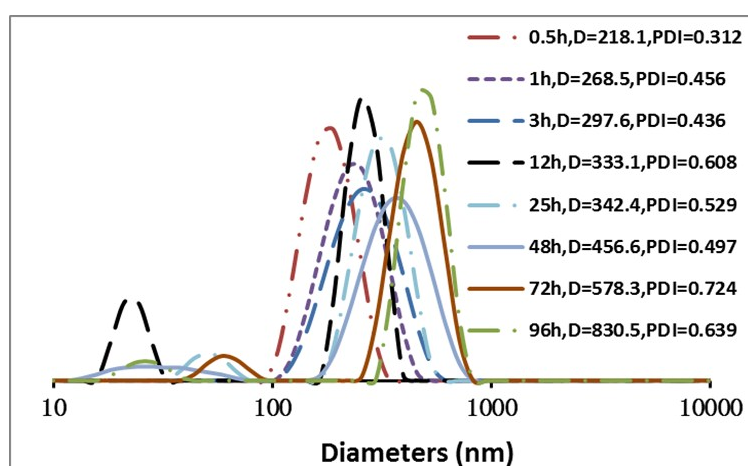


**Figure S74.** The time dependent DLS curves of DOX-loaded micelles of diblock copolymer **PN(Fc-b-TEG)** by using  $1 \text{ mg ml}^{-1}$  of  $\text{FeCl}_3$  as oxidant.

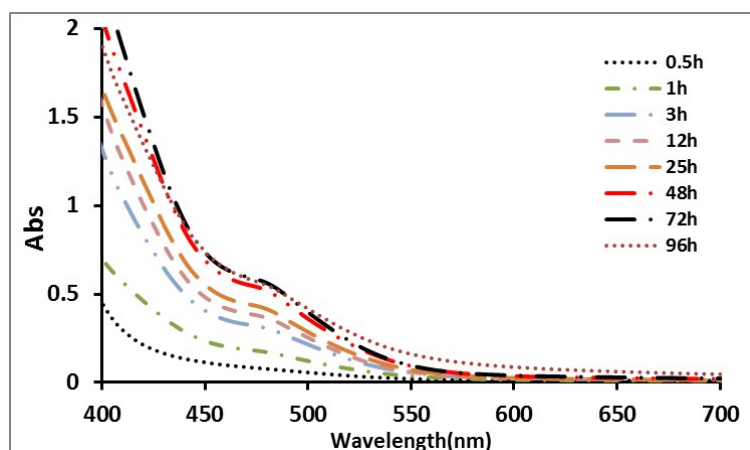


**Figure S75.** UV-vis absorption spectra of DOX releasing from micelles of diblock copolymer PN(Fc-*b*-TEG) at different intervals after the treatment by using 2 mg ml<sup>-1</sup> of FeCl<sub>3</sub> as oxidant.

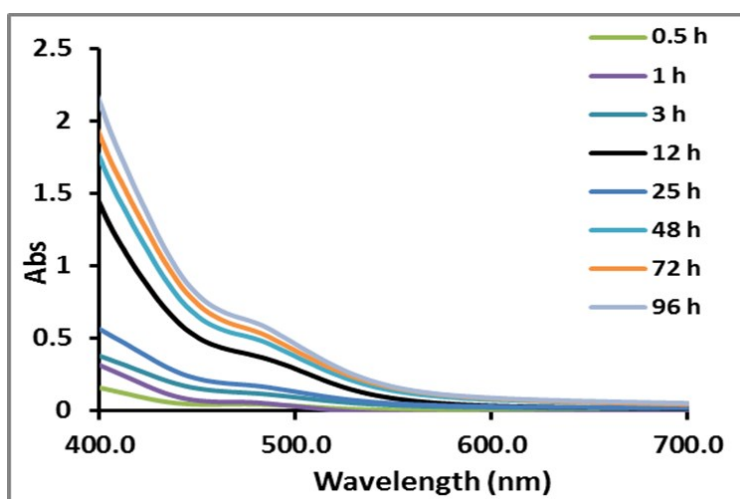


**Figure S76.** UV-vis absorption spectra of DOX releasing from micelles of diblock copolymer PN(Fc-*b*-TEG) at different intervals after the treatment by using 1 mg ml<sup>-1</sup> of FeCl<sub>3</sub> as oxidant.

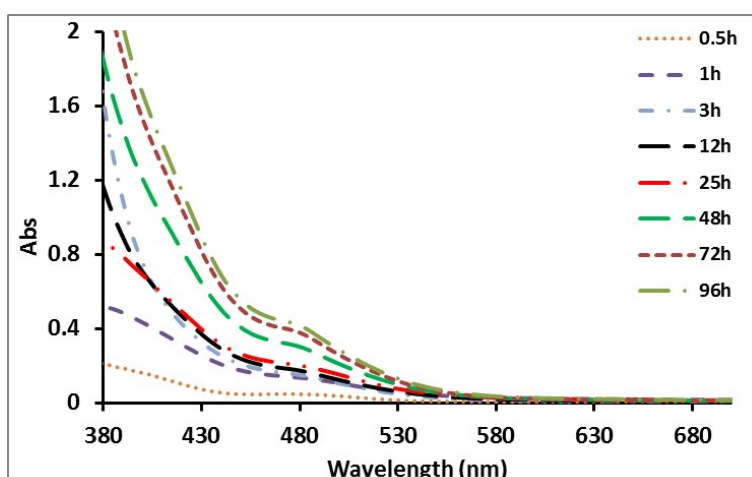


**Figure S77.** UV-vis absorption spectra of DOX releasing from micelles of diblock copolymer PN(Fc-*b*-TEG) at different intervals after the treatment by using 0.5 mg ml<sup>-1</sup> of FeCl<sub>3</sub> as oxidant.

#### 10.4. Loading and release of DOX by micelles of PN(Fc-r-TEG)

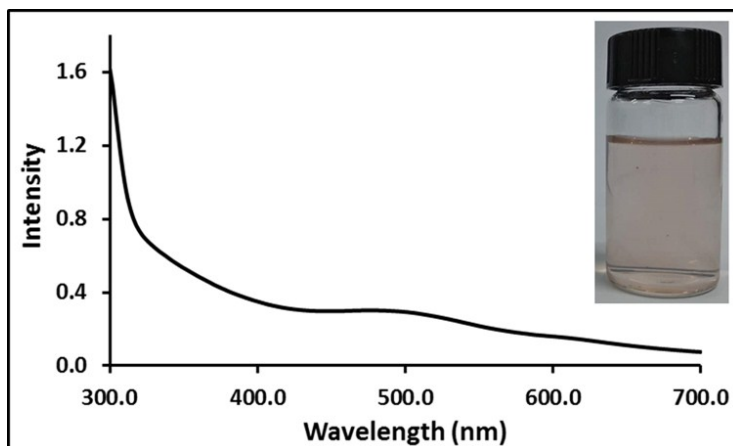


**Figure S78.** UV-vis absorption spectrum of DOX-loaded micelles of random copolymer **PN(Fc-r-TEG)**.

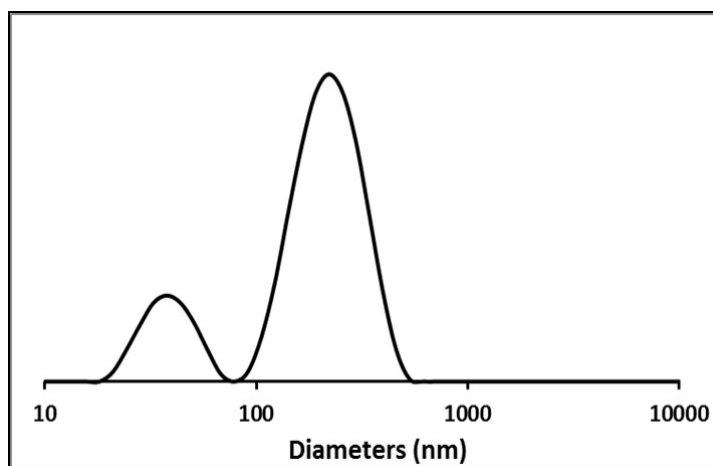


**Figure S79.** DLS curve of the micelles of DOX-loaded micelles of random copolymer **PN(Fc-r-TEG)**. (PDI = 0.712, Average size = 226 nm).

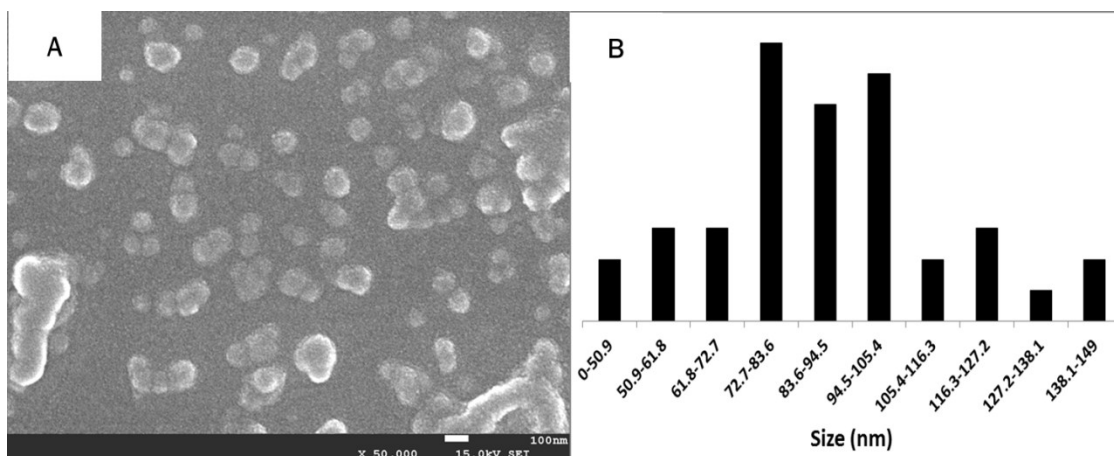


**Figure S80.** SEM image (A) and size distribution (B) of DOX-loaded micelles of random copolymer **PN(Fc-r-TEG)**. (Average size of  $89 \pm 20$  nm)

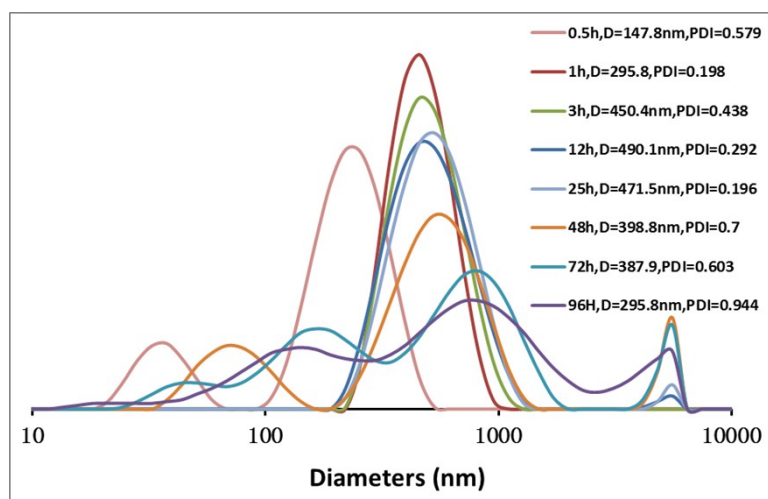


**Figure S81.** The time dependent DLS curves of DOX-loaded micelles of random copolymer **PN(Fc-*r*-TEG)** by using  $1 \text{ mg ml}^{-1}$  of  $\text{FeCl}_3$  as oxidant.

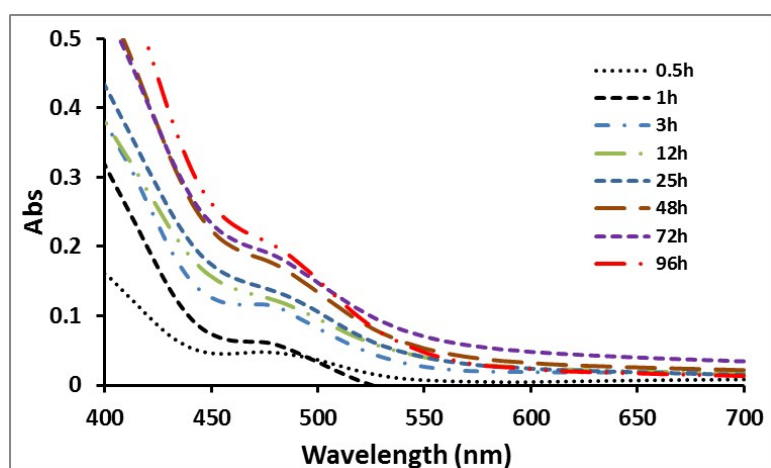


**Figure S82.** The UV-vis absorption spectra of DOX releasing from micelles of random copolymer **PN(Fc-*r*-TEG)** at different intervals after the treatment by using  $1 \text{ mg ml}^{-1}$  of  $\text{FeCl}_3$  as oxidant.

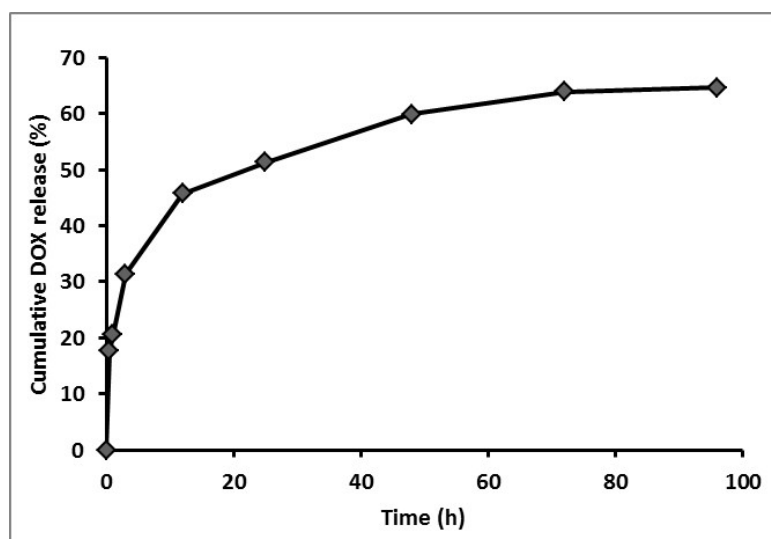


**Figure S83.** The cumulative release curve of DOX from micelles of random copolymer **PN(Fc-r-TEG)** at different time intervals using  $1\text{mg ml}^{-1}$   $\text{FeCl}_3$  as oxidant.

## 11. Biototoxicity evaluation

### 11.1. Evaluation of the biotoxicity by murine fibroblast cells (L-929 cell)

**Table S10.** The relationship between cell relative proliferation rate and cytotoxicity grade

Cell relative proliferation rate (%)	Cytotoxicity classification
$\geq 100$	0
$\geq 80$	1
$\geq 50$	2
$\geq 30$	3
$\geq 0$	4

### 11.2. Evaluation of the biotoxicity by zebrafish embryo

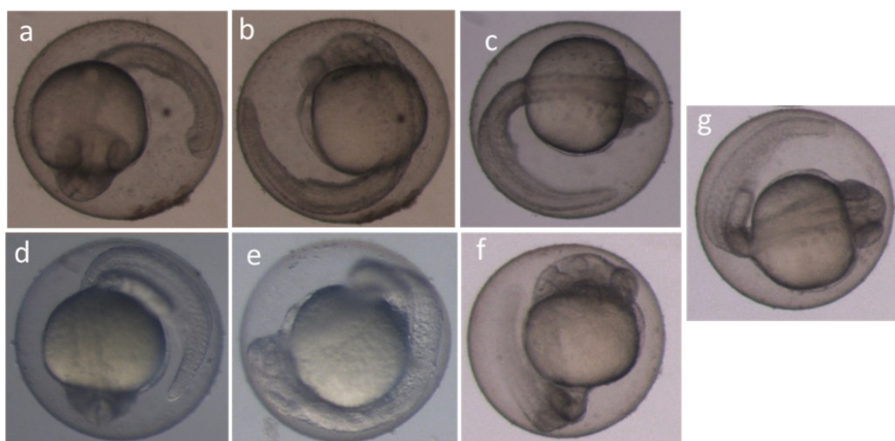


**Figure S84.** The photos of the zebrafish at 24 hpf. (a)-(c) treated with diblock copolymer **PN(Fc-b-TEG)** ((a)  $8\text{ mg ml}^{-1}$ , (b)  $4\text{ mg ml}^{-1}$ , (c)  $0.5\text{ mg ml}^{-1}$ ). (d)-(f) treated with random copolymer **PN(Fc-r-TEG)** (d)  $8\text{ mg ml}^{-1}$ , (e)  $4\text{ mg ml}^{-1}$ , (f)  $0.5\text{ mg ml}^{-1}$ ). (g) control.

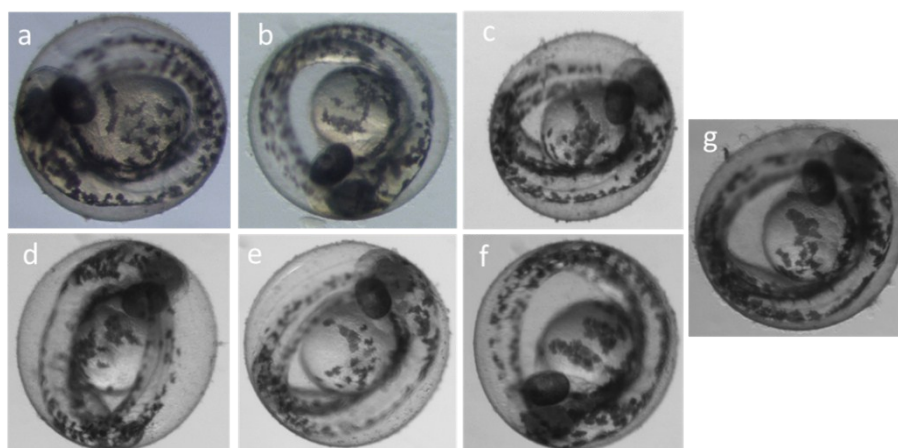


**Figure S85.** The photos of the zebrafish at 48 hpf. (a)-(c) treated with diblock copolymer **PN(Fc-b-TEG)** (a) 8 mg ml<sup>-1</sup>, (b) 4 mg ml<sup>-1</sup>, (c) 0.5 mg ml<sup>-1</sup>). (d)-(f) treated with random copolymer **PN(Fc-r-TEG)** (d) 8 mg ml<sup>-1</sup>, (e) 4 mg ml<sup>-1</sup>, (f) 0.5 mg ml<sup>-1</sup>). (g) control.

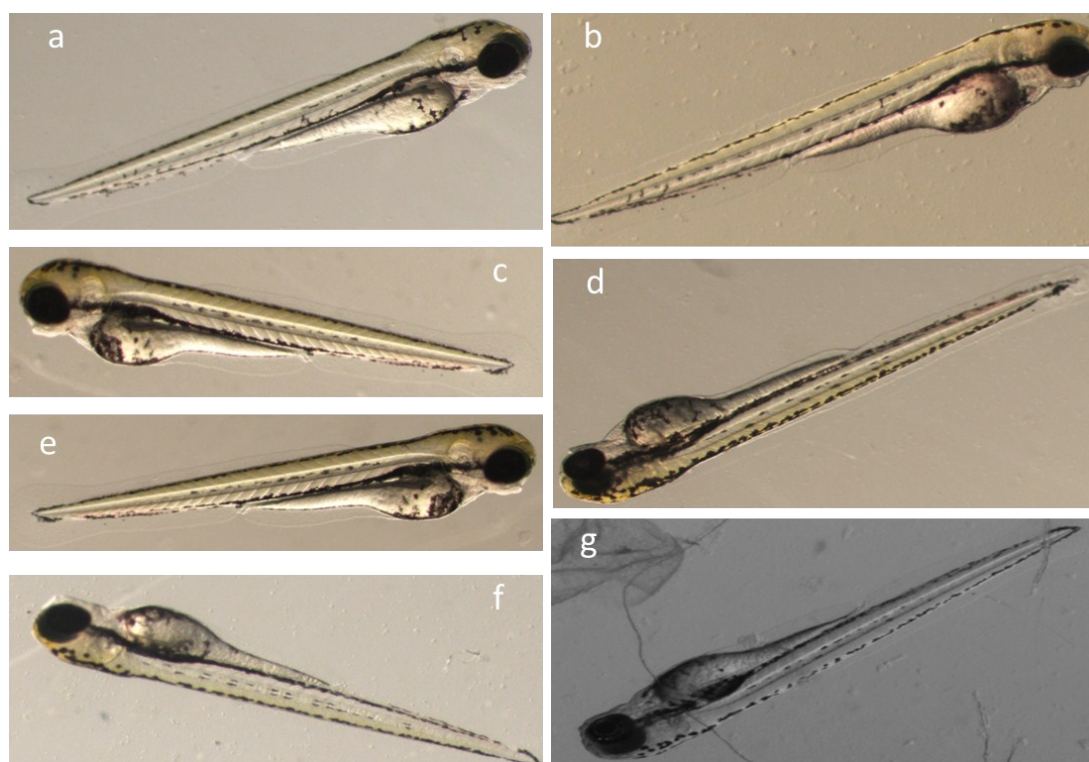


**Figure S86.** The photos of the zebrafish at 72 hpf. (a)-(c) treated with diblock copolymer **PN(Fc-b-TEG)** (a) 8 mg ml<sup>-1</sup>, (b) 4 mg ml<sup>-1</sup>, (c) 0.5 mg ml<sup>-1</sup>). (d)-(f) treated with random copolymer **PN(Fc-r-TEG)** (d) 8 mg ml<sup>-1</sup>, (e) 4 mg ml<sup>-1</sup>, (f) 0.5 mg ml<sup>-1</sup>). (g) control.

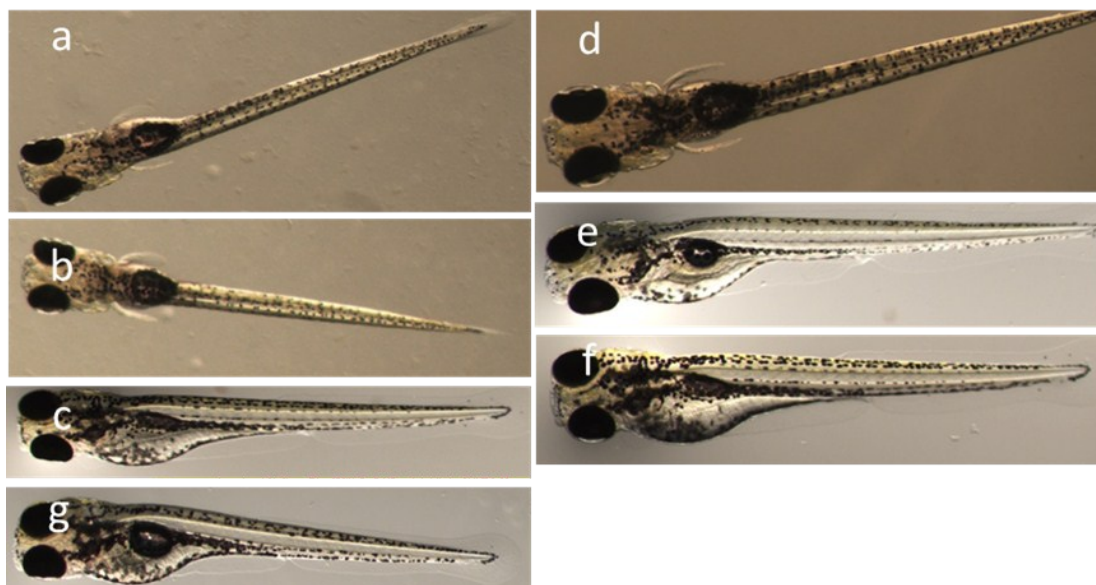


**Figure S87.** The photos of the zebrafish at 96 hpf. (a)-(c) treated with diblock copolymer **PN(Fc-*b*-TEG)** (a) 8 mg ml<sup>-1</sup>, (b) 4 mg ml<sup>-1</sup>, (c) 0.5 mg ml<sup>-1</sup>). (d)-(f) treated with random copolymer **PN(Fc-*r*-TEG)** (d) 8 mg ml<sup>-1</sup>, (e) 4 mg ml<sup>-1</sup>, (f) 0.5 mg ml<sup>-1</sup>). (g) control.

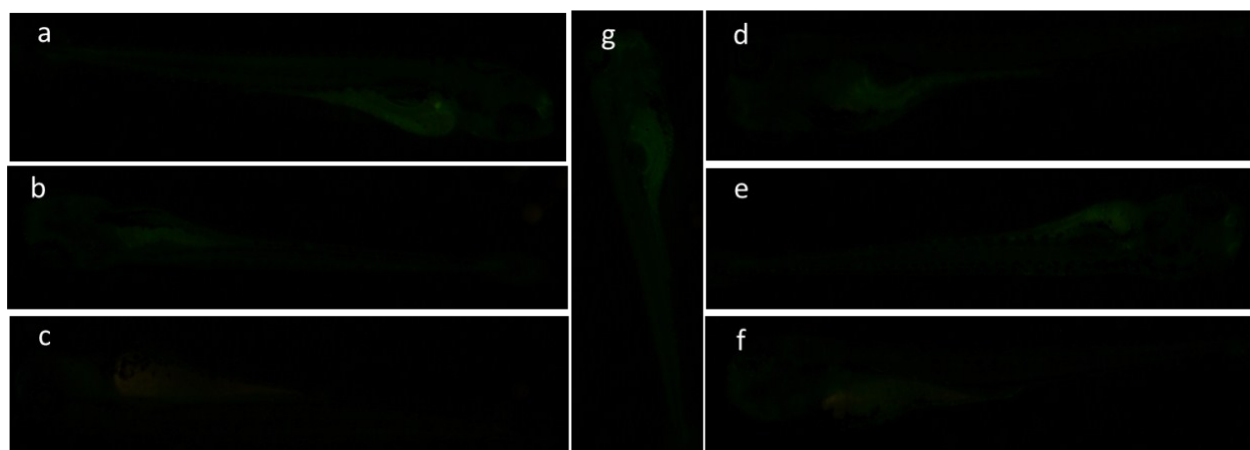


**Figure S88.** The photos of the zebrafish dyed by acridine orange at 96 hpf. (a)-(c) treated with diblock copolymer **PN(Fc-*b*-TEG)** (a) 8 mg ml<sup>-1</sup>, (b) 4 mg ml<sup>-1</sup>, (c) 0.5 mg ml<sup>-1</sup>). (d)-(f) treated with random copolymer **PN(Fc-*r*-TEG)** (d) 8 mg ml<sup>-1</sup>, (e) 4 mg ml<sup>-1</sup>, (f) 0.5 mg ml<sup>-1</sup>). (g) control.

## 12. References

- [S1] L. Zhao, QJ. Ling, X. Liu, CD. Hang, QX. Zhao, FF. Liu, Multifunctional triazolylferrocenyl Janus dendron: Nanoparticle stabilizer, smart drug carrier and supramolecular nanoreactor, *Appl. Organomet. Chem.* 2017, 32, e4000.
- [S2] H. Gu, A. Rapakousiou, P. Castel, N. Guidolin, N. Pinaud, J. Ruiz, D. Astruc, Living Ring-Opening Metathesis–Polymerization Synthesis and Redox-Sensing Properties of Norbornene Polymers and Copolymers Containing Ferrocenyl and Tetraethylene Glycol Groups. *Organometallics* 2014, 33(16), 4323-4335.
- [S3] A. K. Diallo, E. Boisselier, L. Liang, J. Ruiz, D. Astruc, Dendrimer-Induced Molecular Catalysis

in Water: The Example of Olefin Metathesis. *Chem. Eur. J.* 2010, 16(39), 11832-11835.

[S4] Liu, X., et al., Controlled ROMP Synthesis of Ferrocene-Containing Amphiphilic Dendronized Diblock Copolymers as Redox-Controlled Polymer Carriers. *Macromolecular Chemistry and Physics*, 2018. 219(18): p. 1800273

[S5] G Qiu, L Zhao, X Liu, Q Zhao, F Liu, Y Liu, Y Liu, ROMP synthesis of benzaldehyde-containing amphiphilic block polynorbornenes used to conjugate drugs for pH-responsive release. *React. Funct. Polym.* 2018, 128, 1-15.

[S6] USPC .Biological Tests/ Biological Reactivity Tests, in vitro [S] .USP 27, 2004.